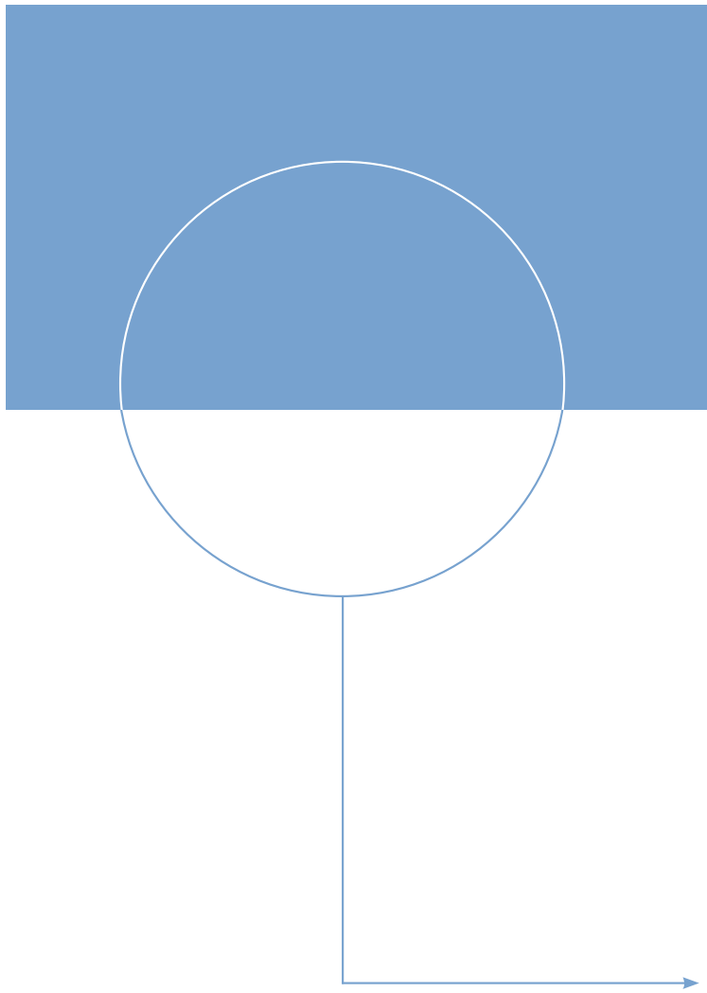

Master's thesis

2021

Martin Spillum Grønli

NTNU
Norwegian University of
Science and Technology
Faculty of Natural Sciences
Department of Physics

Martin Spillum Grønli

Quantum Chromodynamics in Strong Magnetic Fields with Isospin Chemical Potential

Chiral Soliton Lattice and Magnetic Vortex Lattice

June 2021

NTNU
Norwegian University of
Science and Technology

NTNU
Norwegian University of
Science and Technology

NTNU
Norwegian University of
Science and Technology

Quantum Chromodynamics in Strong Magnetic Fields with Isospin Chemical Potential

Chiral Soliton Lattice and Magnetic Vortex Lattice

Martin Spillum Grønli

Applied Physics and Mathematics
Submission date: June 2021
Supervisor: Tomáš Brauner, UiS
Co-supervisor: Jens Oluf Andersen, NTNU

Norwegian University of Science and Technology
Department of Physics

I want to dedicate this thesis to my parents Ruth and Anders, and my sister Oda.

Abstract

This thesis considers the low-energy behavior of two-flavor quantum chromodynamics (QCD) at finite isospin density in an external magnetic field. The ground state of QCD under these conditions will at sufficiently strong magnetic fields be affected by the anomalies of QCD. Hence, we demonstrate how the chiral isospin anomaly is manifested in chiral perturbation theory. Using chiral perturbation theory, the mentioned ground state turns out to be a chiral soliton lattice (CSL) composed of an array of parity-violating topological solitons. In presence of the CSL background, we derive the excitation spectrum when the phonon of the soliton lattice is coupled to dynamical electromagnetic fields. The resulting spectrum consists of two gapped modes and one gapless mode having a nonrelativistic dispersion relation. Moreover, we demonstrate how a Bose-Einstein condensate (BEC), consisting of charged pions, forms when the isospin chemical potential μ_I exceeds the value of the pion mass. This also happens when the external magnetic field H is absent. As a next step, we establish how dynamical electromagnetic fields affect the excitation spectrum of the BEC through the Anderson-Higgs mechanism.

Furthermore, we map out the QCD phase diagram in the μ_I-H plane allowing for three phases to exist. These are the QCD vacuum, the CSL and the BEC. Going to the chiral limit squeezes the QCD vacuum completely out of the phase diagram. Finally, we examine the possibility of a superconducting magnetic vortex lattice as a fourth phase in the phase diagram. We establish a numerical iteration procedure that computes the order parameter and the magnetic field in a system exhibiting this type-II superconductivity. Furthermore, we derive a virial theorem for QCD that makes it possible to determine the Gibbs free energy of the vortex lattice at an arbitrary fixed external magnetic field and isospin density. Consequently, we have a method that can establish where the magnetic vortex lattice is manifested in the QCD phase diagram.

Sammendrag

I denne avhandlingen studerer vi kvantekromodynamikk (QCD) med to kvarktyper ved lave energier. Vi inkluderer et eksternt magnetfelt og et endelig isospinn kjemisk potensial. Under disse forholdene vil grunntilstanden til QCD i et tilstrekkelig høyt magnetfelt være påvirket av anomaliene i QCD. Vi demonstrerer hvordan disse anomaliene er inkludert i kiral perturbasjonsteori. Ved å bruke kiral perturbasjonsteori konstaterer vi at den nevnte grunntilstanden er et kiralt solitongitter (CSL) bestående av en rekke med paritetsbrytende topologiske solitoner. Med en CSL-bakgrunn kobler vi solitongitterets fonon til dynamiske elektromagnetiske felter og utleder eksitasjonsspekteret. Spekteret består av to masseløse moder og én massiv mode med en ikke-relativistisk dispersjonsrelasjon. I tillegg viser vi hvordan et Bose-Einstein-kondensat (BEC) dannes når vi har et isospinn kjemisk potensial μ_I som er større enn verdien til pionmassen. Det samme skjer når det eksterne magnetfeltet H fjernes. Vi undersøker også hvordan dynamiske elektromagnetiske felter endrer eksitasjonsspekteret i et BEC bestående av ladde pioner. Endringene skjer som følge av Anderson-Higgs-mekanismen.

Videre bestemmer vi hvordan fasediagrammet til QCD i μ_I-H-planet ser ut. Dette gjør vi ved å tillate eksistensen av de tre fasene QCD-vakuum, CSL og BEC. I den kirale grensen blir QCD-vakuumet presset helt ut av fasediagrammet. Til slutt undersøker vi muligheten for en fjerde fase bestående av et superledende magnetisk virvelgitter. Vi utleder en numerisk iterasjonsmetode som beregner ordreparameteren og magnetfeltet for et slikt type-II superledende virvelgitter i QCD. Et virialteorem blir utledet for QCD slik at gitterets Gibbs frie energi kan beregnes for et vilkårlig eksternt magnetfelt og isospinntetthet. Vi har derfor en metode som kan bestemme hvor virvelgitteret manifesteres i fasediagrammet til QCD.

Preface

This master's thesis has been written as an integral part of a Master of Science in Applied Physics and Mathematics at the Norwegian University of Science and Technology. The thesis is divided into three parts which are further divided into chapters. Chapters 2-8 are identical to the specialization project written in the autumn of 2020 [1].[1] The purpose of the thesis has been to investigate how quantum chromodynamics behaves in an external magnetic field at finite isospin density. The physics arising from such conditions has at some points been truly fascinating.

I want to thank Tomáš Brauner (UiS) and Jens Oluf Andersen (NTNU) for joyful and illuminating discussions. In particular I would like to thank Tomáš Brauner for letting me work on interesting topics that has challenged and developed all of my scientific abilities. Furthermore, I would like to thank all my friends who have helped me focus and not focus.

Martin Spillum Grønli
Trondheim, Norway
June 14, 2021

[1]The chapters are identical except for some typographical errors that have been corrected.

Contents

List of Figures

Notation and conventions

Here we present a list of different notation and conventions used in the project.

- QCD: quantum chromodynamics.
- QED: quantum electrodynamics
- Vev: vacuum expectation value.
- EFT: effective field theory.
- ChPT: chiral perturbation theory.
- CSL: chiral soliton lattice.
- BEC: Bose-Einstein condensate.
- GW current: Goldstone-Wilczek current
- $\mathscr{L}$: Lagrangian (density).
- $\mathscr{H}$: Hamiltonian (density)
- $\mathrm{Tr}(A)$: trace of matrix A.
- $\mathrm{Det}(A)$: determinant of matrix A.
- $\langle ... \rangle = (1/V) \int_V \mathrm{d}^3 r ...$: spatial average of ... over a unit cell of volume V.
- Boldface letters like $\boldsymbol{p}$ denote three-vectors.
- Greek indices denote spacetime coordinates, $x^\mu = (x^0, \boldsymbol{x})$, where $\mu = (0, 1, 2, 3)$.
- Latin indices denote space coordinates x^i, where $i = (1, 2, 3)$.
- Repeated indices are summed over using the Einstein summation convention.
- Natural units with $\hbar = c = e = 1$ if not stated otherwise.
- Feynman slash notation reads $\not{A} = \gamma^\mu A_\mu$.
- Pauli matrices defined as

$$\tau_1 = \begin{pmatrix} 0 & 1 \\ 1 & 0 \end{pmatrix}, \quad \tau_2 = \begin{pmatrix} 0 & -i \\ i & 0 \end{pmatrix} \quad \text{and} \quad \tau_3 = \begin{pmatrix} 1 & 0 \\ 0 & -1 \end{pmatrix}.$$

- Gamma matrices defined as

$$\gamma^0 = \begin{pmatrix} \mathbb{1} & 0 \\ 0 & -\mathbb{1} \end{pmatrix}, \quad \gamma^i = \begin{pmatrix} 0 & \tau^i \\ -\tau^i & 0 \end{pmatrix} \quad \text{and} \quad \gamma^5 = \begin{pmatrix} 0 & \mathbb{1} \\ \mathbb{1} & 0 \end{pmatrix},$$

  where $\mathbb{1}$ is the 2×2 identity matrix, τ^i are the three Pauli matrices and $\gamma^5 = i\gamma^0\gamma^1\gamma^2\gamma^3$. This satifies the Clifford algebra $\{\gamma^\mu, \gamma^\nu\} = 2\eta^{\mu\nu}$.

- The Minkowski metric is $\eta_{\mu\nu} = \eta^{\mu\nu} = \text{diag}(1, -1, -1, -1)$.

- The Levi-Civita symbol in Euclidean space is defined by $\varepsilon_{1234} = 1$.

- The Levi-Civita symbol in Minkowski space is defined by $\varepsilon_{0123} = 1$.

- The third pion field $\pi_3 = \pi^0$, where π^0 is the neutral pion field.

Chapter 1

Introduction

In this chapter, we will present a brief historical background of Goldstone bosons, quantum chromodynamics (QCD), the chiral soliton lattice and superconductivity. The structure of the thesis is presented at the end of this chapter.

1.1 Historical background

Yoichiro Nambu published in 1960 a paper [2] that came to set the stage for still ongoing research. He was exploring superconductivity and found collective excitations of massless quasiparticle pairs, later known as massless Nambu-Goldstone bosons or Goldstone bosons. The following year, Jeffrey Goldstone conjectured that Goldstone bosons appear if a system, invariant under some group G, has a ground state that is only invariant under a subgroup $H \subset G$ [3]. This is known as spontaneous symmetry breaking (SSB) from a symmetry G down to a symmetry H. The conjecture was proved for Lorentz invariant systems in 1962 by Goldstone, Salam and Weinberg, and is known as the Goldstone theorem [4]. Two months after Nambu published his paper on Goldstone bosons, he also explained why the pions are nearly massless compared to other particles made up of quarks. He argued that pions are nearly massless Goldstone bosons resulting from a hidden, approximate symmetry of the strong interaction [5]. This was more than a decade before the theory of the strong force was firmly established when Fritzsch, Gell-Mann and Leutwyler introduced QCD as the gauge theory of color [6, 7].

A feature of QCD that was discovered in 1973 [8, 9] is asymptotic freedom in which the interaction strength between quarks and gluons decreases with increasing energy. This implies that QCD at high energies can be studied using perturbative methods with an expansion in the QCD coupling constant. However, this is not possible at low energies where the coupling constant is large. The relevant degrees of freedom at low energies are not quarks and gluons but pions. An effective field theory (EFT) written in terms of pion degrees of freedom was therefore derived by Weinberg in 1979 [10]. An EFT approximates the underlying theory. EFTs have been used to gain insight into the different regimes of QCD. One of these regimes is QCD at low energies and finite densities. Several studies of this regime using EFTs have been done in the two last decades [11–13]. The results from EFTs have been complemented by lattice simulations of QCD. These are simulations that solve QCD numerically on a discretized spacetime grid. Examples of results from such

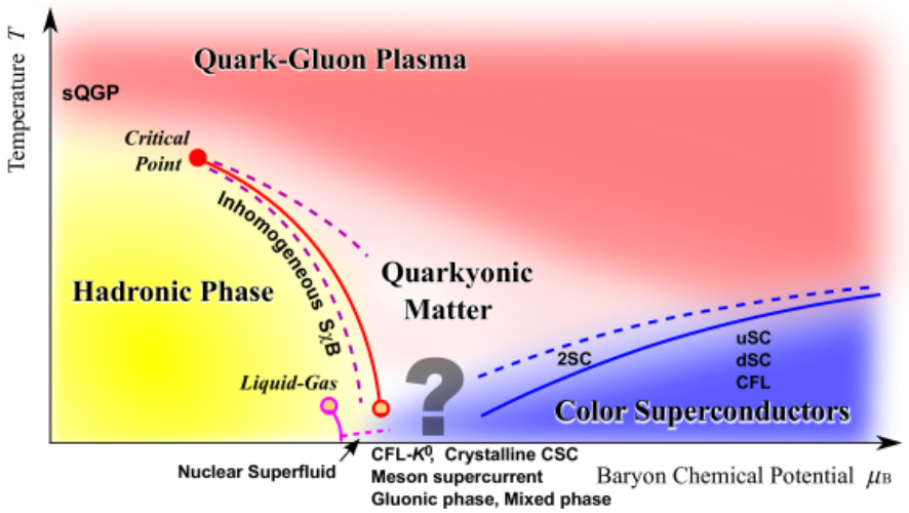

Figure 1.1: QCD phase diagram in the μ_B-T plane. Figure is taken from [19].

lattice simulations can be found in [14, 15]. One of the major limitations on lattice QCD is the NP-hard sign problem [16]. This prevents the use of lattice QCD at an arbitrary baryon chemical potential. A system with finite isospin chemical potential is not hindered by the fermion sign problem [17]. However, including a magnetic field results in the breaking of flavor symmetry because of the differing charge of the up and down quark. This makes the sign problem reappear.[1] EFTs may therefore serve as an advantageous tool in order to gain insight into phases both with and without a sign problem.

The EFTs need to reproduce the correct physics of the underlying theory in a given regime. This means that all relevant features of the underlying theory must be systematically included in the EFT. A feature of QCD that can be important in some regimes is anomalies. An anomaly arises if a classical symmetry of a theory does not survive quantization. In 1969, Adler [20], Bell and Jackiw [21] discovered that an anomaly could explain the decay rate of a neutral pion decaying into two photons. It was dubbed the chiral (or axial) anomaly since it leads to a nonconservation of a chiral current. Son and Stephanov showed in 2008 that an anomaly would affect the ground state in presence of an external magnetic field at finite baryon density [22]. The structure of this ground state was firmly established by Brauner and Yamamoto in 2017 [23]. It takes the form of a periodic array of topological solitons and is called a chiral soliton lattice (CSL).

Other ground states at finite densities have also been established [19]. One of these is the Bose-Einstein condensate (BEC). For two-flavor QCD at finite isospin density, it is shown that the condensed phase is a superfluid where one of the charged pions forms a massless mode [24]. It is therefore expected that such a phase will behave as a superconductor in presence of an external magnetic field. Superconductors expel external magnetic fields by exhibiting either type-I or type-II behavior. In 1957, Abrikosov generalized the experimental and theoretical understanding of type-II superconductors, and demonstrated the existence of a vortex lattice at strong

[1] In [18] they circumvent the sign problem by performing a Taylor expansion in the magnetic field.

magnetic fields [25]. Such a magnetic vortex lattice has recently been discussed in [17, 26] for two-flavor QCD at finite isospin density. However, the structure and the energy of the lattice have only been found for limiting cases of the external magnetic field and the isospin chemical potential. It is neither established where the lattice is manifested in the QCD phase diagram. The QCD phase diagram is a graphical representation of the conditions under which the different phases exist. A conjectured phase diagram for QCD matter at finite temperature T and baryon chemical potential μ_B is shown in figure 1.1.

1.2 Structure of the thesis and general assumptions

This thesis is divided into three parts which are further divided into chapters. Chapters 2-8 present the work done in the specialization project during last semester [1], while chapters 9-12 present the work done this semester.

Part I starts out by studying how the mass spectrum and dispersion relations of specific models are affected by a chemical potential and a magnetic field. These are models that contain Goldstone bosons resulting from SSB.

In part II, we exploit the intuition from the above models and proceed to QCD. We introduce chiral perturbation theory (ChPT) as an EFT of QCD. ChPT is then used to study the low-energy regime of QCD at finite densities. Furthermore, we calculate the chiral isospin anomaly and include it in the ChPT Lagrangian.

In part III, we use the ChPT Lagrangian to determine the ground state of low-energy QCD in a strong magnetic field at finite baryon density. The result is the CSL solution obtained by Brauner and Yamamoto. Next, we replace the baryon chemical potential by an isospin chemical potential resulting in the same CSL structure. In presence of the CSL background, we derive the excitation spectrum when neutral pions are coupled to dynamical electromagnetic fields. The excitation spectrum is also derived in a BEC with dynamical electromagnetic fields. Finally, we determine the phase diagram of low-energy QCD and establish an iteration procedure that can compute the Gibbs free energy of the magnetic vortex lattice at an arbitrary external magnetic field and isospin density.

Throughout the thesis, we will ignore weak interactions as they are small. In addition, we ignore electromagnetic interactions between pions. This is potentially problematic, but a justification of this is found in [17]. All results in this thesis are obtained at tree level.

Part I

Complex scalar field and non-Abelian models

Chapter 2

Complex scalar field

In this chapter we calculate the mass spectrum and dispersion relations of a complex scalar field. This is first done for a complex scalar field in the vacuum, before we introduce a chemical potential. Finally, we observe how Landau level quantization appears by introducing a magnetic field along with the chemical potential. The calculations in section 2.1 and 2.2 follow a procedure similar to the ones in [27].

2.1 Complex scalar field in the vacuum

A complex scalar field ϕ has the Lagrangian

$$\mathscr{L} = \partial_\mu \phi^* \partial^\mu \phi + m^2 \phi^* \phi - \lambda(\phi^* \phi)^2, \tag{2.1}$$

where m is the mass and λ is the coupling constant of the theory. By considering the static part of the Lagrangian we find that the classical potential of the theory reads

$$\mathscr{U} = -m^2 \phi^* \phi + \lambda(\phi^* \phi)^2. \tag{2.2}$$

The vacuum expectation value (vev) of the field is given by the minimum of the potential. Differentiating the potential with respect to the field ϕ^* and setting the derivative equal to zero

$$\frac{\partial \mathscr{U}}{\partial \phi^*} = \left[-m^2 + 2\lambda(\phi^* \phi)\right] \phi = 0, \tag{2.3}$$

gives for $m^2 > 0$ the local maximum

$$\phi = 0, \tag{2.4}$$

and the minima

$$\phi = \frac{m}{\sqrt{2\lambda}} e^{i\delta} \equiv \frac{v}{\sqrt{2}} e^{i\delta}, \tag{2.5}$$

where δ corresponds to an arbitrary phase of the field. The mass spectrum of a theory with nonzero vev is obtained by expanding the field around its vev. We choose $\phi = v/\sqrt{2}$ and the parameterization

$$\phi = \frac{1}{\sqrt{2}}(v + \pi_1 + i\pi_2), \tag{2.6}$$

where π_1 and π_2 are real fields fluctuating around the ground state. Substituting the parameterization for ϕ into our potential in eq. (2.2) yields

$$\mathscr{U} = -\frac{m^4}{4\lambda} + m^2\pi_1^2 + \lambda v\pi_1^3 + \lambda v\pi_1\pi_2^2 + \frac{\lambda}{2}\pi_1^2\pi_2^2 + \frac{\lambda}{4}\pi_1^4 + \frac{\lambda}{4}\pi_2^4. \tag{2.7}$$

The mass spectrum is determined by the eigenvalues of the mass matrix. The mass matrix in a Lorentz invariant theory is diagonal, implying that the masses are given by

$$m_i^2 = \frac{\partial^2\mathscr{U}}{\partial\pi_i^2}\Big|_{\pi_1=\pi_2=0}. \tag{2.8}$$

Consequently, the masses of the two modes π_1 and π_2 are

$$m_{\pi_1} = \sqrt{2}m \tag{2.9}$$

and

$$m_{\pi_2} = 0. \tag{2.10}$$

The nonzero vev of the field has consequently led to one massless mode. When choosing our parameterization we picked the ground state $\phi = v/\sqrt{2}$. The Lagrangian in eq. (2.1) has a $U(1)$ symmetry, but performing a $U(1)$ transformation of the chosen ground state gives $\phi = v/\sqrt{2}e^{i\theta}$, where θ is a phase. Thus, the $U(1)$ symmetry of the Lagrangian is broken in the ground state. $U(1)$ has only one generator and the generator must therefore be broken. In light of the Goldstone theorem this broken generator corresponds to the massless mode π_2.

2.2 Complex scalar field with a chemical potential

2.2.1 Spontaneous symmetry breaking

Consider a Lagrangian

$$\mathscr{L}_0 = \partial_\mu\phi^*\partial^\mu\phi - m^2\phi^*\phi - \lambda(\phi^*\phi)^2, \tag{2.11}$$

which differs from the Lagrangian in eq. (2.1) by an opposite sign of the mass term. By carrying out a Legendre transform we can obtain the corresponding Hamiltonian $\mathscr{H}_0$. A Legendre transformation to $\mathscr{H}_0$ is given by

$$\mathscr{H}_0 = \sum_a \Pi_a\dot{\phi}_a - \mathscr{L}_0, \tag{2.12}$$

summing over the fields ϕ_a. The dot denotes derivative with respect to time and Π_a are the canonical conjugate momenta, not to be confused with π_1 and π_2. The canonical conjugate momenta are given by

$$\Pi = \partial\mathscr{L}_0/\partial\dot{\phi} = \dot{\phi}^* \tag{2.13}$$

and

$$\Pi^* = \partial\mathscr{L}_0/\partial\dot{\phi}^* = \dot{\phi}. \tag{2.14}$$

This gives the Hamiltonian

$$\mathscr{H}_0 = \Pi\,\Pi^* + \boldsymbol{\nabla}\phi^* \cdot \boldsymbol{\nabla}\phi + m^2\phi^*\phi + \lambda(\phi^*\phi)^2. \tag{2.15}$$

In analogy with statistical physics, the grand canonical Hamiltonian is

$$\mathscr{H}_\mu = \mathscr{H}_0 - \mu\mathscr{N}, \tag{2.16}$$

where $\mathscr{N}$ is the Noether charge density corresponding to the global $U(1)$ symmetry of our Lagrangian $\mathscr{L}_0$. The charge density $\mathscr{N}$ can be obtained from the temporal part of the Noether current. The Noether current of a Lagrangian $\mathscr{L}_0 = \mathscr{L}_0(\phi_a, \partial_\mu\phi_a)$ is

$$j^\mu = \frac{\delta\mathscr{L}_0}{\delta\partial_\mu\phi_a}\delta\phi_a. \tag{2.17}$$

Varying our Lagrangian $\mathscr{L}_0$ with respect to the derivative of the fields results in

$$\frac{\delta\mathscr{L}_0}{\delta\partial_\mu\phi} = \partial_\mu\phi^* \quad \text{and} \quad \frac{\delta\mathscr{L}_0}{\delta\partial_\mu\phi^*} = \partial_\mu\phi. \tag{2.18}$$

Furthermore, a $U(1)$ transformation of the fields takes the form

$$\phi \to e^{-i\alpha}\phi \quad \text{and} \quad \phi^* \to e^{i\alpha}\phi^*, \tag{2.19}$$

with α as a constant in spacetime. Assuming that the transformation is infinitesimal leaves us with $\phi \to (1 - i\alpha)\phi$ and $\phi^* \to (1 + i\alpha)\phi^*$, giving the variation of the fields

$$\delta\phi = -i\phi \quad \text{and} \quad \delta\phi^* = i\phi^*. \tag{2.20}$$

Inserting eqs. (2.18) and (2.20) into eq. (2.17) for the Noether current gives

$$j^\mu = i\left[\phi^*\partial^\mu\phi - \phi\partial^\mu\phi^*\right]. \tag{2.21}$$

Taking the temporal part of the Noether current yields the needed Noether charge density

$$\mathscr{N} = j^0 = i\left[\phi^*\Pi^* - \phi\Pi\right]. \tag{2.22}$$

By eq. (2.16), the grand canonical Hamiltonian for a complex scalar field with a chemical potential is[1]

$$\mathscr{H}_\mu = \Pi\,\Pi^* + \boldsymbol{\nabla}\phi^* \cdot \boldsymbol{\nabla}\phi + m^2\phi^*\phi + \lambda(\phi^*\phi)^2 - i\mu\left[\phi^*\Pi^* - \phi\Pi\right]. \tag{2.23}$$

We can derive the corresponding grand canonical Lagrangian $\mathscr{L}_\mu$ by performing an inverse Legendre transform of our grand canonical Hamiltonian $\mathscr{H}_\mu$. Since the Legendre transform is its own inverse, we can in analogy with eq. (2.12) obtain $\mathscr{L}_\mu$ as

$$\mathscr{L}_\mu = \Pi\dot{\phi} + \Pi^*\dot{\phi}^* - \mathscr{H}_\mu. \tag{2.24}$$

Because of the replacement $\mathscr{H}_0 \to \mathscr{H}_\mu$, we need to recalibrate how the conjugate momenta are related to the time derivative of the fields. Using Hamilton's equations, we get

$$\dot{\phi} = \frac{\partial\mathscr{H}_\mu}{\partial\Pi} = \Pi^* + i\mu\phi \quad \text{and} \quad \dot{\phi}^* = \frac{\partial\mathscr{H}_\mu}{\partial\Pi^*} = \Pi - i\mu\phi^*, \tag{2.25}$$

[1]The subscript μ is not a Greek index.

leading to

$$\Pi^* = \dot{\phi} - i\mu\phi \quad \text{and} \quad \Pi = \dot{\phi}^* + i\mu\phi^*. \tag{2.26}$$

Inserting this into $\mathscr{L}_\mu$ in eq. (2.24) yields

$$\mathscr{L}_\mu = D_\mu^* \phi^* D^\mu \phi - m^2 \phi^* \phi - \lambda(\phi^* \phi)^2, \tag{2.27}$$

with $D_\mu \phi = (\partial_\mu - i\delta_{\mu 0}\mu)\phi$ as the covariant derivative. From D_μ, we can see that the chemical potential behaves as the temporal component of a constant gauge field.

To examine if SSB can take place, we need to determine the vev. The Lagrangian $\mathscr{L}_\mu$ can be written as

$$\mathscr{L}_\mu = \partial_\mu \phi^* \partial^\mu \phi - i\mu[\phi \partial_0 \phi^* - \phi^* \partial_0 \phi] + \mu^2 \phi^* \phi - m^2 \phi^* \phi - \lambda(\phi^* \phi)^2, \tag{2.28}$$

resulting in the classical potential

$$\mathscr{U} = (-\mu^2 + m^2)\phi^* \phi + \lambda(\phi^* \phi)^2, \tag{2.29}$$

where we have used that the ground state is time-independent making the second term in the Lagrangian drop out. Setting the derivative of the potential equal to zero

$$\frac{\partial \mathscr{U}}{\partial \phi^*} = (-\mu^2 + m^2)\phi + 2\lambda(\phi^* \phi)\phi = 0, \tag{2.30}$$

gives the two solutions

$$\phi = 0 \quad \text{and} \quad |\phi|^2 = \frac{\mu^2 - m^2}{2\lambda} \equiv \frac{v^2}{2} > 0. \tag{2.31}$$

The second solution is not possible for $\mu < m$, causing $\phi = 0$ to be the vev. Therefore, no SSB is taking place for $\mu < m$. This is called the normal phase. For $\mu > m$, the potential acquires an infinite number of nonzero vevs, given by

$$\phi = \frac{v}{\sqrt{2}} e^{i\delta}, \tag{2.32}$$

where δ is an arbitrary phase. Having multiple vevs means that we have SSB. The phase where $\mu > m$ is therefore called the broken phase. The broken symmetry is the global $U(1)$ symmetry of the Langrangian $\mathscr{L}_\mu$. This follows from the same arguments as for the complex scalar field without a chemical potential in section 2.1.

2.2.2 Mass spectrum

We can now expand the field around the vev by choosing the parameterization

$$\phi = \frac{1}{\sqrt{2}}(v + \pi_1 + i\pi_2), \tag{2.33}$$

where π_1 and π_2 are real fields. The Lagrangian then takes the form

$$\begin{aligned} \mathscr{L}_\mu = {} & \frac{1}{2}\partial_\mu \pi_1 \partial^\mu \pi_1 + \frac{1}{2}\partial_\mu \pi_2 \partial^\mu \pi_2 - \mu(v\partial_0 \pi_2 + \pi_1 \partial_0 \pi_2 - \pi_2 \partial_0 \pi_1) \\ & + \frac{\mu^2 - m^2}{2}(v^2 + 2v\pi_1 + \pi_1^2 + \pi_2^2) \\ & - \frac{\lambda}{4}(v^4 + 4v^3\pi_1 + 6v^2\pi_1^2 + 2v^2\pi_2^2 + 4v\pi_1^3 + 4v\pi_1\pi_2^2 + 2\pi_1^2\pi_2^2 + \pi_1^4 + \pi_2^4). \end{aligned} \tag{2.34}$$

This Lagrangian is not manifestly Lorentz invariant, meaning that we cannot necessarily use the relation in eq. (2.8) to determine the mass spectrum [28]. Furthermore, the dispersion relation will deviate from $E = \sqrt{m^2 + \mathbf{p}^2}$. In order to derive the mass spectrum, we need to work out the dispersion relation and then let $\mathbf{p} \to 0$. The dispersion relation is found from the bilinear part of the Lagrangian $\mathscr{L}_\mu^{(2)}$ taking the form

$$\begin{aligned}\mathscr{L}_\mu^{(2)} = &\frac{1}{2}\partial_\mu\pi_1\partial^\mu\pi_1 + \frac{1}{2}\partial_\mu\pi_2\partial^\mu\pi_2 - \mu(\pi_1\partial_0\pi_2 - \pi_2\partial_0\pi_1) \\ &+ \frac{f(\mu)}{2}\pi_1^2 + \frac{g(\mu)}{2}\pi_2^2,\end{aligned} \tag{2.35}$$

where we have defined

$$f(\mu) \equiv \mu^2 - m^2 - 3\lambda v^2, \tag{2.36}$$
$$g(\mu) \equiv \mu^2 - m^2 - \lambda v^2. \tag{2.37}$$

A partial integration of the two first terms in $\mathscr{L}_\mu^{(2)}$ allows us to write the bilinear Lagrangian in the matrix form

$$\mathscr{L}_\mu^{(2)} = \frac{1}{2}\begin{pmatrix}\pi_1 & \pi_2\end{pmatrix}\begin{pmatrix}-\partial_\mu\partial^\mu + f(\mu) & -2\mu\partial_0 \\ 2\mu\partial_0 & -\partial_\mu\partial^\mu + g(\mu)\end{pmatrix}\begin{pmatrix}\pi_1 \\ \pi_2\end{pmatrix}. \tag{2.38}$$

The middle matrix is the inverse propagator D^{-1} in the (π_1, π_2)-basis. A Fourier transform of the inverse propagator reads,

$$D^{-1} = \begin{pmatrix}P^2 + f(\mu) & 2i\mu E \\ -2i\mu E & P^2 + g(\mu)\end{pmatrix}, \tag{2.39}$$

where $P = (E, \mathbf{p})$ is the four-momentum. The dispersion relations are given by the zero modes of the inverse propagator, found by setting

$$\begin{aligned}\mathrm{Det}(D^{-1}) = 0 &= \left[P^2 + f(\mu)\right]\left[P^2 + g(\mu)\right] - 4\mu^2E^2 \\ &= \left[E^2 - \mathbf{p}^2 + f(\mu)\right]\left[E^2 - \mathbf{p}^2 + g(\mu)\right] - 4\mu^2E^2.\end{aligned} \tag{2.40}$$

We must now distinguish between the normal and the broken phase. In the normal phase, we have the vev $v = 0$. Inserting $v = 0$ into eqs. (2.36) and (2.37) gives

$$f(\mu) = g(\mu) = \mu^2 - m^2. \tag{2.41}$$

Hence, solving eq. (2.40) for E result in the two dispersion relations

$$E_\pm(\mathbf{p}) = \sqrt{\mathbf{p}^2 + m^2} \pm \mu, \tag{2.42}$$

for the two modes π_1 and π_2. In the limit $\mathbf{p} \to 0$, we see that the two modes have masses

$$m_\pm = m \pm \mu \quad \text{for } \mu < m. \tag{2.43}$$

Next, we work out the dispersion relations in the broken phase where $v^2 = (\mu^2 - m^2)/\lambda$, as seen from eq. (2.31). Having $m^2 > 0$ and the fact that $\mu > m$, implies

that we have a nonzero vev. This yields SSB and means that we have relativistic Bose-Einstein condensation. Eqs. (2.36) and (2.37) now read

$$f(\mu) = -2(\mu^2 - m^2), \tag{2.44}$$
$$g(\mu) = 0. \tag{2.45}$$

Thus, eq. (2.40) for the zero modes becomes

$$E^4 - E^2(2\mathbf{p}^2 + 6\mu^2 - 2m^2) + \mathbf{p}^2(\mathbf{p}^2 + 2\mu^2 - 2m^2) = 0. \tag{2.46}$$

By solving this for E, we get the dispersion relations for the two modes π_1 and π_2 in the broken phase,

$$E_\pm(\mathbf{p}) = \sqrt{\mathbf{p}^2 + 3\mu^2 - m^2 \pm \sqrt{4\mu^2\mathbf{p}^2 + (3\mu^2 - m^2)^2}}. \tag{2.47}$$

Letting $\mathbf{p} \to 0$, we find that the mass spectrum of the two modes are,

$$m_+ = \sqrt{6\mu^2 - 2m^2}, \tag{2.48}$$
$$m_- = 0. \tag{2.49}$$

Thus, we have one gapless mode corresponding to the Nambu-Goldstone boson of the spontaneously broken $U(1)$ symmetry. Letting $\mu \to 0$ and taking $m^2 < 0$, we recover the masses in eqs. (2.9) and (2.10) for the complex field without a chemical potential.[2]

2.3 Complex scalar field with a chemical potential and a magnetic field

We will now study how the transition to a BEC is affected by a uniform magnetic field. This amounts to adding an external magnetic field to the covariant derivative $D_\mu = \partial_\mu - iA_\mu$ in eq. (2.27). By orienting the magnetic field in the z-direction, we can choose a gauge such that

$$A_\mu = (\mu, 0, -qBx, 0), \tag{2.50}$$

where q is, up to a sign, the electric charge of the particle annihilated by ϕ or the electric charge of the antiparticle created when ϕ is acting on the vacuum. Furthermore, B is the magnitude of the magnetic field. In this case, finding the dispersion relation directly is a bit more complicated. We will instead start from the fact that the ground state is trivial, $\phi = 0$, when $\mu = B = 0$. From there we assume that this holds also for some nonzero μ and B. We are thus working in the normal phase. The dispersion relation is as before obtained from the bilinear part of the Lagrangian,

$$\mathscr{L}_\mu^{(2)} = D_\mu\phi^* D^\mu\phi - m^2\phi^*\phi, \tag{2.51}$$

which after partial integration results in the inverse propagator

$$D^{-1} = -D_\mu D^\mu - m^2 = -(\partial_0 - i\mu)^2 + (\partial_i + i\delta_{i2}qBx)^2 - m^2. \tag{2.52}$$

[2]The difference between the Lagrangians in eqs. (2.1) and (2.11) is the opposite sign of the mass term.

The eigenfunctions ϕ of the inverse propagator can be found by noting that it commutes with ∂_t, ∂_y and ∂_z. We can therefore find simultaneous eigenstates of these operators, while the x-dependence must be treated separately. Hence, ϕ can be written as

$$\phi = e^{-i(Et - p_y y - p_z z)} f(x), \tag{2.53}$$

where E is the energy of the eigenstate. p_y corresponds to the eigenvalue of the operator $-i\partial_y$ and p_z will be the momentum in the z-direction. Consequently, the zero modes of the inverse propagator is given by

$$-\frac{1}{2m}\frac{\mathrm{d}^2 f(x)}{\mathrm{d}x^2} + \frac{(p_y + qBx)^2}{2m} f(x) = \frac{1}{2m}(E^2 + 2\mu E + \mu^2 - m^2 - p_z^2) f(x). \tag{2.54}$$

This can be recognized as the equation of a harmonic oscillator with frequency $\omega = qB/m$ and energy $(E^2 + 2\mu E + \mu^2 - m^2 - p_z^2)/2m$. On the other hand, the energy levels of a harmonic oscillator is given by $E_n = (1/2 + n)\omega$, where n is a non-negative integer denoting different Landau levels. Equating the two expressions for energy,

$$\frac{E^2 + 2\mu E + \mu^2 - m^2 - p_z^2}{2m} = (\frac{1}{2} + n)\frac{qB}{m} \tag{2.55}$$

yields the dispersion relation for a particle-antiparticle pair,

$$E_{\pm}(n, p_z) = \sqrt{m^2 + p_z^2 + (2n+1)qB} \mp \mu. \tag{2.56}$$

We can see that the energy of a particle drops below zero for certain values of μ and B. This indicates an instability in the normal phase. Bose-Einstein condensation will therefore happen when the particles on the lowest Landau level become gapless. This occurs when

$$\mu = \sqrt{m^2 + qB}. \tag{2.57}$$

Hence, the limit $B \to 0$ recovers the condition $\mu = m$ for Bose-Einstein condensation in the case where we only had a chemical potential and not a magnetic field.

Chapter 3

Non-Abelian models

In this chapter we calculate the mass spectrum and dispersion relations in the linear and nonlinear $SO(3)$ sigma models, where both non-Abelian models exhibit SSB. For the linear $SO(3)$ sigma model, we verify that the number of Goldstone bosons resulting from SSB is in accordance with Goldstone's theorem. Some of the calculations in this chapter follow a similar procedure as in [27].

3.1 Linear $SO(3)$ sigma model

Consider a real, three-component vector field $\vec{\phi}$ with a Lagrangian

$$\mathscr{L} = \frac{1}{2}(\partial_\mu \vec{\phi})^2 + \frac{1}{2}m^2\vec{\phi}^2 - \frac{\lambda}{4}(\vec{\phi}^2)^2, \tag{3.1}$$

having an $SO(3)$ symmetry. We want to show that the $SO(3)$ symmetry gets spontaneously broken resulting in Goldstone bosons. This happens if the field acquires a nonzero vev. The vev is as previously determined by calculating

$$\frac{\partial \mathscr{U}}{\partial|\vec{\phi}|} = (-m^2 + \lambda|\vec{\phi}|^2)\,|\vec{\phi}| = 0, \tag{3.2}$$

giving the local maximum $|\vec{\phi}| = 0$ and the minimum

$$\vec{\phi}_0^{\,2} = \phi_{01}^2 + \phi_{02}^2 + \phi_{03}^2 = \frac{m^2}{\lambda} \equiv v^2. \tag{3.3}$$

This corresponds to the equation of a three-dimensional sphere with radius v^2. The vev of the field is therefore any point on this sphere, implying that we have infinitely many vevs. We can expand the field around its vev by choosing $\vec{\phi}_0 = (\xi_1, \xi_2, v + \xi_3)$, where ξ_i are real fields. The Lagrangian is then written as

$$\begin{aligned}\mathscr{L} = \frac{1}{2}(\partial_\mu \vec{\xi}\,)^2 &- \frac{1}{2}m^2\left[v^2 + 2v\xi_3 + (\xi_1^2 + \xi_2^2) + \xi_3^2\right] \\ &- \frac{\lambda}{4}\left[v^4 + 4v^3\xi_3 + 2v^2(\xi_1^2 + \xi_2^2) + 6v^2\xi_3^2 + 4v(\xi_1^2 + \xi_2^2)\xi_3 + 4v\xi_3^3\right. \\ &\qquad \left. + 2\xi_1^2\xi_2^2 + (\xi_1^2 + \xi_2^2)\xi_3^2 + (\xi_1^4 + \xi_2^4) + \xi_3^4\right].\end{aligned} \tag{3.4}$$

Consequently, the $SO(3)$ symmetry of the Lagrangian is spontaneously broken to an $SO(2)$ symmetry since ξ_1 and ξ_2 are the only fields treated equally. Now that the Lagrangian is diagonal, we can calculate the masses of the three modes by taking the second derivative of the potential as in eq. (2.8). The classical potential is given by the static part of the Lagrangian resulting in the masses,

$$m_{\xi_1} = m_{\xi_2} = 0, \tag{3.5}$$

$$m_{\xi_3} = \sqrt{2}m, \tag{3.6}$$

where we have used that $v^2 = m^2/\lambda$ defined in eq. (3.3). We will argue in the next section that the two massless modes are a result of the SSB from $SO(3)$ to $SO(2)$.

3.1.1 Massless modes from Goldstone's theorem

The number of massless modes can also be derived from Goldstone's theorem. The theorem states that for each broken generator of a continuous symmetry there exists a massless mode called a Goldstone boson. This is valid for a Lorentz invariant theory [29]. We can therefore check if $SO(3)$ has two broken generators corresponding to the two massless modes found in eq. (3.5). An $SO(3)$ transformation of the ground state is given by

$$\vec{\phi}_0 \to \vec{\phi}_0' = e^{i\alpha^a T_a}\vec{\phi}_0 = \left[\mathbb{1} + i\alpha^a T_a + \mathcal{O}(\alpha^2)\right]\vec{\phi}_0, \tag{3.7}$$

where α^a are the Euler angles and T_a are the three generators of $SO(3)$. Hence, the ground state is invariant under an infinitesimal transformation if

$$T_i\vec{\phi}_0 = 0. \tag{3.8}$$

The generators that does not satisfy this equation are therefore broken. Applying each generator to our ground state field gives

$$T_1\vec{\phi}_0 = i\begin{pmatrix}0&0&0\\0&0&-1\\0&1&0\end{pmatrix}\begin{pmatrix}0\\0\\v\end{pmatrix} = -i\begin{pmatrix}0\\v\\0\end{pmatrix}, \tag{3.9}$$

$$T_2\vec{\phi}_0 = i\begin{pmatrix}0&0&1\\0&0&0\\-1&0&0\end{pmatrix}\begin{pmatrix}0\\0\\v\end{pmatrix} = i\begin{pmatrix}v\\0\\0\end{pmatrix}, \tag{3.10}$$

$$T_3\vec{\phi}_0 = i\begin{pmatrix}0&-1&0\\1&0&0\\0&0&0\end{pmatrix}\begin{pmatrix}0\\0\\v\end{pmatrix} = \begin{pmatrix}0\\0\\0\end{pmatrix}. \tag{3.11}$$

The generators T_1 and T_2 do not satisfy eq. (3.8) and are therefore broken. Two broken generators lead to two massless Goldstone bosons as expected.

This can also be seen in an alternative way. Consider a Lagrangian with a symmetry G and a ground state invariant under a subgroup H of G. In that case, a formulation of Goldstone's theorem in a Lorentz invariant theory is: The number of Goldstone bosons equals $\dim(G) - \dim(H)$, or equivalently the dimension $\dim(G/H)$ of the left coset space. For our Lagrangian in eq. (3.1), we have that $G = SO(3)$ and $H = SO(2)$. The number of Goldstone bosons is therefore equal to $\dim(SO(3)) - \dim(SO(2)) = 3 - 1 = 2$.

3.2 Nonlinear $SO(3)$ sigma model with a chemical potential

The nonlinear sigma model contains only the massless modes in the linear sigma model considered in section 3.1. It can be defined by the Lagrangian

$$\mathscr{L}_0 = \frac{1}{2}(\partial_\mu \vec{\chi})^2, \tag{3.12}$$

where $\vec{\chi}$ is a three-component vector field satisfying

$$\chi_1^2 + \chi_2^2 + \chi_3^2 = v^2. \tag{3.13}$$

Adding a chemical potential for one of the $SO(3)$ generators promotes the derivative to a covariant derivative, $D_\mu \vec{\chi} \equiv (\partial_\mu - i\delta_{\mu 0}\mu T_3)\vec{\chi}$, where T_3 is a generator of $SO(3)$. This results in the Lagrangian

$$\mathscr{L}_\mu = \frac{1}{2}(D_\mu \vec{\chi})^2 = \frac{1}{2}(D_0 \vec{\chi})^2 - \frac{1}{2}(\partial_i \vec{\chi})^2. \tag{3.14}$$

The temporal part takes the form

$$D_0\vec{\chi} = (\partial_0 - i\mu T_3)\vec{\chi} = \begin{pmatrix} \partial_0 & -\mu & 0 \\ \mu & \partial_0 & 0 \\ 0 & 0 & \partial_0 \end{pmatrix} \begin{pmatrix} \chi_1 \\ \chi_2 \\ \chi_3 \end{pmatrix} = \begin{pmatrix} \partial_0\chi_1 - \mu\chi_2 \\ \partial_0\chi_2 + \mu\chi_1 \\ \partial_0\chi_3 \end{pmatrix}, \tag{3.15}$$

giving

$$\begin{aligned} \frac{1}{2}(D_0\vec{\chi})^2 &= \frac{1}{2}\begin{pmatrix} \partial_0\chi_1 - \mu\chi_2 & \partial_0\chi_2 + \mu\chi_1 & \partial_0\chi_3 \end{pmatrix} \begin{pmatrix} \partial_0\chi_1 - \mu\chi_2 \\ \partial_0\chi_2 + \mu\chi_1 \\ \partial_0\chi_3 \end{pmatrix} \\ &= \frac{1}{2}(\partial_0\chi_1)^2 + \frac{1}{2}(\partial_0\chi_2)^2 + \frac{1}{2}(\partial_0\chi_3)^2 \\ &\quad + \frac{\mu^2}{2}(\chi_1^2 + \chi_2^2) + \mu(\chi_1\partial_0\chi_2 - \chi_2\partial_0\chi_1). \end{aligned} \tag{3.16}$$

Next, we plug this into eq. (3.14), resulting in

$$\begin{aligned} \mathscr{L}_\mu &= \frac{1}{2}(\partial_\mu\chi_1)^2 + \frac{1}{2}(\partial_\mu\chi_2)^2 + \frac{1}{2}(\partial_\mu\chi_3)^2 \\ &\quad + \frac{\mu^2}{2}(\chi_1^2 + \chi_2^2) + \mu(\chi_1\partial_0\chi_2 - \chi_2\partial_0\chi_1). \end{aligned} \tag{3.17}$$

Finally, we can eliminate χ_1 by exploiting the constraint $\chi_1^2 = v^2 - \chi_2^2 - \chi_3^2$. A Taylor expansion in the fields yields

$$\mathscr{L}_\mu = \frac{1}{2}(\partial_\mu\chi_2)^2 + \frac{1}{2}(\partial_\mu\chi_3)^2 - \frac{\mu^2}{2}\chi_3^2 + \mu v\partial_0\chi_2 + \frac{\mu^2 v^2}{2} + \mathcal{O}(\chi^3), \tag{3.18}$$

where all terms of $\mathcal{O}(\chi^3)$ are non-static. In order to determine the vevs it is sufficient to look at the classical potential. This is because the quadratic part of the

Lagrangian is formally Lorentz invariant, although we have a system with a chemical potential. The classical potential is given by

$$\mathscr{U} = \frac{\mu^2}{2}\chi_3^2 - \frac{\mu^2 v^2}{2}, \tag{3.19}$$

which is minimal for the vev $\chi_3 = 0$. From eq. (3.13), we can conclude that the vev of χ_1 and χ_2 must fulfil $\chi_1^2 + \chi_2^2 = v^2$. This is analogous to the spins in an antiferromagnet exposed to an external magnetic field. Before turning on the magnetic field there is no preferred direction of the spin, but turning it on results in spins aligning perpendicular to the field. The chemical potential in our theory is therefore behaving as an external magnetic field that orients the ground state.

The dispersion relations are as before derived from the bilinear part of the Lagrangian,

$$\begin{aligned}\mathscr{L}_\mu^{(2)} &= \frac{1}{2}(\partial_\mu \chi_2)^2 + \frac{1}{2}(\partial_\mu \chi_3)^2 - \frac{\mu^2}{2}\chi_3^2 \\ &= \frac{1}{2}\begin{pmatrix}\chi_2 & \chi_3\end{pmatrix}\begin{pmatrix}-\partial_\mu\partial^\mu & 0 \\ 0 & -\partial_\mu\partial^\mu - \mu^2\end{pmatrix}\begin{pmatrix}\chi_2 \\ \chi_3\end{pmatrix},\end{aligned} \tag{3.20}$$

where we have performed a partial integration of the two first terms going to the second line. Going to Fourier space yields the inverse propagator

$$D^{-1} = \begin{pmatrix}E^2 - \mathbf{p}^2 & 0 \\ 0 & E^2 - \mathbf{p}^2 - \mu^2\end{pmatrix}. \tag{3.21}$$

The zero modes of D^{-1} are extracted by requiring that

$$\mathrm{Det}(D^{-1}) = 0 = (E^2 - \mathbf{p}^2)(E^2 - \mathbf{p}^2 - \mu^2), \tag{3.22}$$

resulting in the dispersion relations

$$E_{\chi_2}(\mathbf{p}) = |\mathbf{p}|, \tag{3.23}$$

$$E_{\chi_3}(\mathbf{p}) = \sqrt{\mathbf{p}^2 + \mu^2}. \tag{3.24}$$

The mass spectrum is obtained when $\mathbf{p} \to 0$, giving

$$m_{\chi_2} = 0, \tag{3.25}$$

$$m_{\chi_3} = \mu. \tag{3.26}$$

We can see that one of the two massless modes in the previously considered linear $SO(3)$ sigma model has acquired a mass due to the introduction of a chemical potential. The massive mode is called a "massive Goldstone boson". It turns out that this result is valid not only at tree level, but also when all quantum corrections are included [30].

Part II

Anomalies in chiral perturbation theory

Chapter 4

Introduction to QCD and ChPT

This chapter gives a brief introduction to QCD and ChPT. The form of the ChPT Lagrangian is established and used to calculate the mass spectrum of two-flavor QCD in the low-energy regime. The necessary background material for QCD and ChPT has been found in [31].

4.1 QCD

QCD is the theory of strong interactions. These are interactions between quarks and gluons. The theory can be described by the QCD Lagrangian

$$\mathscr{L}_{\mathrm{QCD}} = \sum_{f=\substack{u,d,s,\\c,b,t}} \bar{\psi}_f \left(i\not{D} - m_f\right) \psi_f - \frac{1}{4}\mathcal{G}_{\mu\nu,a}\mathcal{G}_a^{\mu\nu}, \tag{4.1}$$

where f denotes the different quark flavors and the quark field ψ_f is a color triplet

$$\psi_f = \begin{pmatrix} \psi_{f,r} \\ \psi_{f,g} \\ \psi_{f,b} \end{pmatrix}, \tag{4.2}$$

where r, g and b stands for "red", "green" and "blue". Furthermore, the color field tensor is defined by

$$\mathcal{G}_{\mu\nu,a} = \partial_\mu \mathcal{A}_{\nu,a} - \partial_\nu A_{\mu,a} + g f_{abc} \mathcal{A}_{\mu,b} \mathcal{A}_{\nu,c}, \tag{4.3}$$

with f_{abc} being $SU(3)$ structure constants and $\mathcal{A}_{\mu,a}$ are eight independent gauge fields. Finally, the covariant derivative is given by

$$D_\mu \psi_f = \partial_\mu \psi_f - ig\frac{\lambda_a}{2}\mathcal{A}_{\mu,a}\psi_f, \tag{4.4}$$

where λ_a are the eight $SU(3)$ Gell-Mann matrices. It is common to divide the six quark flavors into the three heavy flavors c, b, t and the three light flavors u, d, s having masses

$$\begin{aligned} m_u &= 0.005\,\mathrm{GeV}, & m_c &= (1.15 - 1.35)\,\mathrm{GeV}, \\ m_d &= 0.009\,\mathrm{GeV}, & m_b &= (4.0 - 4.4)\,\mathrm{GeV}, \\ m_s &= 0.175\,\mathrm{GeV}, & m_t &= 174\,\mathrm{GeV}. \end{aligned} \tag{4.5}$$

The masses of the lightest hadrons, that are not Goldstone bosons originating from spontaneous symmetry breaking, are associated with a scale of 1 GeV. The lightest nucleon has for instance a mass of 938 MeV. Since we are interested in a low-energy description of QCD, we only need to consider the quark flavors u, d and s that have masses well below the scale of 1 GeV. As the mass of the strange quark is considerably higher than the mass of the other two light quarks, we will restrict our calculations to only include the u and d quarks.

4.2 QCD in the chiral limit

We will start out by reviewing the symmetries of the QCD Lagrangian in the so-called chiral limit where the quark masses m_f vanish. The Lagrangian in eq. (4.1) will for two-flavor QCD in the chiral limit reduce to

$$\mathscr{L}^0_{\text{QCD}} = \sum_{f=u,d} \left(\bar{\psi}_{L,f} i \not{D} \psi_{L,f} + \bar{\psi}_{R,f} i \not{D} \psi_{R,f} \right) - \frac{1}{4} \mathcal{G}_{\mu\nu,a} \mathcal{G}^{\mu\nu}_a, \tag{4.6}$$

where we have decomposed the Dirac field ψ_f into its left and right chiral components, $\psi_{L,f}$ and $\psi_{R,f}$. This Lagrangian has a $U(2)_L \times U(2)_R \cong SU(2)_L \times SU(2)_R \times U(1)_V \times U(1)_A$ symmetry since the covariant derivative is flavor independent.[1] In lattice QCD it has been shown that the QCD vacuum possesses a nonzero quark condensate. The quark condensate is a vacuum expectation value of QCD, having the form

$$\Sigma_{ji} \equiv \left\langle \bar{\psi}_{iR} \psi_{jL} \right\rangle \neq 0. \tag{4.7}$$

It serves as an order parameter of transitions between phases of quark matter.[2] The nonzero quark condensate tells us that the vacuum is filled with quark-anti-quark pairs. Furthermore, the Vafa-Witten theorem states that vector-like global symmetries in vector-like gauge theories such as QCD cannot be spontaneously broken if the so-called θ-angle is zero [33]. Assuming that the θ-angle is zero [34] means that the vector-like global symmetry $SU(2)_V$ of QCD is not spontaneously broken. This implies that the quark condensate Σ is invariant under an $SU(2)_V$ transformation. It will therefore commute with an irreducible representation of $SU(2)_V$. By Schur's lemma, any matrix that commutes with an irreducible representation of a group must be proportional to the identity in that group [35]. As a result, the quark condensate Σ is proportional to the 2×2 identity matrix,

$$\Sigma = \left\langle \bar{\psi} \psi \right\rangle = \lambda \mathbb{1}, \tag{4.8}$$

where λ is a constant with dimension mass cubed.

We can now turn our attention to an $SU(2)_L \times SU(2)_R$ transformation, which amounts to a transformation of the quark fields given by

$$\psi_{iL} \to L_{ij} \psi_{jL} \quad \text{and} \quad \psi_{jR} \to R_{ij} \psi_{iR}, \tag{4.9}$$

[1] The QCD Lagrangian also has a local $SU(3)_{\text{color}}$ symmetry.

[2] The nonzero chiral condensate is analogous to the condensation of Cooper pairs in superconductors [32].

where L and R are matrices belonging to $SU(2)_L$ and $SU(2)_R$, respectively. As a consequence, the quark condensate transforms as

$$\Sigma \to L\Sigma R^\dagger. \tag{4.10}$$

This implies that the ground state of QCD does not share the $SU(2)_L \times SU(2)_R$ symmetry of the QCD Lagrangian in eq. (4.6).[3] The result is that the QCD Lagrangian in eq. (4.6) has an $SU(2)_L \times SU(2)_R$ symmetry, while the ground state only has an $SU(2)_V$ symmetry. Having a ground state that does not share the symmetry of the Lagrangian means that we have SSB. An SSB from $SU(2)_L \times SU(2)_R$ to $SU(2)_V$ symmetry, will by Goldstone's theorem result in three Goldstone bosons. The Goldstone bosons can be identified with the three pseudoscalar pions.[4]

4.3 ChPT

Due to the nonzero quark condensate, the degrees of freedom at low energies are not quarks, but quark-anti-quark pairs known as pions. Consequently, we want a QCD Lagrangian that is expressed in terms of the pion degrees of freedoms. This cannot be derived directly from QCD, and we must therefore make use of an effective field theory (EFT). An EFT is an approximation to the underlying theory up to some given energy scale. It is written in terms of the relevant degrees of freedom. Chiral perturbation theory (ChPT) is an example of a low-energy EFT that provides us with an applicable Lagrangian. The starting point for the construction of the ChPT Lagrangian is to identify the dynamical variables that will represent the pion degrees of freedom. The pions are Goldstone bosons resulting from SSB of the $SU(2)_L \times SU(2)_R$ symmetry down to an $SU(2)_V$ symmetry. Hence, they must live on the coset space $SU(2)_L \times SU(2)_R / SU(2)_V \cong SU(2)_V$. This space is the Goldstone manifold. The pion degrees of freedom can therefore be parameterized by the matrix $\Sigma \in SU(2)_V$. There are several possible parameterizations, but two common ones are

$$\begin{aligned} &\text{i)} \qquad \Sigma = \exp\left(\frac{i}{f_\pi}\boldsymbol{\tau}\cdot\boldsymbol{\pi}\right), \\ &\text{ii)} \qquad \Sigma = \frac{1}{f_\pi}(\sigma \mathbb{1} + i\boldsymbol{\tau}\cdot\boldsymbol{\pi}), \end{aligned} \tag{4.11}$$

where f_π is the pion decay constant, $\boldsymbol{\tau} = (\tau_1, \tau_2, \tau_3)$ are the three Pauli matrices and $\boldsymbol{\pi} = (\pi_1, \pi_2, \pi_3)$ are the three pion degrees of freedom. The fields σ and $\boldsymbol{\pi}$ must satisfy $\sigma^2 + \boldsymbol{\pi}^2 = f_\pi^2$ in the latter case.[5]

In a perturbation theory, the standard expansion is in powers of the coupling constant. However, this does not work at low energies since a large coupling constant hinders convergence. Instead, ChPT is a derivative expansion in powers of p/Λ, where p is a momentum or mass that must be small compared to Λ. Λ is the energy scale of QCD and can be set to $\Lambda \approx 4\pi f_\pi \approx 1.2$ GeV. ChPT will therefore produce reliable results if and only if $p \ll 4\pi f_\pi$.

[3]The ground state is neither invariant under the $U(1)_A$ symmetry. However, this symmetry is also explicitly broken by an anomaly implying that it does not result in any Goldstone bosons [21].

[4]SSB in three-flavor QCD gives rise to the pseudoscalar octet.

[5]This is a nonlinear constraint and defines the nonlinear sigma model.

The next step in the construction of the ChPT Lagrangian is to realize that ChPT as an EFT must include all terms that respect the symmetries of the underlying theory. First of all, we must require that the ChPT Lagrangian in the chiral limit must be invariant under an $SU(2)_L \times SU(2)_R \times U(1)_V$ transformation, where $\Sigma \to L\Sigma R^\dagger$. One obvious term, $\mathrm{Tr}(\Sigma\Sigma^\dagger) = 2$, is a constant and so does not affect the dynamics. The trace here is over the two flavor indices. In the chiral limit, the only term up to second order in $p/4\pi f_\pi$ that respects the symmetries is

$$\mathscr{L}_2 = \frac{f_\pi^2}{4}\mathrm{Tr}\left[\partial_\mu\Sigma^\dagger\partial^\mu\Sigma\right], \tag{4.12}$$

where each $\partial_\mu\Sigma$ yields a factor of momentum. The Lagrangian is of second order in the momentum implying that the results obtained from this Lagrangian will correspond to tree level results. Corrections from loops can be calculated by including higher order terms in the Lagrangian. We will drop the index 2 of the Lagrangian and consider only tree level results in the rest of this project.

4.3.1 Turning on masses in ChPT

As mentioned, the effective Lagrangian must satisfy the same symmetries as the original theory. However, it must also break any broken symmetries in the same way. We can now turn on the small masses of the u and d quark. Hence, the two-flavor QCD Lagrangian is from eq. (4.1) given as

$$\mathscr{L}_{\mathrm{QCD}} = \sum_{f=u,d}\left(\bar{\psi}_{L,f}i\not{D}\psi_{L,f} + \bar{\psi}_{R,f}i\not{D}\psi_{R,f} - \bar{\psi}_{L,f}m_f\psi_{R,f} - \bar{\psi}_{R,f}m_f\psi_{L,f}\right) - \frac{1}{4}\mathcal{G}_{\mu\nu,a}\mathcal{G}_a^{\mu\nu}, \tag{4.13}$$

where ψ_f is written in terms of the left and right chiral components. This explicitly breaks the $SU(2)_L \times SU(2)_R$ symmetry. If we set $m_u = m_d$, the symmetry is broken to an $SU(2)_V$ symmetry. Setting the quark masses equal is known as the isospin limit. The explicit symmetry breaking can be included in the ChPT Lagrangian as a perturbation since the quark masses are small. We can do this by introducing the quark mass matrix M and demand that under an $SU(2)_L \times SU(2)_R$ it must transform as

$$M \to RML^\dagger. \tag{4.14}$$

The resulting term that can be included in the ChPT Lagrangian is

$$\frac{f_\pi^2 B}{4}\mathrm{Tr}\left(M\Sigma^\dagger + \Sigma M^\dagger\right), \tag{4.15}$$

where B is a parameter that can be related to the quark condensate. This term correctly breaks the $SU(2)_L \times SU(2)_R$ symmetry to an $SU(2)_V$ symmetry when $m_u = m_d$. The term can, in the isopsin limit, be rewritten leading to a ChPT Lagrangian in the form

$$\mathscr{L} = \frac{f_\pi^2}{4}\left[\mathrm{Tr}(\partial_\mu\Sigma^\dagger\partial^\mu\Sigma) + 2m_\pi^2\mathrm{ReTr}\Sigma\right], \tag{4.16}$$

where $m_\pi \approx 140$ MeV is the bare pion mass. The dynamical variable of ChPT is the 2×2 unitary matrix field Σ. The matrix field is an element of $SU(2)$, implying that

it has three degrees of freedom. These are denoted by the pion triplet $\boldsymbol{\pi}$. The ChPT Lagrangian is as needed Lorentz invariant and invariant under charge conjugation and parity. Additionally, it breaks the $SU(2)_L \times SU(2)_R$ symmetry in the same way as the QCD Lagrangian.

4.4 Mass spectrum of ChPT

The ChPT Lagrangian in eq. (4.16) is Lorentz invariant implying that we can determine the mass spectrum from the classical potential of the theory. This is given by the static second term of the Lagrangian. By using parameterization i) in eq. (4.11), we can expand to second order in the fields $\boldsymbol{\pi} = (\pi_1, \pi_2, \pi_3)$,

$$\Sigma = \exp(\frac{i}{f_\pi}\boldsymbol{\tau}\cdot\boldsymbol{\pi}) = 1 + \frac{i}{f_\pi}(\boldsymbol{\tau}\cdot\boldsymbol{\pi}) - \frac{1}{2f_\pi^2}(\boldsymbol{\tau}\cdot\boldsymbol{\pi})^2 + \mathcal{O}(\boldsymbol{\pi}^3), \tag{4.17}$$

where higher-order terms govern the interaction between the pions. The dot product of $\boldsymbol{\tau}$ and $\boldsymbol{\pi}$ in matrix form reads

$$\boldsymbol{\tau}\cdot\boldsymbol{\pi} = \begin{pmatrix} \pi_3 & \pi_1 - i\pi_2 \\ \pi_1 + i\pi_2 & -\pi_3 \end{pmatrix}, \tag{4.18}$$

resulting in

$$(\boldsymbol{\tau}\cdot\boldsymbol{\pi})^2 = \begin{pmatrix} \pi_1^2+\pi_2^2+\pi_3^2 & 0 \\ 0 & \pi_1^2+\pi_2^2+\pi_3^2 \end{pmatrix}. \tag{4.19}$$

Thus, we can extract the potential from the Lagrangian as

$$\mathscr{U} = -\mathscr{L}^{\text{static}} = \frac{1}{2}m_\pi^2(\pi_1^2+\pi_2^2+\pi_3^2) + \mathcal{O}(\boldsymbol{\pi}^3). \tag{4.20}$$

Having this at hand, we can calculate the masses of the three pion fields by using eq. (2.8) with three fields instead of two. We then arrive at

$$m_{\pi_1} = m_{\pi_2} = m_{\pi_3} = m_\pi. \tag{4.21}$$

Two-flavor ChPT is therefore a theory describing the behavior of three pion fields with equal mass.

For later purposes, we want to determine which of the pion fields π_1, π_2 and π_3 that corresponds to the physical neutral pion π^0. This is done by performing a $U(1)_Q$ transformation of the pion fields represented by Σ. A $U(1)_Q$ transformation of Σ reads $\Sigma \to L\Sigma R^\dagger$, where

$$L = R = e^{i\alpha Q}. \tag{4.22}$$

Here we have α as an arbitrary phase, while Q is the charges of the u and d quarks given on matrix form as

$$Q = \begin{pmatrix} 2/3 & 0 \\ 0 & -1/3 \end{pmatrix} = \frac{1}{6}\mathbb{1} + \frac{\tau_3}{2}. \tag{4.23}$$

Hence, Σ transforms as

$$\Sigma \to e^{i\alpha\left(\frac{1}{6}\mathbb{1}+\frac{\tau_3}{2}\right)}\Sigma e^{-i\alpha\left(\frac{1}{6}\mathbb{1}+\frac{\tau_3}{2}\right)} = e^{i\frac{\alpha}{2}\tau_3}e^{\frac{i}{f_\pi}(\tau_1\pi_1+\tau_2\pi_2+\tau_3\pi_3)}e^{-i\frac{\alpha}{2}\tau_3}, \tag{4.24}$$

where τ_3 does not commute with τ_1 and τ_2. Hence, the third pion field π_3 is the only field not affected by a $U(1)_Q$ transformation. The neutral pion π^0 will therefore correspond to π_3 and they will from now on be treated as the same field.

Chapter 5

ChPT with isospin chemical potential

In section 4.2, we saw that the QCD vacuum is invariant under $SU(2)_V$ transformations. This means that one of the generators of $SU(2)_V$ can be used as a quantum number to label particle states. The quantum numbers is known as isospin. The third component of isospin I_3 is given by the generator $T_3 = \tau_3/2$ of $SU(2)_V$. Isospin of a particle is related to its electric charge Q and baryon number B through the Gell-Mann-Nishijima formula, $Q = I_3 + B/2$. Since I_3 is conserved in strong interactions, we can associate an isospin chemical potential μ_I to it.

In this chapter we will see how a nonzero isospin chemical potential affects the ground state of QCD. We find that the ground state has a normal phase corresponding to the QCD vacuum and a phase with charged pion condensation. Moreover, we obtain the isospin density. Finally, the mass spectrum and dispersion relations are derived in both phases. The calculations in section 5.1 and 5.3 follow a procedure similar to the ones in [24, 36].

5.1 Ground state

Adding a chemical potential for isospin μ_I to the ChPT Lagrangian is done by promoting the ordinary derivative of Σ to a covariant derivative, defined by

$$\begin{aligned} D_\mu \Sigma &= \partial_\mu \Sigma - i\delta_{\mu 0}\mu_I \left[T_3, \Sigma\right], \\ D_\mu \Sigma^\dagger &= \partial_\mu \Sigma^\dagger + i\delta_{\mu 0}\mu_I \left[\Sigma^\dagger, T_3\right], \end{aligned} \tag{5.1}$$

where $T_3 = \tau_3/2$ is the third generator of $SU(2)_V$. The ChPT Lagrangian in eq. (4.16) with isospin chemical potential is then

$$\begin{aligned} \mathscr{L} &= \frac{f_\pi^2}{4}\left[\mathrm{Tr}(D_\mu \Sigma^\dagger D^\mu \Sigma) + 2m_\pi^2 \mathrm{ReTr}\Sigma\right] \\ &= \frac{f_\pi^2}{4}\mathrm{Tr}\left\{\partial_\mu \Sigma^\dagger \partial^\mu \Sigma - i\mu_I\left[\partial_0 \Sigma^\dagger [T_3, \Sigma] - [\Sigma^\dagger, T_3]\partial^0 \Sigma\right] + \mu_I^2 [\Sigma^\dagger, T_3][T_3, \Sigma]\right\} \\ &\quad + \frac{f_\pi^2 m_\pi^2}{2}\mathrm{ReTr}\Sigma. \end{aligned} \tag{5.2}$$

By assuming that the ground state is independent of time and space, we can obtain the ground state by minimizing the static Hamiltonian. The static Hamiltonian is

given by the Lagrangian as

$$\begin{aligned}\mathscr{H}^{\text{static}} &= -\frac{f_\pi^2\mu_I^2}{4}\text{Tr}\left\{[\Sigma^\dagger, T_3][T_3, \Sigma]\right\} - \frac{f_\pi^2 m_\pi^2}{2}\text{ReTr}\Sigma \\ &= \frac{f_\pi^2\mu_I^2}{8}\text{Tr}(\Sigma^\dagger\tau_3\Sigma\tau_3 - \mathbb{1}) - \frac{f_\pi^2 m_\pi^2}{2}\text{ReTr}\Sigma.\end{aligned} \tag{5.3}$$

We progress by noting that the $SU(2)$ matrix field can in general be written as

$$\Sigma = \text{e}^{i\alpha\hat{\phi}_i\tau_i} = \cos\alpha + i\hat{\phi}_i\tau_i\sin\alpha, \tag{5.4}$$

where α is an angle, τ_i are the three Pauli matrices and the three parameters $\hat{\phi}_i$ satisfy $\hat{\phi}_i\hat{\phi}_i = 1$, guaranteeing that $\Sigma\Sigma^\dagger = \mathbb{1}$. Thus, the static Hamiltonian takes the form

$$\begin{aligned}\mathscr{H}^{\text{static}} &= \frac{f_\pi^2\mu_I^2}{8}\text{Tr}\left[\left(\cos\alpha - i\hat{\phi}_i\tau_i\sin\alpha\right)\tau_3\left(\cos\alpha + i\hat{\phi}_i\tau_i\sin\alpha\right)\tau_3 - \mathbb{1}\right] \\ &\quad - \frac{f_\pi^2 m_\pi^2}{2}\text{ReTr}\left(\cos\alpha + i\hat{\phi}_i\tau_i\sin\alpha\right) \\ &= -\frac{1}{2}f_\pi^2\mu_I^2\sin^2\alpha(\hat{\phi_1}^2 + \hat{\phi_2}^2) - f_\pi^2 m_\pi^2\cos\alpha.\end{aligned} \tag{5.5}$$

We note that the ground state is determined by a competition between the two terms in the static Hamiltonian. The last term favors the vacuum with $\alpha = 0$, while the first term favors rotation of the vacuum. In a case where $\alpha \neq 0$, the energy of the ground state will be minimized for the vevs $\hat{\phi}_{10}^2 + \hat{\phi}_{20}^2 = 1$, which in turn yields the vev $\hat{\phi}_{30} = 0$. This reduces the static Hamiltonian to

$$\mathscr{H}^{\text{static}} = -\frac{f_\pi^2\mu_I^2}{2}\sin^2\alpha - f_\pi^2 m_\pi^2\cos\alpha. \tag{5.6}$$

The ground state energy is therefore minimal when

$$\alpha = 0 \quad \text{for } \mu_I \leqslant m_\pi \tag{5.7}$$

or

$$\cos\alpha = \frac{m_\pi^2}{\mu_I^2} \quad \text{for } \mu_I \geqslant m_\pi. \tag{5.8}$$

The case $\mu_I \leqslant m_\pi$ corresponds to the QCD vacuum where the matrix field $\Sigma = \mathbb{1}$. Because $\alpha = 0$, the first term in eq. (5.5) will vanish. Hence, it is not necessary to have $\hat{\phi}_1^2 + \hat{\phi}_2^2 = 1$ and $\hat{\phi}_3 = 0$ in the ground state. In the case of $\mu_I \geqslant m_\pi$, our conditions $\hat{\phi}_1^2 + \hat{\phi}_2^2 = 1$ and $\hat{\phi}_3 = 0$ apply. From eq. (4.24), we have that $\hat{\phi}_1$ and $\hat{\phi}_2$ will be charged. Since $\mu_I \geqslant m_\pi$ and $\hat{\phi}_1$ and $\hat{\phi}_2$ acquire a nonzero vev it means that we have a BEC of charged pions. The onset of the condensation is at $\mu_I = m_\pi$ and the rotation of the QCD vacuum increases when μ_I increases as seen from eq. (5.6).

5.2 Isospin density

The isospin density n_I in the condensed phase is given by

$$n_I = -\frac{\partial}{\partial\mu_I}(\mathscr{H}_{\text{norm}} - \mu_I n_I) = -\frac{\partial\mathscr{H}}{\partial\mu_I} = f_\pi^2\mu_I\sin^2\alpha = f_\pi^2\mu_I\left(1 - \frac{m_\pi^4}{\mu_I^4}\right), \tag{5.9}$$

where $\mathscr{H}_{\text{norm}}$ is the Hamiltonian without an isospin chemical potential and α is given by eq. (5.8).

5.3 Excitation spectrum

The excitation spectrum of $\hat{\phi}_1$, $\hat{\phi}_2$ and $\hat{\phi}_3$ are obtained by expanding these fields into fluctuations around the ground state. In section 5.1, we found that the ground state must satisfy $\hat{\phi}_{10}^2 + \hat{\phi}_{20}^2 = 1$ and $\hat{\phi}_{30} = 0$ in the pion condensed phase. We can choose $\hat{\phi}_{10} = 0$ and $\phi_{20} = 1$ without loss of generality. Thus, the ground state will by eq. (5.4) take the form

$$\begin{aligned}\Sigma_0 = e^{i\alpha\hat{\phi}_{i0}\tau_i} = \cos\alpha + i\tau_2 \sin\alpha = \begin{pmatrix} \cos\alpha & \sin\alpha \\ -\sin\alpha & \cos\alpha \end{pmatrix} \\ = e^{i\alpha\tau_2} = e^{i\alpha\frac{\tau_2}{2}}\mathbb{1}e^{i\alpha\frac{\tau_2}{2}} = U_\alpha \mathbb{1} U_\alpha,\end{aligned} \tag{5.10}$$

where $U_\alpha \equiv e^{i\alpha\frac{\tau_2}{2}}$. Hence, the ground state Σ_0 corresponds to a chiral rotation of the QCD vacuum $\Sigma_0 = \mathbb{1}$ by the angle α. In the following, we want to parameterize the fluctuations around the ground state by using parameterization i) in eq. (4.11). This is a parameterization of the fluctuations around the QCD vacuum with $\alpha = 0$. We must therefore rotate the fluctuations such that they fluctuate around the rotated vacuum. The small fluctuations around the vacuum are called Goldstone bosons. Because of the chiral symmetry breaking from $SU(2)_L \times SU(2)_R$ to $SU(2)_V$, the Goldstone manifold, on which the Goldstone bosons live, is $SU(2)_L \times SU(2)_R / SU(2)_V$. This manifold has dimension three, giving the fluctuations three degrees of freedom. Hence, the rotated fluctuations with three degrees of freedom $\boldsymbol{\pi} = (\pi_1, \pi_2, \pi_3)$, is by parameterization i) in eq. (4.11) given as

$$\Sigma = U_\alpha e^{\frac{i}{f_\pi}\boldsymbol{\tau}\cdot\boldsymbol{\pi}} U_\alpha. \tag{5.11}$$

The dispersion relations are obtained from the bilinear part of the Lagrangian. From eqs. (5.2) and (5.3) we have that

$$\begin{aligned}\mathscr{L} = \frac{f_\pi^2}{4}\mathrm{Tr}\Big[\partial_\mu\Sigma^\dagger\partial^\mu\Sigma + i\frac{\mu_I}{2}\tau_3\left(\partial_0\Sigma\Sigma^\dagger - \Sigma\partial_0\Sigma^\dagger + \partial_0\Sigma^\dagger\Sigma - \Sigma^\dagger\partial_0\Sigma\right) \\ -\frac{\mu_I^2}{2}\left(\Sigma^\dagger\tau_3\Sigma\tau_3 - \mathbb{1}\right)\Big] + \frac{f_\pi^2 m_\pi^2}{2}\mathrm{ReTr}\Sigma.\end{aligned} \tag{5.12}$$

We will now calculate each term in our Lagrangian separately by inserting the parameterization in eq. (5.11). The first term is rewritten as

$$\begin{aligned}\frac{f_\pi^2}{4}\mathrm{Tr}\left(\partial_\mu\Sigma^\dagger\partial^\mu\Sigma\right) &= \frac{f_\pi^2}{4}\mathrm{Tr}\left[\partial_\mu\left(U^\dagger e^{-\frac{i}{f_\pi}\boldsymbol{\tau}\cdot\boldsymbol{\pi}}U^\dagger\right)\partial^\mu\left(Ue^{\frac{i}{f_\pi}\boldsymbol{\tau}\cdot\boldsymbol{\pi}}U\right)\right] \\ &= \frac{f_\pi^2}{4}\mathrm{Tr}\left(\partial_\mu e^{-\frac{i}{f_\pi}\boldsymbol{\tau}\cdot\boldsymbol{\pi}}\partial^\mu e^{\frac{i}{f_\pi}\boldsymbol{\tau}\cdot\boldsymbol{\pi}}\right) \\ &= \frac{1}{2}\partial_\mu\pi_a\partial^\mu\pi_a + \mathcal{O}(\boldsymbol{\pi}^3),\end{aligned} \tag{5.13}$$

by using the cyclic property of the trace and Taylor expanding in the fields. It is important to keep in mind that we are taking the derivative of matrix exponentials. In order to evaluate the next terms in eq. (5.12) we note that

$$\begin{aligned}\mathrm{Tr}\left(\partial_0\Sigma\Sigma^\dagger - \Sigma\partial_0\Sigma^\dagger\right) &= \mathrm{Tr}\left(-2\Sigma\partial_0\Sigma^\dagger\right) \\ &= \mathrm{Tr}\left[-2\int_0^1 \mathrm{d}u\, e^{\frac{i}{f_\pi}u\boldsymbol{\tau}\cdot\boldsymbol{\pi}}\left(-\frac{i}{f_\pi}\boldsymbol{\tau}\cdot\partial_0\boldsymbol{\pi}\right)e^{-\frac{i}{f_\pi}u\boldsymbol{\tau}\cdot\boldsymbol{\pi}}\right] \\ &= \mathrm{Tr}\left(\frac{2i}{f_\pi}\boldsymbol{\tau}\cdot\partial_0\boldsymbol{\pi} - \frac{1}{f_\pi^2}[\boldsymbol{\tau}\cdot\boldsymbol{\pi}, \boldsymbol{\tau}\cdot\partial_0\boldsymbol{\pi}]\right) + \mathcal{O}(\boldsymbol{\pi}^3)\end{aligned} \tag{5.14}$$

and

$$\begin{aligned}\mathrm{Tr}\left(\partial_0\Sigma^\dagger\Sigma - \Sigma^\dagger\partial_0\Sigma\right) &= \mathrm{Tr}\left(-2\Sigma^\dagger\partial_0\Sigma\right)\\ &= \mathrm{Tr}\left[-2\int_0^1 \mathrm{d}u\, e^{-\frac{i}{f_\pi}u\boldsymbol{\tau}\cdot\boldsymbol{\pi}}\left(\frac{i}{f_\pi}\boldsymbol{\tau}\cdot\partial_0\boldsymbol{\pi}\right)e^{\frac{i}{f_\pi}u\boldsymbol{\tau}\cdot\boldsymbol{\pi}}\right]\\ &= \mathrm{Tr}\left(-\frac{2i}{f_\pi}\boldsymbol{\tau}\cdot\partial_0\boldsymbol{\pi} - \frac{1}{f_\pi^2}[\boldsymbol{\tau}\cdot\boldsymbol{\pi}, \boldsymbol{\tau}\cdot\partial_0\boldsymbol{\pi}]\right) + \mathcal{O}(\boldsymbol{\pi}^3),\end{aligned} \tag{5.15}$$

where we have used that Σ is unitary. The integral originates from the fact that we are taking the derivative of a matrix exponential. Furthermore, we find that

$$U^\dagger\tau_3 U = \cos\alpha\,\tau_3 + \sin\alpha\,\tau_1, \tag{5.16}$$

$$U\tau_3 U^\dagger = \cos\alpha\,\tau_3 - \sin\alpha\,\tau_1. \tag{5.17}$$

The second and third term in eq. (5.12) are therefore

$$\begin{aligned}\frac{if_\pi^2\mu_I}{8}\mathrm{Tr}\left[\tau_3\left(\partial_0\Sigma\Sigma^\dagger - \Sigma\partial_0\Sigma^\dagger\right)\right] &= \frac{if_\pi^2\mu_I}{8}\mathrm{Tr}\left(U^\dagger\tau_3 U e^{\frac{i}{f_\pi}\boldsymbol{\tau}\cdot\boldsymbol{\pi}}\partial_0 e^{-\frac{i}{f_\pi}\boldsymbol{\tau}\cdot\boldsymbol{\pi}}\right)\\ &= \frac{f_\pi\mu_I}{2}\Bigg[\sin\alpha\,\partial_0\pi_1 + \cos\alpha\,\partial_0\pi_3\\ &\qquad -\frac{1}{f_\pi}\sin\alpha\,(\boldsymbol{\pi}\times\partial_0\boldsymbol{\pi})_1 - \frac{1}{f_\pi}\cos\alpha\,(\boldsymbol{\pi}\times\partial_0\boldsymbol{\pi})_3\Bigg] + \mathcal{O}(\boldsymbol{\pi}^3),\end{aligned} \tag{5.18}$$

where we have used eqs. (5.14) and (5.16). The fourth and fifth term in eq. (5.12) are rewritten using eqs. (5.15) and (5.17), resulting in

$$\begin{aligned}\frac{if_\pi^2\mu_I}{8}\mathrm{Tr}\left[\tau_3\left(\partial_0\Sigma^\dagger\Sigma - \Sigma^\dagger\partial_0\Sigma\right)\right] &= \frac{if_\pi^2\mu_I}{8}\mathrm{Tr}\left(U\tau_3 U^\dagger e^{-\frac{i}{f_\pi}\boldsymbol{\tau}\cdot\boldsymbol{\pi}}\partial_0 e^{\frac{i}{f_\pi}\boldsymbol{\tau}\cdot\boldsymbol{\pi}}\right)\\ &= \frac{f_\pi\mu_I}{2}\Bigg[\sin\alpha\,\partial_0\pi_1 - \cos\alpha\,\partial_0\pi_3\\ &\qquad +\frac{1}{f_\pi}\sin\alpha\,(\boldsymbol{\pi}\times\partial_0\boldsymbol{\pi})_1 - \frac{1}{f_\pi}\cos\alpha\,(\boldsymbol{\pi}\times\partial_0\boldsymbol{\pi})_3\Bigg] + \mathcal{O}(\boldsymbol{\pi}^3).\end{aligned} \tag{5.19}$$

The sixth term in eq. (5.12) is by eqs. (5.16) and (5.17) cast into

$$\begin{aligned}-\frac{f_\pi^2\mu_I^2}{8}\mathrm{Tr}\left(\Sigma^\dagger\tau_3\Sigma\tau_3 - \mathbb{1}\right) &= -\frac{f_\pi^2\mu_I^2}{8}\mathrm{Tr}\left(U\tau_3 U^\dagger e^{-\frac{i}{f_\pi}\boldsymbol{\tau}\cdot\boldsymbol{\pi}}U^\dagger\tau_3 U e^{\frac{i}{f_\pi}\boldsymbol{\tau}\cdot\boldsymbol{\pi}}\right)\\ &= \frac{f_\pi^2\mu_I^2}{4}\Bigg(2\sin^2\alpha + \frac{2}{f_\pi}\sin 2\alpha\,\pi_2 + \frac{2}{f_\pi^2}\cos^2\alpha\,\pi_1^2\\ &\qquad +\frac{2}{f_\pi^2}\cos 2\alpha\,\pi_2^2 - \frac{2}{f_\pi^2}\sin^2\alpha\,\pi_3^2\Bigg) + \mathcal{O}(\boldsymbol{\pi}^3).\end{aligned} \tag{5.20}$$

Finally, the last term in eq. (5.12) is found to be

$$\begin{aligned}\frac{f_\pi^2 m_\pi^2}{2}\mathrm{ReTr}\Sigma &= \frac{f_\pi^2 m_\pi^2}{2}\mathrm{ReTr}\left(U e^{\frac{i}{f_\pi}\boldsymbol{\tau}\cdot\boldsymbol{\pi}}U\right)\\ &= f_\pi^2 m_\pi^2\left(\cos\alpha - \frac{1}{f_\pi}\sin\alpha\,\pi_2 - \frac{1}{2f_\pi^2}\cos\alpha\,\boldsymbol{\pi}^2\right) + \mathcal{O}(\boldsymbol{\pi}^3).\end{aligned} \tag{5.21}$$

Adding all the bilinear terms in eqs. (5.13), (5.18), (5.19), (5.20) and (5.21), we arrive at the bilinear Lagrangian

$$\mathscr{L}^{(2)} = \frac{1}{2}\partial_\mu \pi_a \partial^\mu \pi_a - \frac{1}{2} m_{12}(\pi_1 \partial_0 \pi_2 - \pi_2 \partial_0 \pi_1) - \frac{1}{2}\left(\pi_1^2 m_1^2 + \pi_2^2 m_2^2 + \pi_3^2 m_3^2\right), \quad (5.22)$$

where we have defined

$$\begin{aligned} m_{12}^2 &\equiv 4\mu_I^2 \cos^2\alpha, \\ m_1^2 &\equiv m_\pi^2 \cos\alpha - \mu_I^2 \cos^2\alpha, \\ m_2^2 &\equiv m_\pi^2 \cos\alpha - \mu_I^2 \cos 2\alpha, \\ m_3^2 &\equiv m_\pi^2 \cos\alpha + \mu_I^2 \sin^2\alpha. \end{aligned} \quad (5.23)$$

Performing a partial integration of the first term yields

$$\mathscr{L}^{(2)} = \frac{1}{2}\begin{pmatrix}\pi_1 & \pi_2 & \pi_3\end{pmatrix} \begin{pmatrix} -\partial_\mu\partial^\mu - m_1^2 & m_{12}\partial_0 & 0 \\ -m_{12}\partial_0 & -\partial_\mu\partial^\mu - m_2^2 & 0 \\ 0 & 0 & -\partial_\mu\partial^\mu - m_3^2 \end{pmatrix} \begin{pmatrix}\pi_1 \\ \pi_2 \\ \pi_3\end{pmatrix}, \quad (5.24)$$

where the sandwiched matrix is the inverse propagator. Going to Fourier space gives the inverse propagator

$$D^{-1} = \begin{pmatrix} P^2 - m_1^2 & -iEm_{12} & 0 \\ iEm_{12} & P^2 - m_2^2 & 0 \\ 0 & 0 & P^2 - m_3^2 \end{pmatrix}, \quad (5.25)$$

where $P = (E, \mathbf{p})$. The dispersion relations are as before given by the zero modes of D^{-1}. The zero modes satisfy

$$\begin{aligned} \mathrm{Det}(D^{-1}) = 0 =& (E^2 - \mathbf{p}^2 - m_1^2)(E^2 - \mathbf{p}^2 - m_2^2)(E^2 - \mathbf{p}^2 - m_3^2) \\ &- E^2 m_{12}^2 (E^2 - \mathbf{p}^2 - m_3^2). \end{aligned} \quad (5.26)$$

In the normal phase, where the rotation angle $\alpha = 0$, we find that the neutral pion has the relativistic dispersion relation

$$E_0(\mathbf{p}) = \sqrt{\mathbf{p}^2 + m_\pi^2}, \quad (5.27)$$

while the charged pions experience a Zeeman-like splitting of the relativistic dispersion relation, reading

$$E_\pm(\mathbf{p}) = \sqrt{\mathbf{p}^2 + m_\pi^2} \pm \mu_I. \quad (5.28)$$

Taking the limit $\mathbf{p} \to 0$ in eqs. (5.27) and (5.28) yields the mass spectrum

$$\begin{aligned} m_0 &= m_\pi, \\ m_\pm &= m_\pi \pm \mu_I. \end{aligned} \quad (5.29)$$

Next, we turn our attention to the BEC where charged pions condense and $\cos\alpha = m_\pi^2/\mu_I^2$. We find immediately from eq. (5.26) that the dispersion relation of neutral pions remains relativistic but with mass μ_I,

$$E_0(\mathbf{p}) = \sqrt{\mathbf{p}^2 + \mu_I^2}. \quad (5.30)$$

The solutions of eq. (5.26) for the dispersion relations of charged pions read

$$\begin{aligned} E_{\pm}(\mathbf{p}) &= \sqrt{\mathbf{p}^2 + \frac{1}{2}(m_1^2 + m_2^2 + m_{12}^2) \pm \frac{1}{2}\sqrt{4\mathbf{p}^2 m_{12}^2 + (m_1^2 + m_2^2 + m_{12}^2)^2 - 4m_1^2 m_2^2}} \\ &= \sqrt{\mathbf{p}^2 + \frac{1}{2}\mu_I^2(1 + 3\cos^2\alpha) \pm \mu_I\sqrt{16\mathbf{p}^2\cos^2\alpha + \mu_I^2(1 + 3\cos^2\alpha)^2}}. \end{aligned} \tag{5.31}$$

Evaluating eqs. (5.30) and (5.31) in the limit $\mathbf{p} \to 0$ results in the mass spectrum

$$\begin{aligned} m_0 &= \mu_I, \\ m_+ &= \mu_I\sqrt{1 + 3\cos^2\alpha}, \\ m_- &= 0. \end{aligned} \tag{5.32}$$

Thus, ChPT with an isospin chemical potential results in one Goldstone boson and two modes with a gap.[1]

[1] The previously mentioned formulation of Goldstone's theorem is not valid here since the theory is not Lorentz invariant. However, there exists formulations of the theorem valid for nonrelativistic systems as well [29].

Chapter 6

Anomalies

In section 4.2 we pointed out that the QCD Lagrangian has a global $U(1)_A$ symmetry. Noether's theorem states that any global continuous symmetry of a Lagrangian leads classically to a locally conserved current. To see if the same symmetry is present after quantization, we have to decide whether the generating functional has the same symmetry or not. If not, we are dealing with an anomaly. Some examples of anomalies are the breaking of conformal invariance in string theory, the trace anomaly and the chiral (or axial) anomaly [28]. Since the anomalies manifest themselves in the generating functional, they will also affect the Lagrangian of the theory. Hence, the Lagrangian of the EFT must also include the anomaly. It turns out that a chiral isospin anomaly will be important for neutral pions in background gauge fields. We will therefore start this chapter by calculating the chiral isospin anomaly in presence of an external magnetic field and a chemical potential for baryon number and isospin. Furthermore, we will include the anomaly in the ChPT Lagrangian for neutral pions and see how it contributes to the electromagnetic, baryon number and isospin currents. Finally, we derive the form of the ChPT Lagrangian in presence of an external magnetic field at finite baryon density or at finite isospin density.

6.1 Chiral isospin anomaly from background gauge fields

We can probe the symmetry properties of the neutral pion by coupling the mass term in the QCD Lagrangian to a constant source θ, so that $m \to me^{-i\theta\tau_3\gamma_5}$. The relevant part of the two-flavor QCD Lagrangian in Euclidean space [37] then reads

$$\mathscr{L}_{\text{QCD}} = \bar{\psi}\left(\not{D} + m_f e^{-i\theta\tau_3\gamma_5}\right)\psi, \tag{6.1}$$

where we have defined the gamma matrices in accordance with [38], leading to an anti-Hermitian Dirac operator $\not{D}$ in Euclidean space. The covariant derivative is

$$D_\mu\psi = \left(\partial_\mu - i\mathcal{A}_\mu - ig\frac{\lambda_a}{2}\mathcal{A}_{\mu,a}\right)\psi, \tag{6.2}$$

where ψ contains only the u and d quarks. $\mathcal{A}_{\mu,a}$ are the gluon gauge fields that must be contracted with the Gell-Mann matrices λ_a. In addition, we introduce the

electromagnetic gauge field A_μ^{Q}, baryon number gauge field A_μ^{B} and isospin gauge field A_μ^{I} through the matrix gauge field

$$\mathcal{A}_\mu = QA_\mu^{\mathrm{Q}} + BA_\mu^{\mathrm{B}} + I_3 A_\mu^{\mathrm{I}}, \tag{6.3}$$

where Q, B and I_3 are respectively the electric charge, baryon number and isospin of the u and d quarks written on matrix form as

$$Q = \begin{pmatrix} 2/3 & 0 \\ 0 & -1/3 \end{pmatrix}, \quad B = \begin{pmatrix} 1/3 & 0 \\ 0 & 1/3 \end{pmatrix} \quad \text{and} \quad I_3 = \begin{pmatrix} 1/2 & 0 \\ 0 & -1/2 \end{pmatrix}. \tag{6.4}$$

The Lagrangian in eq. (6.1) has a classical symmetry under a simultaneous chiral isospin transformation,

$$\psi \to e^{i\alpha\tau_3\gamma_5}\psi \quad \text{and} \quad \theta \to \theta + 2\alpha. \tag{6.5}$$

We are now in the position to integrate out the quark fields in the generating functional in Euclidean space,

$$Z[\theta] = e^{-W[\theta]} = \mathrm{Det}\left(\not{D} + me^{-i\theta\tau_3\gamma_5}\right) \equiv \mathrm{Det}\mathscr{D} = \prod_n \lambda_n, \tag{6.6}$$

where have taken the functional determinant and λ_n are the eigenvalues of $\mathscr{D}$. Because $\not{D}$ is anti-Hermitian it will have purely imaginary eigenvalues and the eigenstates will come in pairs since $\not{D}$ anticommutes with γ_5 and commutes with τ_3. We can therefore introduce the eigenstates of $\not{D}$ as pairs of spinors φ_n and $\tilde{\varphi}_n = \tau_3\gamma_5\varphi_n$, that each contain the u and d quarks. The eigenstates are related as

$$\not{D}\varphi_n = i\lambda_n\varphi_n \quad \text{and} \quad \not{D}\tilde{\varphi}_n = -i\lambda_n\tilde{\varphi}_n, \tag{6.7}$$

where $\lambda \in \mathbb{R}$ and n denotes the different eigenfunctions. The eigenvalues of $\mathscr{D}$ can be split into the two sectors $\lambda = 0$ and $\lambda \neq 0$. Thereafter, the eigenvalues from each sector can be multiplied giving the determinant of $\mathscr{D}$.

At first we assume $\lambda \neq 0$. The matrix $\mathscr{D}$ acting on two of the eigenstates φ_n and $\tilde{\varphi}_n$ takes the form

$$\mathscr{D}\begin{pmatrix} \varphi_n \\ \tilde{\varphi}_n \end{pmatrix} = \begin{pmatrix} i\lambda_n + m\cos\theta & -im\sin\theta \\ -im\sin\theta & -i\lambda_n + m\cos\theta \end{pmatrix}\begin{pmatrix} \varphi_n \\ \tilde{\varphi}_n \end{pmatrix}, \tag{6.8}$$

resulting in a determinant $\mathrm{Det}\mathscr{D} = \lambda_n^2 + m^2$ independent of θ. Next, we assume $\lambda = 0$. This means that we are considering the zero modes of $\not{D}$, where φ_n and $\tilde{\varphi}_n = \tau_3\gamma_5\varphi_n$ both have the eigenvalue zero. As a consequence, we can find simultaneous eigenstates of $\not{D}$ and γ_5. These are

$$\begin{aligned} \varphi_n^R &= \begin{pmatrix} u_n^R \\ d_n^R \end{pmatrix} \equiv \frac{1}{2}(1+\gamma_5)\varphi_n = \frac{\varphi_n - \tilde{\varphi}_n}{2}, \\ \varphi_n^L &= \begin{pmatrix} u_n^L \\ d_n^L \end{pmatrix} \equiv \frac{1}{2}(1-\gamma_5)\varphi_n = \frac{\varphi_n + \tilde{\varphi}_n}{2}, \end{aligned} \tag{6.9}$$

which satisfy

$$\begin{aligned} &\not{D}\varphi_n^R = 0 \quad \text{and} \quad \not{D}\varphi_n^L = 0, \\ &\gamma_5\varphi_n^R = +1\varphi_n^R \quad \text{and} \quad \gamma_5\varphi_n^L = -1\varphi_n^L. \end{aligned} \tag{6.10}$$

Applying $\not{D}$ to φ_n^R and φ_n^L yields

$$\not{D}\varphi_n^R = me^{-i\theta\tau_3\gamma_5}\varphi_n^R = \begin{pmatrix} me^{-i\theta}u_n^R \\ me^{i\theta}d_n^R \end{pmatrix} \tag{6.11}$$

and

$$\not{D}\varphi_n^L = me^{-i\theta\tau_3\gamma_5}\varphi_n^L = \begin{pmatrix} me^{i\theta}u_n^L \\ me^{-i\theta}d_n^L \end{pmatrix}, \tag{6.12}$$

which reveals that $\not{D}$ has eigenfunctions u_n^R, d_n^R, u_n^L and d_n^L with eigenvalues $me^{-i\theta}$, $me^{i\theta}$, $me^{i\theta}$ and $me^{-i\theta}$, respectively. The total contribution of eigenvalues from both the $\lambda = 0$ and $\lambda \neq 0$ sector will by eq. (6.6) result in a generating functional of the form

$$\begin{aligned} Z[\theta] &= f(m)(me^{-i\theta})^{N_u^R}(me^{i\theta})^{N_u^L}(me^{i\theta})^{N_d^R}(me^{-i\theta})^{N_d^L} \\ &\equiv \tilde{f}(m)e^{-i\theta(N_u^R - N_u^L)+i\theta(N_d^R - N_d^L)}, \end{aligned} \tag{6.13}$$

where we have written the total contribution from the $\lambda \neq 0$ sector as $f(m)$. Moreover, $N_a^{R,L}$ refer to the number of eigenfunctions of each sort $a^{R,L}$. The expected $\theta \to \theta + 2\alpha$ symmetry is violated in the generating functional. However, this does not come from the quark masses, but from the zero modes of $\not{D}$. By exploiting the property $\mathrm{Det}(A) = e^{\mathrm{Tr}\ln \mathrm{A}}$ for a matrix A, we find from eq. (6.6) that

$$\begin{aligned} W[\theta] - W[\theta = 0] &= i\theta(N_u^R - N_u^L) - i\theta(N_d^R - N_d^L) \\ &= -\mathrm{Tr}\ln\left(\not{D} + me^{-i\theta\tau_3\gamma_5}\right) + \mathrm{Tr}\ln\left(\not{D} + m\right). \end{aligned} \tag{6.14}$$

Taking the derivative with respect to θ gives

$$\left(N_u^R - N_u^L\right) - \left(N_d^R - N_d^L\right) = \mathrm{Tr}\left(\tau_3\gamma_5\right), \tag{6.15}$$

where we are tracing over flavor space, Dirac space and color space. The number of different eigenfunctions can be computed by introducing an arbitrary mass scale Λ.[1] By eq. (6.14), this results in

$$\begin{aligned} W[\theta] - W[0] &= \lim_{\Lambda\to\infty} i\theta\,\mathrm{Tr}\left(\tau_3\gamma_5 e^{\frac{\not{D}^2}{\Lambda^2}}\right) = \lim_{\Lambda\to\infty} i\theta\mathrm{Tr}\left[\tau_3\gamma_5\, g\left(-\not{D}^2/\Lambda^2\right)\right] \\ &= \lim_{\Lambda\to\infty} i\theta\int\frac{\mathrm{d}^4p\,\mathrm{d}^4x}{(2\pi)^4}\mathrm{Tr}\left[e^{-ip\cdot x}\tau_3\gamma_5\, g\left(-\not{D}^2/\Lambda^2\right)e^{ip\cdot x}\right] \\ &= \frac{i\theta}{2}\int\frac{\mathrm{d}^4p}{(2\pi)^4}g''(p^2)\int\mathrm{d}^4x\,\mathrm{Tr}\left[\tau_3\gamma_5(\not{D}^2)^2\right] \\ &= \frac{i\theta}{32\pi^2}\int\mathrm{d}^4x\,\varepsilon^{\mu\nu\alpha\beta}\left(F_{\mu\nu}^Q + F_{\mu\nu}^I\right)\left(F_{\alpha\beta}^Q + 2F_{\alpha\beta}^B\right), \end{aligned} \tag{6.16}$$

where $F_{\mu\nu}^Q$, $F_{\mu\nu}^I$ and $F_{\mu\nu}^B$ are the field strength tensors of the corresponding gauge fields A_μ^Q, A_μ^I and A_μ^B. In addition, $g(x)$ is a smooth function satisfying $g(0) = 1$, $g(\infty) = 0$ and $\lim_{x\to\infty} xg'(x) = 0$. The calculation has been performed by evaluating the trace in terms of plane waves so that we could use $e^{-ip\cdot x}\partial_\mu e^{ip\cdot x} = \partial_\mu + ip_\mu$. The result is the chiral isospin anomaly in presence of the three background gauge fields.

[1]The number of different eigenfunctions are also related through the Atiyah-Singer index theorem. In fact, the anomaly is a manifestation of this theorem [39].

6.2 Chiral isospin anomaly in the ChPT Lagrangian

From the previous section, we note that

$$W[0] = W[\theta] - \frac{i\theta}{32\pi^2}\int \mathrm{d}^4x\, \varepsilon^{\mu\nu\alpha\beta}\left(F^Q_{\mu\nu} + F^I_{\mu\nu}\right)\left(F^Q_{\alpha\beta} + 2F^B_{\alpha\beta}\right) \tag{6.17}$$

should be invariant under a simultaneous transformation, $\psi \to e^{i\alpha\tau_3\gamma_5}\psi$ and $\theta \to \theta + 2\alpha$, as there is no dependence on θ. We must therefore find a way to incorporate this into the ChPT Lagrangian. In section 2.3, we showed that charged particles undergo Landau level quantization. Thus, a strong enough magnetic field causes the low-energy spectrum of QCD to consist solely of neutral pions. The ChPT matrix field will therefore reduce to

$$\Sigma = \exp(\frac{i}{f_\pi}\tau_3\pi^0), \tag{6.18}$$

using parameterization i) in eq. (4.11). The transformation $\psi \to e^{i\alpha\tau_3\gamma_5}\psi$ is by eq. (4.10) corresponding to a transformation $\Sigma \to L\Sigma R^\dagger$, where

$$L = e^{-i\alpha\tau_3} \quad \text{and} \quad R = e^{i\alpha\tau_3}. \tag{6.19}$$

Here, the eigenvalues of γ_5 are given by eq. (6.10). The transformation $\psi \to e^{i\alpha\tau_3\gamma_5}\psi$ leads to a transformation, $\pi^0/f_\pi \to \pi^0/f_\pi - 2\alpha$, of the neutral pion field. Hence, in order to make

$$\mathscr{L}_{\mathrm{ChPT}} - \frac{i\theta}{32\pi^2}\varepsilon^{\mu\nu\alpha\beta}\left(F^Q_{\mu\nu} + F^I_{\mu\nu}\right)\left(F^Q_{\alpha\beta} + 2F^B_{\alpha\beta}\right) \tag{6.20}$$

invariant under a simultaneous transformation of both π^0 and θ, we must include a term

$$-\frac{i\pi^0}{32\pi^2 f_\pi}\varepsilon^{\mu\nu\alpha\beta}\left(F^Q_{\mu\nu} + F^I_{\mu\nu}\right)\left(F^Q_{\alpha\beta} + 2F^B_{\alpha\beta}\right) \tag{6.21}$$

in the ChPT Lagrangian. As a result, the complete ChPT Lagrangian in presence of the three background gauge fields is

$$\begin{aligned}\mathscr{L} = {} & \frac{f_\pi^2}{4}\left[\mathrm{Tr}(\partial_\mu\Sigma^\dagger\partial^\mu\Sigma) + 2m_\pi^2\mathrm{ReTr}\Sigma\right] \\ & - \frac{\pi^0}{32\pi^2 f_\pi}\varepsilon^{\mu\nu\alpha\beta}\left(F^Q_{\mu\nu} + F^I_{\mu\nu}\right)\left(F^Q_{\alpha\beta} + 2F^B_{\alpha\beta}\right),\end{aligned} \tag{6.22}$$

where we have returned to Minkowski space. The last term is known as the Wess-Zumino-Witten term for neutral pions [40]. Like the chiral anomaly, the chiral isospin anomaly will contribute to the decay of the neutral pion into two photons since the anomalous term is linear in the neutral pion field and quadratic in the photon field.

6.3 Anomalous contribution to currents

The anomalous part of the effective Lagrangian in eq. (6.22) is given by

$$\mathscr{L}_{\text{anom}} = -\frac{\pi^0}{32\pi^2 f_\pi}\varepsilon^{\mu\nu\alpha\beta}(F^Q_{\mu\nu} + F^I_{\mu\nu})(F^Q_{\alpha\beta} + 2F^B_{\alpha\beta}). \tag{6.23}$$

It will contribute to electromagnetic, baryon number and isospin currents. The Noether current of an Abelian global symmetry can be obtained by varying the action with respect to the corresponding gauge field,

$$j^\mu = \frac{\delta S}{\delta A_\mu}. \tag{6.24}$$

From eq. (6.23), we find that the anomalous action can be written as

$$\begin{aligned} S &= -\frac{1}{32\pi^2 f_\pi}\int \mathrm{d}^4x\, \pi^0 \varepsilon^{\mu\nu\alpha\beta}(F^Q_{\mu\nu}F^Q_{\alpha\beta} + 2F^Q_{\mu\nu}F^B_{\alpha\beta} + F^Q_{\mu\nu}F^I_{\alpha\beta} + 2F^B_{\mu\nu}F^I_{\alpha\beta}) \\ &\equiv S^{QQ} + 2S^{QB} + S^{QI} + 2S^{BI}. \end{aligned} \tag{6.25}$$

All these terms have the same form. We can therefore calculate the variation of the action by considering the variation of a term S^{UV}, where $(U, V) \in \{Q, B, I\}$. The variation of S^{UV} reads

$$\begin{aligned} \delta S^{UV} &\equiv -\frac{1}{32\pi^2 f_\pi}\int \mathrm{d}^4x\, \varepsilon^{\mu\nu\alpha\beta}\delta(\pi^0 F^U_{\mu\nu}F^V_{\alpha\beta}) \\ &= -\frac{1}{32\pi^2 f_\pi}\int \mathrm{d}^4x\, \varepsilon^{\mu\nu\alpha\beta}\left[\pi^0(\delta F^U_{\mu\nu})F^V_{\alpha\beta} + \pi^0 F^U_{\mu\nu}(\delta F^V_{\alpha\beta})\right] \\ &\quad -\frac{1}{32\pi^2 f_\pi}\int \mathrm{d}^4x\, \varepsilon^{\mu\nu\alpha\beta}(\delta\pi^0)F^U_{\mu\nu}F^V_{\alpha\beta}. \end{aligned} \tag{6.26}$$

Furthermore, it is possible to write

$$\varepsilon^{\mu\nu\alpha\beta}\delta F^U_{\mu\nu} = \varepsilon^{\mu\nu\alpha\beta}(\partial_\mu\delta A^U_\nu - \partial_\nu\delta A^U_\mu) = -2\varepsilon^{\mu\nu\alpha\beta}\partial_\nu\delta A^U_\mu. \tag{6.27}$$

Here we used the complete antisymmetry of $\varepsilon^{\mu\nu\alpha\beta}$ and the fact that $\delta\partial_\mu = \partial_\mu\delta$. Having this at hand we get

$$\begin{aligned} \delta S^{UV} &= \frac{1}{16\pi^2 f_\pi}\int \mathrm{d}^4x\, \varepsilon^{\mu\nu\alpha\beta}\pi^0\left[F^U_{\mu\nu}\partial_\beta\delta A^V_\alpha + F^V_{\alpha\beta}\partial_\nu\delta A^U_\mu\right] \\ &\quad -\frac{1}{32\pi^2 f_\pi}\int \mathrm{d}^4x\, \varepsilon^{\mu\nu\alpha\beta}(\delta\pi^0)F^U_{\mu\nu}F^V_{\alpha\beta} \\ &= -\frac{1}{16\pi^2 f_\pi}\int \mathrm{d}^4x\, \varepsilon^{\mu\nu\alpha\beta}\left[(\partial_\beta\pi^0)F^U_{\mu\nu}\delta A^V_\alpha + (\partial_\beta\pi^0)F^V_{\mu\nu}\delta A^U_\alpha\right] \\ &\quad -\frac{1}{32\pi^2 f_\pi}\int \mathrm{d}^4x\, \varepsilon^{\mu\nu\alpha\beta}(\delta\pi^0)F^U_{\mu\nu}F^V_{\alpha\beta}, \end{aligned} \tag{6.28}$$

where we have performed a partial integration and used the Bianchi identity, $\varepsilon^{\mu\nu\alpha\beta}\partial_\nu F_{\alpha\beta} = 0$. The second term in the variation of S^{UV} will drop out in the currents since it does not contain any variation of the gauge field. By eq. (6.24),

we can conclude that the total contribution from the anomalous Lagrangian to the electromagnetic, baryon number and isospin currents is given by

$$j^\mu_{\mathrm{Q}} = \frac{\delta S}{\delta A^Q_\mu} = -\frac{1}{16\pi^2 f_\pi}\varepsilon^{\mu\nu\alpha\beta}(\partial_\nu\pi^0)(2F^Q_{\alpha\beta} + 2F^B_{\alpha\beta} + F^I_{\alpha\beta}), \tag{6.29}$$

$$j^\mu_{\mathrm{B}} = \frac{\delta S}{\delta A^B_\mu} = -\frac{1}{16\pi^2 f_\pi}\varepsilon^{\mu\nu\alpha\beta}(\partial_\nu\pi^0)(2F^Q_{\alpha\beta} + 2F^I_{\alpha\beta}), \tag{6.30}$$

$$j^\mu_{\mathrm{I}} = \frac{\delta S}{\delta A^I_\mu} = -\frac{1}{16\pi^2 f_\pi}\varepsilon^{\mu\nu\alpha\beta}(\partial_\nu\pi^0)(F^Q_{\alpha\beta} + 2F^B_{\alpha\beta}). \tag{6.31}$$

The anomaly is therefore giving nonuniform *neutral* pion fields an electric charge, a baryon number and an isospin. We can argue that a nonuniform neutral pion field is acting as a baryon since it carries baryon number.

6.4 Anomalous Lagrangian in magnetic field at finite density

Furthermore, we want to study the form of the Lagrangian in the case where we only have a constant background magnetic field and a chemical potential for baryon number. The isospin field strength tensor, $F^I_{\alpha\beta}$, in eq. (6.23) will thus vanish, reducing the anomalous Lagrangian to

$$\mathscr{L}_{\mathrm{anom}} = -\frac{\pi^0}{32\pi^2 f_\pi}\varepsilon^{\mu\nu\alpha\beta}F^Q_{\mu\nu}(F^Q_{\alpha\beta} + 2F^B_{\alpha\beta}). \tag{6.32}$$

By pointing the magnetic field in the z-direction, we can choose $A^Q_\mu = (0, 0, -Bx, 0)$ without loss of generality. Hence, the electromagnetic field strength tensor reads

$$F^Q_{\mu\nu} = \begin{pmatrix} 0 & 0 & 0 & 0 \\ 0 & 0 & -B & 0 \\ 0 & B & 0 & 0 \\ 0 & 0 & 0 & 0 \end{pmatrix}. \tag{6.33}$$

The first term in the anomalous Lagrangian is then rewritten as

$$\begin{aligned} -\frac{\pi^0}{32\pi^2 f_\pi}\varepsilon^{\mu\nu\alpha\beta}F^Q_{\mu\nu}F^Q_{\alpha\beta} &= \frac{2}{32\pi^2 f_\pi}\varepsilon^{\mu\nu\alpha\beta}(\partial_\mu\pi^0)A^Q_\nu F^Q_{\alpha\beta} \\ &= \frac{-2}{32\pi^2 f_\pi}\varepsilon^{\mu 2\alpha\beta}Bx(\partial_\mu\pi^0)F^Q_{\alpha\beta} \\ &= 0, \end{aligned} \tag{6.34}$$

where the first equality follows from eq. (6.27) and a partial integration together with the Bianchi identity. Going to the last line, we contracted $\varepsilon^{\mu 2\alpha\beta}$ with $F^Q_{\alpha\beta}$ and used that the Levi-Civita symbol with two equal indices vanishes. Since $A^B_\mu =$

$(\mu_B, 0, 0, 0)$, the remaining term of the anomalous Lagrangian is

$$\begin{aligned}
-\frac{2\pi^0}{32\pi^2 f_\pi}\varepsilon^{\mu\nu\alpha\beta}F^Q_{\mu\nu}F^B_{\alpha\beta} &= \frac{4\pi^0}{32\pi^2 f_\pi}\varepsilon^{\mu\nu\alpha\beta}F^Q_{\mu\nu}\partial_\beta A^B_\alpha \\
&= \frac{-4}{32\pi^2 f_\pi}\varepsilon^{\mu\nu\alpha\beta}(\partial_\beta\pi^0)F^Q_{\mu\nu}A^B_\alpha \\
&= \frac{-4\mu_B}{32\pi^2 f_\pi}\left[\varepsilon^{210k}(\partial_k\pi^0)B - \varepsilon^{120k}(\partial_k\pi^0)B\right] \\
&= \frac{8\mu_B}{32\pi^2 f_\pi}B\,\partial_3\pi^0,
\end{aligned} \tag{6.35}$$

where the first equality follows from eq. (6.27) and the second line follows from a partial integration along with the Bianchi identity. The system can be generalized to a magnetic field pointing in all directions by choosing $A^Q_\mu = (0, -B_y z, -B_z x, -B_x y)$, giving four more nonzero elements to the electromagnetic field strength tensor in eq. (6.33). The resulting changes will be to replace ∂_3 with $\boldsymbol{\nabla}$ and B with $\boldsymbol{B} = (B_x, B_y, B_z)$ in eq. (6.35). Thus, the anomalous effective Lagrangian in presence of a background magnetic field and a chemical potential for baryon number reduces to

$$\mathscr{L}_{\text{anom}} = \frac{\mu_B}{4\pi^2 f_\pi}\boldsymbol{B}\cdot\boldsymbol{\nabla}\pi^0. \tag{6.36}$$

Naively, this could be surprising since the neutral pion has a baryon number equal to zero. However, as shown in eqs. (6.29)-(6.31), nonuniform neutral pion field configurations can carry *all* the three charges Q, B and I_3.

We can easily replace the chemical potential for baryon number with one for isospin, having $A^I_\mu = (\mu_I, 0, 0, 0)$. Since the two terms $2F^B_{\alpha\beta}$ and $F^I_{\alpha\beta}$ in eq. (6.23) have a different prefactor of 2, the only change will be to let $\mu_B \to \mu_I/2$. Thus, the anomalous effective Lagrangian in presence of a background magnetic field and a chemical potential for isospin becomes

$$\mathscr{L}_{\text{anom}} = \frac{\mu_I}{8\pi^2 f_\pi}\boldsymbol{B}\cdot\boldsymbol{\nabla}\pi^0. \tag{6.37}$$

Chapter 7

Anomaly in ChPT including charged pions

The ChPT Lagrangian has up to now included the chiral isospin anomaly only for neutral pions. We will in the following also include the anomaly for charged pions. The starting point is the Goldstone-Wilczek (GW) current, which we first determine the divergence of. We then find the anomalous contribution to the Lagrangian by coupling the GW current to the baryon gauge field [22]. The resulting new term in the Lagrangian is the Wess-Zumino-Witten term. However, this term has an undetermined coefficient. The coefficient will be determined by matching the resulting Lagrangian to our previously obtained Lagrangian for neutral pions.

7.1 Divergence of the Goldstone-Wilczek current

The form of the GW current was derived by Goldstone and Wilczek in [41]. It is applied to QCD in strong magnetic fields in [22] and is written as

$$j^{\mu}_{\mathrm{GW}} = \lambda\varepsilon^{\mu\nu\alpha\beta}\mathrm{Tr}\left\{(\Sigma D_{\nu}\Sigma^{\dagger})(\Sigma D_{\alpha}\Sigma^{\dagger})(\Sigma D_{\beta}\Sigma^{\dagger}) - \frac{3i}{2}\left[(D_{\nu}\Sigma\Sigma^{\dagger})\mathcal{F}^{L}_{\alpha\beta} - (D_{\nu}\Sigma^{\dagger}\Sigma)\mathcal{F}^{R}_{\alpha\beta}\right]\right\}, \tag{7.1}$$

where λ is a numerical coefficient that we will determine later and Σ is the matrix field variable of ChPT. Since QCD with two light quark flavors has an approximate global chiral symmetry $SU(2)_L \times SU(2)_R$, we can introduce matrix gauge fields $\mathcal{A}^L_\mu$ and $\mathcal{A}^R_\mu$, and define the covariant derivative of Σ as

$$D_{\mu}\Sigma = \partial_{\mu} - i\mathcal{A}^{L}_{\mu}\Sigma + i\Sigma\mathcal{A}^{R}_{\mu}. \tag{7.2}$$

The corresponding field-strength tensors are then

$$\mathcal{F}^{L,R}_{\mu\nu} = \partial_{\mu}\mathcal{A}^{L,R}_{\nu} - \partial_{\nu}\mathcal{A}^{L,R}_{\mu} - i\left[\mathcal{A}^{L,R}_{\mu}, \mathcal{A}^{L,R}_{\nu}\right]. \tag{7.3}$$

The GW current j^{μ}_{GW} is gauge-invariant, implying that $\partial_{\mu}j^{\mu}_{GW} = D_{\mu}j^{\mu}_{GW}$. Thus, by keeping manifest covariance, we can calculate the divergence of the current using

the product rule and the cyclic property of the trace. The result is

$$\begin{aligned}\partial_\mu j^\mu_{\mathrm{GW}} &= D_\mu j^\mu_{\mathrm{GW}} \\ &= \lambda\varepsilon^{\mu\nu\alpha\beta}\mathrm{Tr}\Big\{3(D_\mu\Sigma)(D_\nu\Sigma^\dagger)(\Sigma D_\alpha\Sigma^\dagger)(\Sigma D_\beta\Sigma^\dagger) \\ &\qquad +3\Sigma(D_\mu D_\nu\Sigma^\dagger)(\Sigma D_\alpha\Sigma^\dagger)(\Sigma D_\beta\Sigma^\dagger) \\ &\qquad -\frac{3i}{2}\left[(D_\mu D_\nu\Sigma)\Sigma^\dagger\mathcal{F}^L_{\alpha\beta} - (D_\mu D_\nu\Sigma^\dagger)\Sigma\mathcal{F}^R_{\alpha\beta}\right. \\ &\qquad\qquad +(D_\nu\Sigma)(D_\mu\Sigma^\dagger)\mathcal{F}^L_{\alpha\beta} - (D_\nu\Sigma^\dagger)(D_\mu\Sigma)\mathcal{F}^R_{\alpha\beta} \\ &\qquad\qquad \left.+(D_\nu\Sigma\Sigma^\dagger)D_\mu\mathcal{F}^L_{\alpha\beta} - (D_\nu\Sigma^\dagger\Sigma)D_\mu\mathcal{F}^R_{\alpha\beta}\right]\Big\}.\end{aligned} \tag{7.4}$$

We will in the following calculate each term by itself before collecting the terms into a final answer for the divergence of the GW current. Appendix A presents proofs of different properties that we will use along the way. The first term in eq. (7.4) can be rewritten using the property $D_\mu\Sigma = -\Sigma(D_\mu\Sigma^\dagger)\Sigma$, resulting in

$$\begin{aligned}&3\lambda\varepsilon^{\mu\nu\alpha\beta}\mathrm{Tr}\left[(D_\mu\Sigma)(D_\nu\Sigma^\dagger)(\Sigma D_\alpha\Sigma^\dagger)(\Sigma D_\beta\Sigma^\dagger)\right] \\ &= -3\lambda\varepsilon^{\mu\nu\alpha\beta}\mathrm{Tr}\left[(\Sigma D_\mu\Sigma^\dagger)(\Sigma D_\nu\Sigma^\dagger)(\Sigma D_\alpha\Sigma^\dagger)(\Sigma D_\beta\Sigma^\dagger)\right] \\ &= -3\lambda\varepsilon^{\mu\nu\alpha\beta}\mathrm{Tr}\left[(\Sigma D_\beta\Sigma^\dagger)(\Sigma D_\mu\Sigma^\dagger)(\Sigma D_\nu\Sigma^\dagger)(\Sigma D_\alpha\Sigma^\dagger)\right] \\ &= 3\lambda\varepsilon^{\mu\nu\alpha\beta}\mathrm{Tr}\left[(\Sigma D_\mu\Sigma^\dagger)(\Sigma D_\nu\Sigma^\dagger)(\Sigma D_\alpha\Sigma^\dagger)(\Sigma D_\beta\Sigma^\dagger)\right] \\ &= 0,\end{aligned} \tag{7.5}$$

where we used the trace property going to the third line and the complete antisymmetry of $\varepsilon^{\mu\nu\alpha\beta}$ going to the fourth line. Comparing the second and fourth lines, we conclude that the first term in eq. (7.4) needs to vanish. The second term in eq. (7.4) can be cast into a different form utilizing the properties

$$\varepsilon^{\mu\nu\alpha\beta}D_\mu D_\nu\Sigma^\dagger = \frac{1}{2}\varepsilon^{\mu\nu\alpha\beta}\left[D_\mu, D_\nu\right]\Sigma^\dagger, \tag{7.6}$$

$$\varepsilon^{\mu\nu\alpha\beta}[D_\mu, D_\nu]\Sigma^\dagger = \varepsilon^{\mu\nu\alpha\beta}\left(i\Sigma^\dagger\mathcal{F}^L_{\mu\nu} - i\mathcal{F}^R_{\mu\nu}\Sigma^\dagger\right), \tag{7.7}$$

$$D_\mu\Sigma^\dagger = -\Sigma^\dagger D_\mu\Sigma\Sigma^\dagger, \tag{7.8}$$

yielding

$$\begin{aligned}&3\lambda\varepsilon^{\mu\nu\alpha\beta}\mathrm{Tr}\left[\Sigma(D_\mu D_\nu\Sigma^\dagger)(\Sigma D_\alpha\Sigma^\dagger)(\Sigma D_\beta\Sigma^\dagger)\right] \\ &= \frac{3}{2}\lambda\varepsilon^{\mu\nu\alpha\beta}\mathrm{Tr}\left[(\Sigma[D_\mu, D_\nu]\Sigma^\dagger)(\Sigma D_\alpha\Sigma^\dagger)(\Sigma D_\beta\Sigma^\dagger)\right] \\ &= \frac{3i}{2}\lambda\varepsilon^{\mu\nu\alpha\beta}\mathrm{Tr}\left[(-\Sigma\mathcal{F}^R_{\mu\nu}\Sigma^\dagger + \Sigma\Sigma^\dagger\mathcal{F}^L_{\mu\nu})(\Sigma D_\alpha\Sigma^\dagger)(\Sigma D_\beta\Sigma^\dagger)\right] \\ &= \frac{3i}{2}\lambda\varepsilon^{\mu\nu\alpha\beta}\mathrm{Tr}\left[\mathcal{F}^R_{\mu\nu}(D_\alpha\Sigma^\dagger)(D_\beta\Sigma) - \mathcal{F}^L_{\mu\nu}(D_\alpha\Sigma)(D_\beta\Sigma^\dagger)\right].\end{aligned} \tag{7.9}$$

The third term in eq. (7.4) is calculated using the properties

$$\varepsilon^{\mu\nu\alpha\beta}D_\mu D_\nu\Sigma = \frac{1}{2}\varepsilon^{\mu\nu\alpha\beta}\left[D_\mu, D_\nu\right]\Sigma, \tag{7.10}$$

$$\varepsilon^{\mu\nu\alpha\beta}[D_\mu, D_\nu]\Sigma = \varepsilon^{\mu\nu\alpha\beta}\left(i\Sigma\mathcal{F}^R_{\mu\nu} - i\mathcal{F}^L_{\mu\nu}\Sigma\right), \tag{7.11}$$

resulting in

$$\begin{aligned}-\frac{3i}{2}\lambda\varepsilon^{\mu\nu\alpha\beta}\mathrm{Tr}\left[(D_\mu D_\nu\Sigma)\Sigma^\dagger\mathcal{F}^L_{\alpha\beta}\right] &= -\frac{3i}{4}\lambda\varepsilon^{\mu\nu\alpha\beta}\mathrm{Tr}\left[([D_\mu,D_\nu]\Sigma)\Sigma^\dagger\mathcal{F}^L_{\alpha\beta}\right]\\ &= \frac{3}{4}\lambda\varepsilon^{\mu\nu\alpha\beta}\mathrm{Tr}\left[\Sigma\mathcal{F}^R_{\mu\nu}\Sigma^\dagger\mathcal{F}^L_{\alpha\beta}-\mathcal{F}^L_{\mu\nu}\mathcal{F}^L_{\alpha\beta}\right].\end{aligned} \tag{7.12}$$

The fourth term in eq. (7.4) is rewritten in the same way as eq. (7.12) but using the properties in eqs. (A.4) and (A.6) instead of the properties in eqs. (A.3) and (A.5). This results in

$$\begin{aligned}\frac{3i}{2}\lambda\varepsilon^{\mu\nu\alpha\beta}\mathrm{Tr}\left[(D_\mu D_\nu\Sigma^\dagger)\Sigma\mathcal{F}^R_{\alpha\beta}\right] &= \frac{3}{4}\lambda\varepsilon^{\mu\nu\alpha\beta}\mathrm{Tr}\left[\mathcal{F}^R_{\mu\nu}\mathcal{F}^R_{\alpha\beta}-\Sigma^\dagger\mathcal{F}^L_{\mu\nu}\Sigma\mathcal{F}^R_{\alpha\beta}\right]\\ &= \frac{3}{4}\lambda\varepsilon^{\mu\nu\alpha\beta}\mathrm{Tr}\left[\mathcal{F}^R_{\mu\nu}\mathcal{F}^R_{\alpha\beta}-\Sigma\mathcal{F}^R_{\mu\nu}\Sigma^\dagger\mathcal{F}^L_{\alpha\beta}\right],\end{aligned} \tag{7.13}$$

where we went to the last line by interchanging $\mu,\nu\leftrightarrow\alpha,\beta$ and using the cyclic property of the trace. The fifth and sixth term in eq. (7.4) takes the form

$$\begin{aligned}&-\frac{3i}{2}\lambda\varepsilon^{\mu\nu\alpha\beta}\mathrm{Tr}\left[(D_\nu\Sigma)(D_\mu\Sigma^\dagger)\mathcal{F}^L_{\alpha\beta}-(D_\nu\Sigma^\dagger)(D_\mu\Sigma)\mathcal{F}^R_{\alpha\beta}\right]\\ &=\frac{3i}{2}\lambda\varepsilon^{\mu\nu\alpha\beta}\mathrm{Tr}\left[\mathcal{F}^L_{\mu\nu}(D_\alpha\Sigma)(D_\beta\Sigma^\dagger)-\mathcal{F}^R_{\mu\nu}(D_\alpha\Sigma^\dagger)(D_\beta\Sigma)\right],\end{aligned} \tag{7.14}$$

where we let $\mu,\nu,\alpha,\beta\to\beta,\alpha,\mu,\nu$ and used the complete antisymmetry of $\varepsilon^{\mu\nu\alpha\beta}$. The two last terms in eq. (7.4) are zero because of the Bianchi identity $\varepsilon^{\mu\nu\alpha\beta}D_\nu F_{\alpha\beta}=0$. The divergence of the GW current in eq. (7.4) is determined by collecting all the calculated terms in eqs. (7.5), (7.9), (7.12), (7.13) and (7.14) yielding

$$\begin{aligned}\partial_\mu j^\mu_{GW} = \frac{3}{2}\lambda\varepsilon^{\mu\nu\alpha\beta}\mathrm{Tr}\Bigg[&i\mathcal{F}^R_{\mu\nu}(D_\alpha\Sigma^\dagger)(D_\beta\Sigma)-i\mathcal{F}^L_{\mu\nu}(D_\alpha\Sigma)(D_\beta\Sigma^\dagger)\\ &+\frac{1}{2}\Sigma\mathcal{F}^R_{\mu\nu}\Sigma^\dagger\mathcal{F}^L_{\alpha\beta}-\frac{1}{2}\mathcal{F}^L_{\mu\nu}\mathcal{F}^L_{\alpha\beta}\\ &+\frac{1}{2}\mathcal{F}^R_{\mu\nu}\mathcal{F}^R_{\alpha\beta}-\frac{1}{2}\Sigma\mathcal{F}^R_{\mu\nu}\Sigma^\dagger\mathcal{F}^L_{\alpha\beta}\\ &+i\mathcal{F}^L_{\mu\nu}(D_\alpha\Sigma)(D_\beta\Sigma^\dagger)-i\mathcal{F}^R_{\mu\nu}(D_\alpha\Sigma^\dagger)(D_\beta\Sigma)\Bigg]\\ =\frac{3}{4}\lambda\varepsilon^{\mu\nu\alpha\beta}&\mathrm{Tr}\left(\mathcal{F}^R_{\mu\nu}\mathcal{F}^R_{\mu\nu}-\mathcal{F}^L_{\mu\nu}\mathcal{F}^L_{\mu\nu}\right).\end{aligned} \tag{7.15}$$

We can observe that the divergence of the GW current is independent of the matrix field Σ. When the background gauge field becomes purely vector-like, that is $\mathcal{A}^R_\mu=\mathcal{A}^L_\mu$, we have that $\mathcal{F}^R_{\mu\nu}=\mathcal{F}^L_{\mu\nu}$. This causes the divergence of the GW current to vanish,

$$\partial_\mu j^\mu_{\mathrm{GW}}=0. \tag{7.16}$$

7.2 Wess-Zumino-Witten term in the ChPT Lagrangian

We will now introduce the Wess-Zumino-Witten term $\mathscr{L}_{\mathrm{WZW}}$ into the ChPT Lagrangian. This term captures the anomalies of QCD and is the only anomalous term

that can be added to the two-flavor Lagrangian. It is found by coupling the GW current to a background gauge field A^1_μ for the $U(1)_\mathrm{B}$ baryon number symmetry of QCD [22],

$$\mathscr{L}_\mathrm{WZW} = j^\mu_\mathrm{GW} A^1_\mu. \tag{7.17}$$

By eq. (4.16), the complete ChPT Lagrangian including the chiral isospin anomaly is

$$\mathscr{L} = \frac{f_\pi^2}{4}\left[\mathrm{Tr}(\partial_\mu\Sigma^\dagger\partial^\mu\Sigma) + 2m_\pi^2\mathrm{ReTr}\Sigma\right] + \mathscr{L}_\mathrm{WZW}. \tag{7.18}$$

We will restrict our attention to the three Abelian background gauge fields for electric charge Q, baryon number B and the third component of isospin I_3. Hence, the full gauge field reads

$$\mathcal{A}_\mu = \mathcal{A}^R_\mu = \mathcal{A}^L_\mu = QA^\mathrm{Q}_\mu + I_3A^\mathrm{I}_\mu + BA^\mathrm{B}_\mu = I_3\left(A^\mathrm{I}_\mu + A^\mathrm{Q}_\mu\right) + B\left(A^\mathrm{B}_\mu + \frac{A^\mathrm{Q}_\mu}{2}\right), \tag{7.19}$$

where the Gell-Mann-Nishijima formula $Q = I_3 + B/2$ have been used. However, j^μ_GW is gauged under an $SU(2)_L \times SU(2)_R$ symmetry, while A^1_μ is a $U(1)_\mathrm{B}$ gauge field. Thereby, j^μ_GW will only include the part of $\mathcal{A}_\mu$ belonging to $SU(2)$. This is the term proportional to I_3 since the generator of I_3 is $\tau_3/2$ which belongs to $SU(2)$. The second term in eq. (7.19) is belonging to $U(1)_\mathrm{B}$ and will hence be included in A^1_μ. The Wess-Zumino-Witten term is therefore taking the form

$$\begin{aligned}\mathscr{L}_\mathrm{WZW} =& \lambda\varepsilon^{\mu\nu\alpha\beta}\left(A^B_\mu + \frac{A^Q_\mu}{2}\right) \\ &\times \mathrm{Tr}\left[(\Sigma D_\nu\Sigma^\dagger)(\Sigma D_\alpha\Sigma^\dagger)(\Sigma D_\beta\Sigma^\dagger) - \frac{3i}{4}\tau_3(D_\nu\Sigma\Sigma^\dagger - D_\nu\Sigma^\dagger\Sigma)(F^I_{\alpha\beta} + F^Q_{\alpha\beta})\right],\end{aligned} \tag{7.20}$$

where the covariant derivative is written as

$$D_\mu\Sigma = \partial_\mu\Sigma - \frac{i}{2}\left(A^\mathrm{I}_\mu + A^\mathrm{Q}_\mu\right)[\tau_3, \Sigma], \tag{7.21}$$

and the field strength tensor is given by

$$\mathcal{F}_{\mu\nu} = \mathcal{F}^L_{\mu\nu} = \mathcal{F}^R_{\mu\nu} = \frac{\tau_3}{2}\left(F^\mathrm{Q}_{\mu\nu} + F^\mathrm{I}_{\mu\nu}\right). \tag{7.22}$$

7.2.1 Restricting to neutral pions

We can now restrict the Lagrangian in eq. (7.20) to neutral pions in order to determine the coefficient λ. Using parameterization i) in eq. (4.11) yields

$$\Sigma = \exp\left(\frac{i}{f_\pi}\tau_3\pi^0\right). \tag{7.23}$$

There are three different terms in eq. (7.20) that contain the matrix field Σ. The first term is made up of three factors of the form $\Sigma D_\nu\Sigma^\dagger$. Inserting eq. (7.23) into

one of these factors gives

$$\begin{aligned}\Sigma D_\nu \Sigma^\dagger &= \mathrm{e}^{\frac{i}{f_\pi}\tau_3\pi^0}\left\{\partial_\nu \mathrm{e}^{-\frac{i}{f_\pi}\tau_3\pi^0} - \frac{i}{2}(A^I_\nu + A^Q_\nu)\left[\tau_3, \mathrm{e}^{-\frac{i}{f_\pi}\tau_3\pi^0}\right]\right\} \\ &= \mathrm{e}^{\frac{i}{f_\pi}\tau_3\pi^0}\left(-\frac{i}{f_\pi}\tau_3\right)\left(\partial_\nu\pi^0\right)\mathrm{e}^{-\frac{i}{f_\pi}\tau_3\pi^0} \\ &= -\frac{i}{f_\pi}\tau_3\partial_\nu\pi^0.\end{aligned} \tag{7.24}$$

This results in

$$\mathrm{Tr}\left\{(\Sigma D_\nu\Sigma^\dagger)(\Sigma D_\alpha\Sigma^\dagger)(\Sigma D_\beta\Sigma^\dagger)\right\} = \mathrm{Tr}\left\{\frac{i}{f_\pi^3}(\partial_\nu\pi^0)(\partial_\alpha\pi^0)(\partial_\beta\pi^0)\tau_3\right\} = 0, \tag{7.25}$$

where we used that $\mathrm{Tr}(\tau_3) = 0$. Thus, the first term in eq. (7.20) is zero and we are left with

$$\begin{aligned}\mathscr{L}_{\mathrm{WZW}} &= -\frac{3i}{4}\lambda\varepsilon^{\mu\nu\alpha\beta}\left(A^B_\mu + \frac{A^Q_\mu}{2}\right)\mathrm{Tr}\left[\tau_3(D_\nu\Sigma\Sigma^\dagger - D_\nu\Sigma^\dagger\Sigma)(F^I_{\alpha\beta} + F^Q_{\alpha\beta})\right] \\ &= -\frac{3i}{4}\lambda\varepsilon^{\mu\nu\alpha\beta}\left(A^B_\mu + \frac{A^Q_\mu}{2}\right)\mathrm{Tr}\left[\left(\frac{i}{f_\pi}\partial_\nu\pi^0 + \frac{i}{f_\pi}\partial_\nu\pi^0\right)\left(F^I_{\alpha\beta} + F^Q_{\alpha\beta}\right)\right] \\ &= \frac{3}{f_\pi}\lambda\varepsilon^{\mu\nu\alpha\beta}\left(A^B_\mu + \frac{A^Q_\mu}{2}\right)\left(F^I_{\alpha\beta} + F^Q_{\alpha\beta}\right)\partial_\nu\pi^0 \\ &= -\frac{3\pi^0}{f_\pi}\lambda\varepsilon^{\mu\nu\alpha\beta}\left(\partial_\nu A^B_\mu + \frac{1}{2}\partial_\nu A^Q_\mu\right)\left(F^Q_{\alpha\beta} + F^I_{\alpha\beta}\right) \\ &= \frac{3\pi^0}{4f_\pi}\lambda\varepsilon^{\mu\nu\alpha\beta}\left(F^Q_{\mu\nu} + F^I_{\mu\nu}\right)\left(F^Q_{\alpha\beta} + 2F^B_{\alpha\beta}\right),\end{aligned} \tag{7.26}$$

where we in the fourth line have performed a partial integration and used the Bianchi identity $\varepsilon^{\mu\nu\alpha\beta}\partial_\nu F_{\alpha\beta} = 0$. The last line is obtained by using the complete antisymmetry of the Levi-Civita symbol $\varepsilon^{\mu\nu\alpha\beta}$. Hence, we have now derived an additional form of the anomalous Lagrangian in presence of the three background gauge fields for electric charge Q, baryon number B and isospin I_3. The coefficient λ in the GW current can therefore be determined by matching eq. (7.26) to the anomalous Lagrangian in eq. (6.23), resulting in

$$\lambda = -\frac{1}{24\pi^2}. \tag{7.27}$$

The remaining two a priori undetermined couplings, f_π and m_π, in the complete ChPT Lagrangian in eq. (7.18) need to be determined by experiment.

Part III

Chiral soliton lattice and the QCD phase diagram

Chapter 8

Chiral soliton lattice

In this chapter, we will study how the ground state of low-energy QCD is affected by a baryon chemical potential and an external magnetic field. This has been studied by Son and Stephanov, and in 2008 they conjectured the existence of a "stack of parallel π^0 domain walls" [22]. Similar structures can be found in condensed matter systems such as chiral magnets, where they are called chiral soliton lattices (CSL) [42].[1] In 2017, Brauner and Yamamoto gave the exact solution to the equation of motion for the CSL structure in QCD [23]. This chapter reproduces their findings and provides some extra background material. It starts out by setting up the EFT before the equation of motion is solved. Furthermore, we discuss how the solution is an array of topological solitons. Finally, we determine the ground state of this solution and show how it appears as the ground state of QCD.

8.1 Chiral soliton lattice in the chiral limit

Since we want to study the low-energy regime of QCD, we can use ChPT to determine the ground state. This will be done in presence of a baryon chemical potential and an external magnetic field. In section 2.3, we showed that charged particles in a magnetic field undergo Landau level quantization. The low-energy regime of QCD will therefore consist solely of neutral pions if the magnetic field is strong enough. An external magnetic gauge field A_μ is taken into the ChPT Lagrangian in eq. (4.16) by promoting the ordinary derivatives to covariant derivatives of the form

$$D_\mu \Sigma \equiv \partial_\mu \Sigma - i[Q_\mu, \Sigma], \tag{8.1}$$

where $Q_\mu \equiv A_\mu \tau_3/2$. In eq. (6.36) we found that in presence of a background electromagnetic field $\boldsymbol{H}$ and baryon density μ_B the ChPT Lagrangian for neutral pions acquires an anomalous term. Adding this term to the ChPT Lagrangian results in

$$\mathscr{L} = \frac{f_\pi^2}{4}\left[\mathrm{Tr}(D_\mu \Sigma^\dagger D^\mu \Sigma) + 2m_\pi^2 \mathrm{ReTr}\Sigma\right] + \frac{\mu_B}{4\pi^2}\boldsymbol{H}\cdot\boldsymbol{\nabla}\phi, \tag{8.2}$$

where we have defined the dimensionless neutral pion field $\phi \equiv \pi^0/f_\pi$. Furthermore, we have restricted $\Sigma = \mathrm{e}^{i\tau_3\phi}$ to neutral pions using parameterization i) in eq. (4.11).

[1] "Chiral symmetry" in condensed-matter physics refers to a discrete parity symmetry and not the $SU(2)_L \times SU(2)_R$ chiral symmetry of two-flavor QCD. Hence, the CSL is chiral in the sense that it breaks parity spontaneously.

As in section 5.1, the QCD vacuum has $\Sigma = \mathbb{1}$. The baryon chemical potential can be replaced by an isospin chemical potential μ_I by letting $\mu_B \to \mu_I/2$. Inserting our parameterization of Σ into the Lagrangian yields

$$\mathscr{L} = \frac{f_\pi^2}{2}\dot{\phi}\dot{\phi} - \frac{f_\pi^2}{2}\left(\boldsymbol{\nabla}\phi\right)^2 + f_\pi^2 m_\pi^2(\cos\phi - 1) + \frac{\mu_B}{4\pi^2}\boldsymbol{H}\cdot\boldsymbol{\nabla}\phi, \tag{8.3}$$

where we have introduced an offset $f_\pi^2 m_\pi^2$ such that the Lagrangian vanishes in the QCD vacuum, $\phi = 0$. The Hamiltonian is determined by a Legendre transformation of the Lagrangian as in section 2.2.1. This gives

$$\begin{aligned}\mathscr{H} &= \sum_a \pi_a \dot{\phi}_a - \mathscr{L} = f_\pi^2\dot{\phi}^2 - \mathscr{L} \\ &= \frac{f_\pi^2}{2}\left[\dot{\phi}^2 + \left(\partial_x\phi\right)^2 + \left(\partial_y\phi\right)^2 + \left(\partial_z\phi\right)^2\right] + m_\pi^2 f_\pi^2(1-\cos\phi) - \frac{\mu_B H}{4\pi^2}\partial_z\phi,\end{aligned} \tag{8.4}$$

where we have oriented the uniform magnetic field in the z-direction, $\boldsymbol{H} = (0,0,H)$, without loss of generality. The Hamiltonian is quadratic in the derivatives of ϕ with respect to t, x and y. Consequently, a pion field configuration independent of t, x and y reduces the energy and leaves us with the Hamiltonian

$$\mathscr{H} = \frac{f_\pi^2}{2}\left(\partial_z\phi\right)^2 + m_\pi^2 f_\pi^2(1-\cos\phi) - \frac{\mu_B H}{4\pi^2}\partial_z\phi. \tag{8.5}$$

The ground state is determined by minimizing the Hamiltonian. In the chiral limit, it is straightforward to show that our Hamiltonian is minimal when

$$\phi(z) = \frac{\mu_B H z}{4\pi^2 f_\pi^2}. \tag{8.6}$$

Calculating $\partial_\mu\phi$ yields a new momentum scale of our effective theory,

$$p_{\mathrm{CSL}} = \frac{\mu_{\mathrm{B}} H}{4\pi^2 f_\pi^2}. \tag{8.7}$$

The momentum scale must satisfy $p_{\mathrm{CSL}} \ll 4\pi f_\pi$ in order to maintain the validity of the derivative expansion in ChPT. This was explained in section 4.3.

8.2 Equation of motion

By keeping the magnetic field oriented in the z-direction, we see from eq. (8.5) that our system can be considered as an effective one dimensional system. The equation of motion is obtained by requiring that the variation of the action S is zero,

$$\begin{aligned}\delta S &= \int \mathrm{d}^4x\, \delta\mathscr{L} = -\int \mathrm{d}^4x\, \delta\mathscr{H} \\ &= \int \mathrm{d}^4x\, \left[-f_\pi^2\left(\partial_z\phi\right)\partial_z\delta\phi - f_\pi^2 m_\pi^2 \sin\phi\,\delta\phi + \frac{\mu_B H}{4\pi^2}\partial_z\delta\phi\right], \\ &= \int \mathrm{d}^4x\, \left[f_\pi^2\left(\partial_z^2\phi\right) - f_\pi^2 m_\pi^2\sin\phi\right]\delta\phi = 0,\end{aligned} \tag{8.8}$$

where we have used that ϕ is independent of t, x and y in the ground state. In addition, we used that $\partial_z \delta = \delta \partial_z$ and performed a partial integration. Hence, the integrand must vanish and we are left with the equation of motion

$$\partial_z^2 \phi = m_\pi^2 \sin \phi. \tag{8.9}$$

We can see that the equation of motion is not affected by the anomalous term. However, it will affect the energy. The equation can be recognized as the equation of motion for a simple pendulum with angle ϕ. If we let $\phi \to \theta - \pi$ and introduce $x \equiv z m_\pi$, we obtain the well-known Sine-Gordon equation,

$$\partial_x^2 \theta = -\sin \theta. \tag{8.10}$$

The first step in order to solve this equation is to multiply by $\partial_x \theta$ on both sides and integrate once. Thus, we are left with

$$\frac{1}{2} (\partial_x \theta)^2 - \cos \theta = E, \tag{8.11}$$

where E is an integration constant. Let us define $\theta \equiv t$ and choose the initial condition $\theta(0) = t(0) = 0$. Eq. (8.11) can then be cast into the form

$$\int_0^x \mathrm{d}x = \int_0^\theta \frac{\mathrm{d}t}{\sqrt{2\,(E + \cos t)}} = k \int_0^{\theta/2} \frac{\mathrm{d}t}{\sqrt{1 - k^2 \sin^2 t}}, \tag{8.12}$$

in which we have defined the elliptic modulus $k \equiv \sqrt{\frac{2}{E+1}}$. The integral on the right-hand side is known as the incomplete elliptic integral of the first kind [43]. Consequently, by defining the dimensionless coordinate $\bar{z} \equiv \frac{z m_\pi}{k}$, we obtain

$$\sin\left(\frac{\theta(\bar{z})}{2}\right) = \mathrm{sn}(\bar{z}, k), \tag{8.13}$$

where $\mathrm{sn}(\bar{z}, k)$ is the Jacobi elliptic sine function with k as a free parameter satisfying $0 \leq k \leq 1$. Going back to $\phi = \theta - \pi$, we arrive at

$$\cos\left(\frac{\phi(\bar{z})}{2}\right) = \mathrm{sn}(\bar{z}, k) \quad \Leftrightarrow \quad \phi(\bar{z}) = 2\mathrm{am}(\bar{z}, k) - \pi. \tag{8.14}$$

When $\bar{z}$ varies between $\bar{z}_1 = (2n-1)K(k)$ and $\bar{z}_2 = (2n+1)K(k)$, having n as an integer and $K(k)$ as the complete elliptical integral of the first kind, the angle ϕ will vary between $2(n-1)\pi$ and $2n\pi$. This can be seen in figure 8.1(A) for $k = 0.999$. Thus, our solution has a lattice structure with period

$$\ell = z_2 - z_1 = \frac{k}{m_\pi}(\bar{z}_2 - \bar{z}_1) = \frac{2kK(k)}{m_\pi}. \tag{8.15}$$

8.3 Topological solitons

From our Hamiltonian in eq. (8.5), we find that $\phi = 2n\pi$ and $\phi = 2(n-1)\pi$ correspond to different vacua. When ϕ varies between $2(n-1)\pi$ and $2n\pi$, our

solution in eq. (8.14) is therefore joining different vacua. This is illustrated in figure 8.1(A). Solutions that join different vacua in a localized and smooth manner are called soliton solutions [44]. Soliton solutions are topological and stable if they join different vacua that cannot be continuously transformed into each other. In our case, we can think of ϕ as an angle if we identify $\phi = \phi + 2n\pi$ for any $n \in \mathbb{Z}$. This is reasonable since our Hamiltonian in eq. (8.5) is unchanged when ϕ is shifted by $2n\pi$. The ChPT variable Σ is also unchanged by this shift. Consequently, the values of ϕ are not in $\mathbb{R}$, but in $\mathbb{R}/2\pi\mathbb{Z} \cong S^1$. Our field ϕ is therefore a map[2]

$$\phi : \mathbb{R} \mapsto S^1. \tag{8.16}$$

We will define the winding number ν as the number of times ϕ covers the circle S^1, going from $z = -\infty$ to $z = +\infty$. Strictly speaking, ν is the degree of a continuous mapping. When ϕ goes from one vacuum to another, it is changed by a value of 2π as illustrated in figure 8.1(A). Our solution can therefore be thought of as winding around the circle once for every two vacua it connects. Hence, the winding number of ϕ will be different in each vacuum. In the context of homotopy groups, different winding numbers correspond to different equivalence classes of the corresponding homotopy group. Maps belonging to different equivalence classes cannot be continuously transformed into each other [28]. Thus, having a map ϕ with different winding number in each vacuum means that we have an array of topological solitons. Quantizing the field theory reveals that these solitons have particle-like properties [45]. If we limit our system from $z = 0$ to $z = L$, the total number of solitons will be equal to the winding number acquired going from $z = 0$ to $z = L$.

8.4 Topological charges

Our solution in eq. (8.14) with $0 \leq k \leq 1$ corresponds to a simple pendulum that has enough energy to complete a full swing. The winding number picked up after one swing can be associated with topological charges. In eq. (6.30), we obtained an expression for the baryon current due to the anomalous term in the Lagrangian. Having only a background magnetic field and a baryon chemical potential, the baryon current reduces to

$$j^\mu_{\mathrm{B}} = -\frac{1}{8\pi^2}\varepsilon^{\mu\nu\alpha\beta}(\partial_\nu\phi)F^Q_{\alpha\beta}, \tag{8.17}$$

where $F^{\mathrm{Q}}_{\alpha\beta}$ takes the same form as in eq. (6.33) because the magnetic field points in the z-direction. This produces a local baryon charge given by the zeroth component of the baryon current,[3]

$$n_{\mathrm{B}}(z) = j^0_{\mathrm{B}} = \frac{H}{4\pi^2}\partial_z\phi. \tag{8.18}$$

[2] $\mathbb{R}$ can be compactified to S^1 using for instance a stereographic projection. Hence, we have a map $\phi : S^1 \mapsto S^1$.

[3] We can also calculate the local electric and isospin charge in a similar way. Additionally, it is argued in [46] that the anomalous term in the Lagrangian leads to a nonzero magnetization.

Thus, the baryon number, per unit area in the xy-plane, carried by a unit cell of the lattice is

$$\frac{N_{\mathrm{B}}}{S} = \frac{H}{4\pi^2}\int_{-\ell/2}^{\ell/2} \mathrm{d}z \frac{\partial\phi(z)}{\partial z} = \frac{H}{4\pi^2}\left[\phi(\ell/2) - \phi(-\ell/2)\right] = \frac{H}{2\pi}. \tag{8.19}$$

We can see that the baryon number is only dependent on the boundary values $\phi(\ell/2)$ and $\phi(-\ell/2)$, and not dependent on the behavior of $\phi(z)$ throughout the unit cell. The baryon number is therefore a topological charge generated by the change of winding number over one unit cell.

A topological soliton connecting two different vacua in $3+1$ dimensions gives rise to a two-dimensional domain wall. The domain wall is the boundary between these vacua. Figure 8.1 (A) shows that for k close to one, we have a series of such domain walls that are uniform in the xy-plane. Figures 8.1 (A) and (B) illustrates how the domain walls align with maximal local baryon charge. This makes the array structure of the solution more obvious. We can conclude that the solution with k close to one corresponds to an array of topological solitons carrying baryon charge. The solution will break parity since it is coordinate-dependent and consists of pseudoscalar pions. An analogous structure called Chiral Soliton Lattice (CSL) can be found in chiral magnets. Our solution is therefore termed CSL.

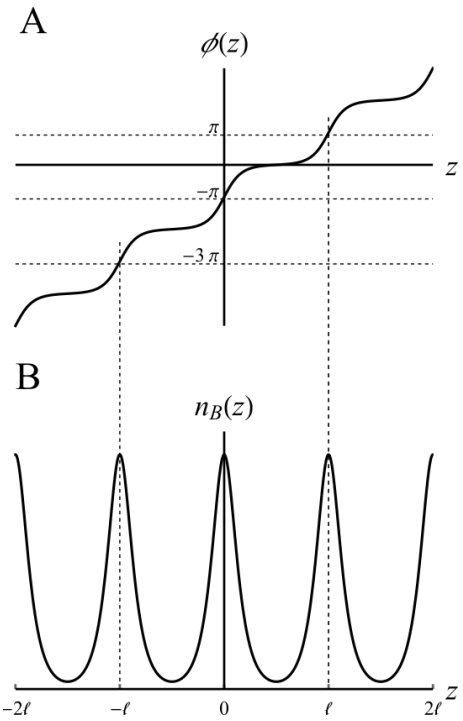

Figure 8.1: (A) Spatial distribution of ϕ with $k = 0.999$. (B) Spatial distribution of the local baryon charge with $k = 0.999$.

8.5 Ground state

The CSL can be studied more closely by determining the value of the parameter k in the ground state. This can be done by minimizing the total energy of each soliton

with respect to k. By eq. (8.5), the energy of each soliton with period ℓ per unit area in the xy-plane is

$$\begin{aligned}\frac{\mathscr{E}}{S} &= \int_{-\ell/2}^{\ell/2} \mathrm{d}z \mathscr{H} = \int_{-\ell/2}^{\ell/2} \mathrm{d}z \left[\frac{f_\pi^2}{2}(\partial_z\phi)^2 + m_\pi^2 f_\pi^2(1-\cos\phi) - \frac{\mu_B H}{4\pi^2}\partial_z\phi\right] \\ &= \int_{-\ell/2}^{\ell/2} \mathrm{d}z \left[\frac{f_\pi^2}{2}(\partial_z\phi)^2 - m_\pi^2 f_\pi^2 \cos\phi\right] + 2m_\pi f_\pi^2 k K(k) - \frac{\mu_B H}{2\pi}.\end{aligned} \tag{8.20}$$

The integral of the first term in the square bracket is given by

$$\begin{aligned}\frac{f_\pi^2}{2}\int_{-\ell/2}^{\ell/2} \mathrm{d}z(\partial_z\phi)^2 &= \frac{2m_\pi^2 f_\pi^2}{k^2}\int_{-\ell/2}^{\ell/2} \mathrm{d}z\, \mathrm{dn}^2(\bar{z},k) = \frac{4m_\pi f_\pi^2}{k}\int_0^K \mathrm{d}\bar{z}\, \mathrm{dn}^2(\bar{z},k) \\ &= \frac{4m_\pi f_\pi^2}{k}E(k),\end{aligned} \tag{8.21}$$

where $\mathrm{dn}(\bar{z},k)$ is the Jacobi delta amplitude and $E(k)$ is the complete elliptic integral of the second kind. By exploiting properties of the Jacobi elliptic functions found in [43], we can rewrite the second term in eq. (8.20) as

$$\begin{aligned}-m_\pi^2 f_\pi^2 \int_{-\ell/2}^{\ell/2} \mathrm{d}z \cos\phi &= m_\pi^2 f_\pi^2 \int_{-\ell/2}^{\ell/2} \mathrm{d}z \left(1 - \frac{2}{k^2} + \frac{2}{k^2}\mathrm{dn}^2(\bar{z},k)\right) \\ &= \frac{2m_\pi f_\pi^2}{k}\left[k^2 K(k) - 2K(k) + 2E(k)\right].\end{aligned} \tag{8.22}$$

Having eqs. (8.21) and (8.22) at hand, the resulting energy of each soliton per unit area in the xy-plane is

$$\frac{\mathscr{E}}{S} = 4m_\pi f_\pi^2\left[\frac{2E(k)}{k} + \left(k - \frac{1}{k}\right)K(k)\right] - \frac{\mu_B H}{2\pi} = \frac{\mathscr{E}_{\mathrm{norm}}}{S} - \frac{\mu_B N_B}{S}, \tag{8.23}$$

where $\mathscr{E}_{\mathrm{norm}}$ is the energy arising from the non-anomalous part of the Hamiltonian in eq. (8.5). This is consistent with the usual expression, $\mathscr{H} = \mathscr{H}_{\mathrm{norm}} - \mu_B n_B$, for the Hamiltonian at finite baryon density. $\mathscr{H}_{\mathrm{norm}}$ is the Hamiltonian in the absence of a baryon chemical potential. The total energy of the system with length L and volume $V = LS$ is

$$\mathscr{E}_{\mathrm{tot}} = L\frac{\mathscr{E}}{\ell} = \frac{V m_\pi}{2kK(k)}\left[F(k) - \frac{\mu_B H}{2\pi}\right], \tag{8.24}$$

where we have defined

$$F(k) \equiv 4m_\pi f_\pi^2\left[\frac{2E(k)}{k} + \left(k - \frac{1}{k}\right)K(k)\right]. \tag{8.25}$$

Letting $k \to 1$ will by eq. (8.15) lead to a period $\ell \to \infty$. This corresponds to a single domain wall. Thus, in the absence of a magnetic field, the energy of each soliton per unit area in the xy-plane will reduce to the familiar result [22]

$$\frac{\mathscr{E}}{S} = F(1) = 8m_\pi f_\pi^2. \tag{8.26}$$

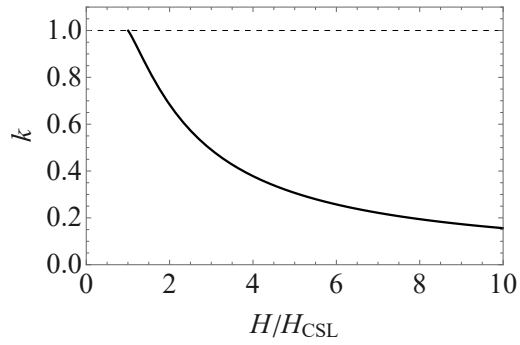

Figure 8.2: The ground state value of the elliptic modulus k as a function of external magnetic field with $f_\pi = 92$ Mev.

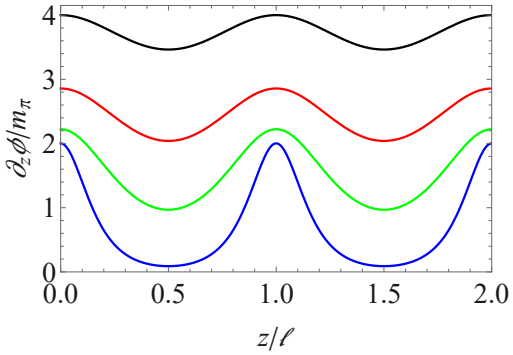

Figure 8.3: The gradient of ϕ as a function of position. The different curves correspond to $k = 0.999$ (blue), $k = 0.9$ (green), $k = 0.7$ (red) and $k = 0.5$ (black). All numerical values are obtained with $f_\pi = 92$ MeV.

We can now minimize the total energy $\mathscr{E}_{\text{tot}}$ of the system with respect to k at fixed volume V. It is helpful to note that

$$\frac{\mathrm{d}K}{\mathrm{d}k} = \frac{1}{k}\left(\frac{E(k)}{1-k^2} - K(k)\right), \tag{8.27}$$

$$\frac{\mathrm{d}E}{\mathrm{d}k} = \frac{1}{k}\left(E(k) - K(k)\right). \tag{8.28}$$

These derivatives can be used to show that

$$\frac{\mathrm{d}\mathscr{E}_{\text{tot}}}{\mathrm{d}k} = \frac{-2Vm_\pi^2 f_\pi^2 E(k)}{k^2(1-k^2)K(k)}\left(\frac{2E(k)}{k} - \frac{\mu_B H}{8\pi m_\pi f_\pi^2}\right), \tag{8.29}$$

which equated to zero yields a condition for the ground state value of k reading

$$\frac{E(k)}{k} = \frac{\mu_B H}{16\pi m_\pi f_\pi^2}. \tag{8.30}$$

Therefore, the CSL solution exists if and only if k satisfies this condition for the given external parameters μ_B and H. Now that $0 \leq k \leq 1$, the left-hand side is bounded from below and the condition for the CSL solution to exist can be written as

$$\mu_B H \geq (\mu_B H)_{\text{CSL}} \equiv 16\pi m_\pi f_\pi^2. \tag{8.31}$$

The CSL solution can therefore exist at an arbitrary small magnetic field in the chiral limit. The ground state value of k is plotted in figure 8.2. We can see that the case of a single domain wall having $k = 1$ is obtained at a critical magnetic field H_{CSL}. Figure 8.3 shows how the gradient of ϕ is affected by the value of k. The gradient of ϕ gives information about how the soliton solutions interpolate between two vacua. Additionally, it is proportional to the local baryon charge by eq. (8.18). Comparing figure 8.2 to figure 8.3 reveals that magnetic fields close to H_{CSL} yields a CSL consisting of thin domain walls. As the magnetic field increases, the CSL turns into a smooth, cosine-like profile. Moreover, we can illustrate how the period of the

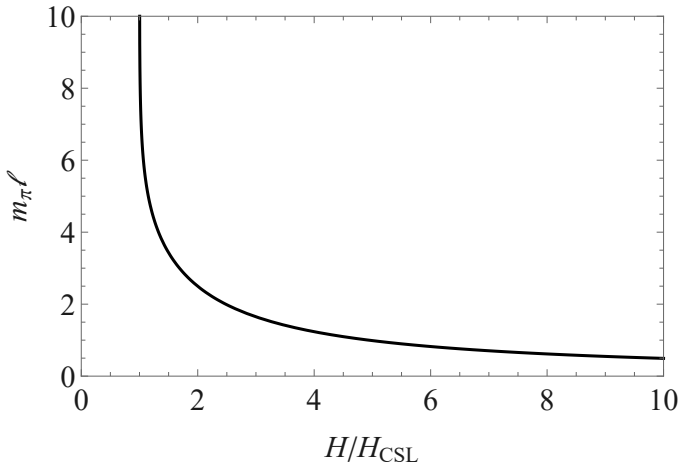

Figure 8.4: The period of the CSL ℓ in units of inverse pion mass as a function of external magnetic field with $f_\pi = 92$ MeV.

CSL changes with magnetic field using eq. (8.15). In figure 8.4, we have plotted the period in units of inverse pion mass as a function of the magnetic field. We observe that the period is large close to the critical magnetic field. To sum up, the CSL with a magnetic field close to $H_{\rm CSL}$ consists of thin domain walls with large separation.

8.6 Chiral soliton lattice as the ground state of QCD

We will now turn our attention to where the CSL can be realized in QCD. Firstly, there is not enough energy to excite any particles if $\mu_{\rm B} \leq m_{\rm N}$, where $m_{\rm N}$ is the nucleon mass. In that case, we have a QCD vacuum with $\phi = 0$. Consequently, by eq. (8.5), the energy density is zero. However, if we obtain the soliton energy in the CSL ground state by combining eqs. (8.23) and (8.30) we find

$$\frac{\mathscr{E}}{S} = 4m_\pi f_\pi^2 \left(k - \frac{1}{k}\right) K(k) < 0, \tag{8.32}$$

where we have used that $K(k) > 0$ and $0 \leq k < 1$. As a result, the CSL ground state is energetically more favorable than the QCD vacuum when $\mu_{\rm B} \leq m_N$. In other words, nature will prefer the CSL over the QCD vacuum if $\mu_{\rm B} \leq m_{\rm N}$ and $\mu_{\rm B} H \geq (\mu_{\rm B} H)_{\rm CSL}$ is fulfilled.

Finally, nuclear matter is a substance consisting of an infinite number of nucleons. It is distributed with uniform density over an infinite volume. Nucleons have baryon number one, causing nuclear matter to have energy $m_{\rm N} - \mu_{\rm B}$ per baryon number. The soliton energy per baryon number in the CSL ground state is given by eqs. (8.23), (8.19) and (8.30), and reads

$$\frac{\mathscr{E}}{N_{\rm B}} = \frac{8\pi m_\pi f_\pi^2}{H} \left(k - 1/k\right) K(k)) < 0. \tag{8.33}$$

The CSL ground state is therefore energetically more favorable than nuclear matter when $\mu_{\rm B} \approx m_{\rm N}$. The binding energy of nucleons reduces the total energy of nucleons

implying that μ_B can be slightly less than m_N. We conclude that the CSL is realized when the condition in eq. (8.31) is fulfilled.

In order to determine the validity of the derivative expansion in ChPT, we can obtain the momentum scale associated with the exact solution in eq. (8.14). This scale is given by the maximum value of

$$\partial_z \phi(\bar{z}) = \frac{2m_\pi}{k}\mathrm{dn}(\bar{z}, k) = \frac{\mu H}{8\pi f_\pi^2 E(k)}\mathrm{dn}(\bar{z}, k), \tag{8.34}$$

where we have inserted the value of k using eq. (8.30). This has the maximal value

$$p_{\mathrm{CSL}} = \frac{\mu H}{8\pi f_\pi^2}. \tag{8.35}$$

When $\mu_B H = (\mu_B H)_{\mathrm{CSL}}$, which satisfies eq. (8.31), we have a maximal value of

$$p_{\mathrm{CSL}} = 2m_\pi \approx 280\,\mathrm{MeV} \ll 4\pi f_\pi \approx 1156\,\mathrm{MeV}. \tag{8.36}$$

We can see that this satisfies the constraint on ChPT given in section 4.3 when $m_\pi \approx 140$ MeV and $f_\pi \approx 92$ MeV. The ChPT Lagrangian in eq. (8.2) is of second order in the derivative expansion, meaning that it includes all corrections up to the order $(p_{\mathrm{CSL}}/4\pi f_\pi)^2$. Any higher order corrections can be neglected as long as $p_{\mathrm{CSL}} \ll 4\pi f_\pi$.

Chapter 9

Excitation spectrum in a chiral soliton lattice

In the previous chapter, we observed how the CSL leads to a modulation of the background in the direction of the external magnetic field. We will in this chapter see how this gives rise to a phonon of the soliton lattice. The rest of this thesis will focus on a finite isospin density instead of a finite baryon density. This amounts to letting $\mu_B \to \mu_I/2$ in the previous chapter. First, we will derive the dispersion relation of the phonon in a fixed external magnetic field. This was done for a CSL with finite baryon density in [23]. Next, we introduce dynamical electromagnetic fields, which alter the excitation spectrum in presence of the CSL background. The dispersion relations are obtained by solving the equations of motion linearized around the CSL background. Closed analytic solutions are found in the chiral limit and for pion-like excitations propagating along the direction of the external magnetic field. In other cases, we provide approximate solutions to the dispersion relations. We will use the same method as in [47] where the excitation spectrum is derived in presence of a baryon chemical potential. It is interesting to note that the system has three gapless modes in the absence of pion-photon coupling. These are the phonon of the soliton lattice and the two photon polarizations. However, turning on the coupling will give rise to two gapped excitations and only one gapless mode. This happens even though the Higgs mechanism for photons is absent and the fact that spontaneous breaking of spatial translations occurs.

9.1 Phonons

The dispersion relation of the phonon of the soliton lattice is derived from the Lagrangian in presence of a fixed external magnetic field $\boldsymbol{H}$ and an isospin chemical potential μ_I. The full Lagrangian has the form

$$\mathscr{L} = \mathscr{L}_{\text{ChPT}} + \mathscr{L}_{\text{WZW}} = \frac{f_\pi^2}{4}\left[\text{Tr}(D_\mu\Sigma^\dagger D^\mu\Sigma) + 2m_\pi^2\text{ReTr}\Sigma\right] + \frac{\mu_I}{8\pi^2}\boldsymbol{H}\cdot\boldsymbol{\nabla}\phi, \quad (9.1)$$

where the ChPT Lagrangian is given by eq. (4.16). Furthermore, the ordinary derivative has been promoted to a covariant derivative reading

$$D_\mu\Sigma \equiv \partial_\mu\Sigma - i[\delta_{\mu 0}\mu_I I_3 - Q_\mu, \Sigma] = \partial_\mu\Sigma - \frac{1}{2}i\left(\delta_{\mu 0}\mu_I - A_\mu\right)[\tau_3, \Sigma] = \partial_\mu\Sigma, \quad (9.2)$$

where $Q_\mu \equiv A_\mu \tau_3/2$. The commutator is zero since the CSL consists solely of neutral pions, implying that $\Sigma = e^{i\tau_3\phi}$. The last term of the Lagrangian is the Wess-Zumino-Witten term given by eq. (6.37). Following similar arguments as in sections 8.1 and 8.2 results in an identical equation of motion

$$\partial_z^2 \phi = m_\pi^2 \sin\phi, \tag{9.3}$$

with the CSL solution

$$\cos\left(\frac{\phi(\bar{z})}{2}\right) = \mathrm{sn}(\bar{z}, k) \quad \Leftrightarrow \quad \phi(\bar{z}) = 2\mathrm{am}(\bar{z}, k) - \pi, \tag{9.4}$$

where $\bar{z} = \frac{z m_\pi}{k}$. We will in the following see how this solution gives rise to a phonon of the soliton lattice. First, we note that SSB leads to broken generators of the broken symmetry. If the Noether charge densities of the broken generators are linearly dependent, it will lead to redundant Goldstone bosons [48]. The Noether charge densities for translation T^{0i} and rotation R^{0i} are related by

$$R^{0i} = \varepsilon_{ijk} x^j T^{0k}. \tag{9.5}$$

The CSL spontaneously breaks continuous translational symmetry down to a discrete one in the z-direction. In addition, it spontaneously breaks continuous rotational symmetry down to rotational symmetry around the z-axis. The Noether charge densities associated with the generators of these broken symmetries are related through eq. (9.5). Consequently, we expect exactly one Goldstone boson of the CSL. This is the phonon of the soliton lattice. The dispersion relation of the phonon can be obtained by examining the linear perturbations of the CSL solution. We start out by introducing linear perturbations, $\pi(x)$, of the neutral pion field ϕ such that $\phi \to \phi + \pi(x)$, where x is a four-vector. From eq. (9.3), we conclude that fluctuations with full spacetime dependence yield the linearized equation of motion

$$\left(\Box^2 + m_\pi^2 \cos\phi\right)\pi = 0. \tag{9.6}$$

Observing that the CSL background only depends on the z-coordinate, we can carry out a Fourier transform in x, y and t, resulting in

$$\left[-\partial_{\bar{z}}^2 + 2k^2 \mathrm{sn}^2(\bar{z}, k)\right]\pi = \frac{k^2}{m_\pi^2}\left[m_\pi^2 + \omega^2 - \left(p_x^2 + p_y^2\right)\right]\pi, \tag{9.7}$$

where we used eq. (9.4) and the fact that $\cos(2\mathrm{am}(\bar{z}, k)) = 1 - 2\mathrm{sn}^2(\bar{z}, k)$. The left-hand side is known as the Lamé operator with $n = 1$ [49]. The general form of the Lamé equation is

$$\left[-\partial_{\bar{z}}^2 + n(n+1)k^2 \mathrm{sn}^2(\bar{z}, k)\right]\psi(\bar{z}) = A\psi(\bar{z}). \tag{9.8}$$

Having $n = 1$ gives the solution

$$\psi(\bar{z}) = \frac{H(\bar{z} + \sigma, k)}{\Theta(\bar{z}, k)} e^{-\bar{z} Z(\sigma, k)}, \tag{9.9}$$

where H, Θ and Z are the Jacobi's eta, theta and zeta functions, respectively. Moreover, σ is a complex parameter related to A by

$$A = 1 + k^2 \mathrm{cn}^2(\sigma, k). \tag{9.10}$$

We can cast eq. (9.9) into a Bloch form reading

$$\psi(\bar{z}) = \frac{H(\bar{z}+\sigma,k)}{\Theta(\bar{z},k)}\exp\left[-i\pi\frac{\bar{z}}{2K(k)}\right]\exp\left\{i\bar{z}\left[iZ(\sigma,k)+\frac{\pi}{2K(k)}\right]\right\}. \tag{9.11}$$

The two first factors are together periodic in $\bar{z}$ with period $2K(k)$, meaning that the period of z is $2kK(k)/m_\pi = \ell$. The last factor has the form $e^{ip_z z} = e^{ik\bar{z}p_z/m_\pi}$. Hence, the crystal momentum associated with the phonon of the soliton lattice is

$$p_z = \frac{m_\pi}{k}\left[iZ(\sigma,k)+\frac{\pi}{2K(k)}\right] = \frac{im_\pi}{k}Z(\sigma,k)+\frac{\pi}{\ell}. \tag{9.12}$$

The solution in eq. (9.11) is only physically acceptable when it is bounded. Hence, $Z(\sigma,k)$ has to be purely imaginary. This happens for $\mathrm{Re}(\sigma)=0$ or $\mathrm{Re}(\sigma)=K(k)$. The Lamé equation with $n=1$ thus has two solutions corresponding to the two bands

$$\begin{aligned}\sigma_{\mathrm{v}} =& K(k)+i\kappa,\\ \sigma_{\mathrm{c}} =& i\kappa,\end{aligned} \tag{9.13}$$

where σ_{v} corresponds to the "valence band" with the phonon excitation, while σ_{c} corresponds to the "conduction band".[1] The next step in finding the dispersion relation of the phonon is to identify A in eq. (9.8). We start out by observing that the minimum of the valence band appears at $\kappa = K(k')$, where $k' \equiv \sqrt{1-k^2}$ is the complementary elliptic modulus. We shift κ to the minimum by $\delta\kappa \equiv \kappa - K(k')$. This allows us to show that

$$\mathrm{cn}(\sigma_{\mathrm{v}},k) = -\frac{ik'}{k}\mathrm{cn}(\delta\kappa,k'), \tag{9.14}$$

where we have exploited the periodicity of the Jacobi elliptic functions given by eq. (16.8.2) in [43]. Thus, eq. (9.10) becomes

$$A = 1-k'^2\mathrm{cn}^2(\delta\kappa,k'). \tag{9.15}$$

A purely longitudinal motion where $p_x = p_y = 0$ will from eqs. (9.7) and (9.8) give

$$\frac{\omega}{m_\pi} = \frac{k'}{k}\mathrm{sn}(\delta\kappa,k') \approx \frac{k'}{k}\delta\kappa + \mathcal{O}\left(\delta\kappa^3\right), \tag{9.16}$$

in which we expect that $\delta\kappa$ is small since $\kappa = K(k')$ at the bottom of the valence band. A relation between κ and the crystal momentum p_z is found by exploiting the identity

$$\frac{\mathrm{d}Z(\sigma,k)}{\mathrm{d}\sigma} = \mathrm{dn}^2(\sigma,k) - \frac{E(k)}{K(k)}. \tag{9.17}$$

Again, we rewrite the Jacobi elliptic function at the valence band in terms of $\delta\kappa$, yielding

$$\mathrm{dn}(\sigma_{\mathrm{v}},k) = -k'\mathrm{sn}(\delta\kappa,k'), \tag{9.18}$$

which vanishes to all orders when $\delta\kappa = 0$. Combining eqs. (9.12) and (9.17) provides the relation

$$\frac{\mathrm{d}p_z}{\mathrm{d}\kappa} = \frac{m_\pi E(k)}{kK(k)} \tag{9.19}$$

[1] A study of the band structure resulting from the Lamé equation can be found in [50].

at the bottom of the valence band. Keeping a purely longitudinal motion and using eqs. (9.16) and (9.19) gives the phonon group velocity

$$c_{\rm ph} = \frac{\mathrm{d}\omega}{\mathrm{d}p_z} = \frac{\mathrm{d}\omega/\mathrm{d}\kappa}{\mathrm{d}p_z/\mathrm{d}\kappa} = \sqrt{1-k^2}\frac{K(k)}{E(k)}. \tag{9.20}$$

The group velocity rapidly increases towards the speed of light as the magnetic field increases above the critical magnetic field for the formation of the CSL. Restoring transverse motion on the CSL background gives by eq. (9.7) the full phonon dispersion relation

$$\omega^2 = p_x^2 + p_y^2 + (1-k^2)\left[\frac{K(k)}{E(k)}\right]^2 p_z^2 + \mathcal{O}(p_z^4), \tag{9.21}$$

where the crystal momentum p_z is measured from the bottom of the valence band. The neutral pion fluctuations of the CSL are represented by this phonon.[2]

9.2 ChPT including dynamical electromagnetic fields

We will in the following couple the neutral pion fluctuation, found in the previous section, to photon fluctuations of the CSL background. The full Lagrangian with an isospin chemical potential and dynamical electromagnetic fields A_μ reads

$$\mathscr{L} = \mathscr{L}_{\rm ChPT} + \mathscr{L}_{\rm WZW} + \mathscr{L}_{\rm QED}, \tag{9.22}$$

where the ChPT Lagrangian remains the same as in eq. (9.1). Allowing for fluctuations in the electromagnetic fields A_μ changes the Wess-Zumino-Witten term given by eq. (7.26) to

$$\begin{aligned}\mathscr{L}_{\rm WZ} &= -\frac{\pi^0}{32\pi^2 f_\pi}\varepsilon^{\mu\nu\alpha\beta}F_{\mu\nu}(F_{\alpha\beta}+F^{\rm I}_{\alpha\beta}) \\ &= -\frac{\pi^0}{32\pi^2 f_\pi}\varepsilon^{\mu\nu\alpha\beta}F_{\mu\nu}F_{\alpha\beta} - \frac{\mu_I}{16\pi^2 f_\pi}\varepsilon^{0\mu\nu\alpha}F_{\mu\nu}\partial_\alpha\pi^0,\end{aligned} \tag{9.23}$$

where $A^I_\mu = (\mu_I, \mathbf{0})$ and we defined the electromagnetic field strength tensor $F^{\rm Q}_{\mu\nu} \equiv F_{\mu\nu}$. Finally, we have the Lagrangian of quantum electrodynamics (QED)

$$\mathscr{L}_{\rm QED} = -\frac{1}{4}F_{\mu\nu}F^{\mu\nu} + \frac{1}{2\xi}\left(\partial_\mu A^\mu\right)^2 - j^\mu_{\rm back}A_\mu, \tag{9.24}$$

which describes the dynamics of the dynamical electromagnetic fields. The second term is a gauge-fixing term. The Faddeev-Popov procedure for adding gauge-fixing terms will be described in chapter 10. A coupling to a classical charged background is given by the third term. Hence, the full Lagrangian in eq. (9.22) with $\Sigma = \exp(\frac{i}{f_\pi}\tau_3\pi^0)$ becomes

$$\begin{aligned}\mathscr{L} = &\frac{1}{2}\left(\partial_\mu\pi^0\right)^2 + m_\pi^2 f_\pi^2\cos\left(\frac{\pi^0}{f_\pi}\right) - \frac{\mu_I C}{4}\varepsilon^{0\mu\nu\alpha}F_{\mu\nu}\partial_\alpha\pi^0 - \frac{C}{8}\pi^0\varepsilon^{\mu\nu\alpha\beta}F_{\mu\nu}F_{\alpha\beta} \\ &- \frac{1}{4}F_{\mu\nu}F^{\mu\nu} + \frac{1}{2\xi}\left(\partial_\mu A^\mu\right)^2 - j^\mu_{\rm back}A_\mu,\end{aligned} \tag{9.25}$$

[2]Dispersion relations for the charged pion fluctuations of the CSL are obtained in [23].

where the constant $C \equiv \frac{1}{4\pi^2 f_\pi}$. The non-relativistic version of the Lagrangian can be obtained by noting that $A^\mu = (\varphi, \boldsymbol{A})$ and $j^\mu = (\rho, \boldsymbol{j})$. This gives

$$\begin{aligned}\mathscr{L} = &\frac{1}{2}\left[\left(\dot{\pi}^0\right)^2 - \left(\boldsymbol{\nabla}\pi^0\right)^2\right] + m_\pi^2 f_\pi^2 \cos\left(\frac{\pi^0}{f_\pi}\right) + \frac{\mu_I C}{2}\boldsymbol{B}\cdot\boldsymbol{\nabla}\pi^0 + C\pi^0\boldsymbol{E}\cdot\boldsymbol{B} \\ &+ \frac{1}{2}\left(\boldsymbol{E}^2 - \boldsymbol{B}^2\right) + \frac{1}{2\xi}\left(\dot{\varphi} + \boldsymbol{\nabla}\cdot\boldsymbol{A}\right) - \rho_{\text{back}}\varphi + \boldsymbol{j}_{\text{back}}\cdot\boldsymbol{A},\end{aligned} \tag{9.26}$$

where the term proportional to μ_I is found using eq. (6.35). We can now derive the equations of motion in the Lorenz gauge $\partial_\mu A^\mu = 0$. Starting with the Euler-Lagrange equations for π^0, using the Lagrangian in eq. (9.25), we find

$$\frac{\partial\mathscr{L}}{\partial\pi^0} = -m_\pi^2 f_\pi \sin\left(\frac{\pi^0}{f_\pi}\right) + C\boldsymbol{E}\cdot\boldsymbol{B} \tag{9.27}$$

and

$$\begin{aligned}\partial_\gamma\left(\frac{\partial\mathscr{L}}{\partial\left(\partial_\gamma\pi^0\right)}\right) &= \ddot{\pi}^0 - \boldsymbol{\nabla}^2\pi^0 + \frac{\mu_I C}{4}\varepsilon^{0\mu\nu\gamma}\partial_\gamma F^Q_{\mu\nu} \\ &= \ddot{\pi}^0 - \boldsymbol{\nabla}^2\pi^0,\end{aligned} \tag{9.28}$$

where the term proportional to μ_I vanishes due to the Bianchi identity. The resulting equation of motion is therefore

$$\ddot{\pi}^0 - \boldsymbol{\nabla}^2\pi^0 + m_\pi^2 f_\pi \sin\left(\frac{\pi^0}{f_\pi}\right) = C\boldsymbol{E}\cdot\boldsymbol{B}. \tag{9.29}$$

Next, we derive the equations of motion resulting from each component of the electromagnetic four-potential. The Euler-Lagrange equations take the form

$$\frac{\partial\mathscr{L}}{\partial A_\delta} = \partial_\gamma\left(\frac{\partial\mathscr{L}}{\partial\left(\partial_\gamma A_\delta\right)}\right), \tag{9.30}$$

where

$$\frac{\partial\mathscr{L}}{\partial A_\delta} = -j^\delta_{\text{back}} \tag{9.31}$$

and

$$\begin{aligned}\frac{\partial\mathscr{L}}{\partial\left(\partial_\gamma A_\delta\right)} &= -\frac{C}{8}\pi^0\varepsilon^{\mu\nu\alpha\beta}\frac{\partial}{\partial\left(\partial_\gamma A_\delta\right)}\left[\left(\partial_\mu A_\nu - \partial_\nu A_\mu\right)\left(\partial_\alpha A_\beta - \partial_\beta A_\alpha\right)\right] - F^{\gamma\delta} \\ &= -\frac{C}{2}\pi^0\varepsilon^{\mu\nu\gamma\delta}F_{\mu\nu} - F^{\gamma\delta}.\end{aligned} \tag{9.32}$$

Thus, the equations of motion (9.30) are cast as

$$j^\delta_{\text{back}} = \frac{C}{2}\varepsilon^{\mu\nu\gamma\delta}F_{\mu\nu}\partial_\gamma\pi^0 + \partial_\gamma F^{\gamma\delta}, \tag{9.33}$$

where we have performed a partial integration of the first term. The equation of motion resulting from $\delta = 0$ reads

$$\begin{aligned}\rho_{\text{back}} &= \frac{C}{2}\varepsilon^{\mu\nu\gamma 0}F_{\mu\nu}\partial_\gamma\pi^0 + \partial_\gamma F^{\gamma 0} \\ &= C\boldsymbol{B}\cdot\boldsymbol{\nabla}\pi^0 + \partial_\gamma F^{\gamma 0} \\ &= C\boldsymbol{B}\cdot\boldsymbol{\nabla}\pi^0 + \boldsymbol{\nabla}\cdot\boldsymbol{E},\end{aligned} \tag{9.34}$$

where we have used that $\boldsymbol{E} = -\boldsymbol{\nabla}\varphi - \dot{\boldsymbol{A}}$. The equation of motion resulting from $\delta = i$ is

$$j^i_{\text{back}} = \frac{C}{2}\varepsilon^{\mu\nu\gamma i}F_{\mu\nu}\partial_\gamma\pi^0 + \partial_\gamma F^{\gamma i}, \tag{9.35}$$

where the first term can be cast as

$$\begin{aligned}\frac{C}{2}\varepsilon^{\mu\nu\gamma i}F_{\mu\nu}\partial_\gamma\pi^0 &= \frac{C}{2}\varepsilon^{\mu\nu 0 i}F_{\mu\nu}\dot{\pi}^0 + \frac{C}{2}\varepsilon^{\mu\nu j i}F_{\mu\nu}\partial_j\pi^0 \\ &= -CB_i\dot{\pi}^0 - \frac{C}{2}\varepsilon^{i\mu\nu j}F_{\mu\nu}\partial_j\pi^0 \\ &= -CB_i\dot{\pi}^0 + C\varepsilon^{ik0j}F_{0k}\partial_j\pi^0 \\ &= -CB_i\dot{\pi}^0 + C\varepsilon^{0ikj}E_k\partial_j\pi^0 \\ &= -CB_i\dot{\pi}^0 + C\varepsilon_{ijk}E_j\partial_k\pi^0,\end{aligned} \tag{9.36}$$

in which we have used that $\varepsilon^{0ikj} = \varepsilon^{ikj}$ making it possible to exploit the relations $B_i = -\frac{1}{2}\varepsilon_{ijk}F^{jk}$ and $F_{0k} = E_k$. The second term in eq. (9.35) reads

$$\partial_\gamma F^{\gamma i} = \ddot{A}_i + \partial_i\dot{\varphi} - \left(\boldsymbol{\nabla}^2\boldsymbol{A}\right)_i + \left[\boldsymbol{\nabla}\cdot(\boldsymbol{\nabla}\cdot\boldsymbol{A})\right]_i = (\boldsymbol{\nabla}\times\boldsymbol{B})_i - \dot{E}_i, \tag{9.37}$$

where $\boldsymbol{B} = \boldsymbol{\nabla}\times\boldsymbol{A}$. Hence, eq. (9.35) yields

$$\boldsymbol{\nabla}\times\boldsymbol{B} = \boldsymbol{j}_{\text{back}} + \dot{\boldsymbol{E}} + C\boldsymbol{B}\dot{\pi}^0 + C\boldsymbol{E}\times\boldsymbol{\nabla}\pi^0. \tag{9.38}$$

To summarize, the equations of motion given by eqs. (9.29), (9.34) and (9.38) read

$$\begin{aligned}\ddot{\pi}^0 - \boldsymbol{\nabla}^2\pi^0 + m_\pi^2 f_\pi \sin\left(\frac{\pi^0}{f_\pi}\right) &= C\boldsymbol{E}\cdot\boldsymbol{B}, \\ \boldsymbol{\nabla}\cdot\boldsymbol{E} &= \rho_{\text{back}} - C\boldsymbol{B}\cdot\boldsymbol{\nabla}\pi^0, \\ \boldsymbol{\nabla}\times\boldsymbol{B} &= \boldsymbol{j}_{\text{back}} + \dot{\boldsymbol{E}} + C\boldsymbol{B}\dot{\pi}^0 + C\boldsymbol{E}\times\boldsymbol{\nabla}\pi^0.\end{aligned} \tag{9.39}$$

The first equation is the Klein-Gordon equation for the pion field, where the source is the Pontryagin density for the electromagnetic field. The second and third equations are Maxwell's equations in presence of the chiral isospin anomaly. These are the basic equations of axion electrodynamics [51]. We want to study the electrodynamics of neutral pions in a uniform external magnetic field $\boldsymbol{H}$. Thus, we need a ground state where $\boldsymbol{B} = \boldsymbol{H}$ and $\boldsymbol{E} = \boldsymbol{0}$. In order to ensure zero electric field, the system has to be locally electrically neutral. Overall electrical neutrality is also necessary to guarantee the existence of a thermodynamic limit. This is because the electric energy scales with the system size R to the power five. On the contrary, the energy resulting from strong interactions and the interaction with the external magnetic field only scales as R^3 within the regime of validity of ChPT [17]. We must therefore assume that the background neutralizes the electric charge arising from the nonuniform pion field configuration,

$$\rho_{\text{back}} = C\boldsymbol{H}\cdot\left\langle\boldsymbol{\nabla}\pi^0\right\rangle \quad \text{and} \quad \boldsymbol{j}_{\text{back}} = 0. \tag{9.40}$$

The angular brackets represent the ground state expectation value which is equal to the CSL solution ϕ found in eq. (9.4) when $\boldsymbol{H} = (0, 0, H)$. We will assume that the background charge density is fixed and unaffected by fluctuations of the pion and electromagnetic field. This is justified in section 9.7 for sufficiently low energies.

9.3 Equations of motion

In this section, we derive the equations of motion linearized around the CSL background. We do so by introducing the field fluctuations $\delta\pi^0$, $\delta\boldsymbol{E}$ and $\delta\boldsymbol{B}$ around the ground state, such that

$$\begin{aligned}\pi^0 &= \langle\pi^0\rangle + \delta\pi^0,\\ \boldsymbol{E} &= \delta\boldsymbol{E},\\ \boldsymbol{B} &= \boldsymbol{H} + \delta\boldsymbol{B},\end{aligned} \tag{9.41}$$

where $\boldsymbol{H} = (0, 0, H)$ is the external magnetic field pointing in z-direction. Inserting this into the equations of motion (9.39) and expanding to first order in the fluctuations, we find

$$\delta\ddot{\pi}^0 - \boldsymbol{\nabla}^2\delta\pi^0 + m_\pi^2\delta\pi^0\cos\left(\frac{\langle\pi^0\rangle}{f_\pi}\right) = C\boldsymbol{H}\cdot\delta\boldsymbol{E}, \tag{9.42}$$

$$\boldsymbol{\nabla}\cdot\delta\boldsymbol{E} = -C\delta\boldsymbol{B}\cdot\left\langle\boldsymbol{\nabla}\pi^0\right\rangle - C\boldsymbol{H}\cdot\boldsymbol{\nabla}\delta\pi^0, \tag{9.43}$$

$$\boldsymbol{\nabla}\times\delta\boldsymbol{B} = \delta\dot{\boldsymbol{E}} + C\boldsymbol{H}\delta\dot{\pi}^0 - C\delta\boldsymbol{E}\times\left\langle\boldsymbol{\nabla}\pi^0\right\rangle, \tag{9.44}$$

where we used eq. (9.40) in order to obtain the last two equations. Furthermore, we exploited the equation of motion (9.4) for the CSL background. We can perform a Fourier transform of the fluctuations in x, y and t since the background only depends on the z-coordinate. The z-dependence is isolated by introducing the complex amplitudes $\Pi(z)$, $\boldsymbol{e}(z)$ and $\boldsymbol{b}(z)$, yielding

$$\begin{aligned}\delta\pi^0(\boldsymbol{r},t) &= \Pi(z)e^{-i\omega t}e^{i\boldsymbol{p}_\perp\cdot\boldsymbol{r}_\perp},\\ \delta\boldsymbol{E}(\boldsymbol{r},t) &= \boldsymbol{e}(z)e^{-i\omega t}e^{i\boldsymbol{p}_\perp\cdot\boldsymbol{r}_\perp},\\ \delta\boldsymbol{B}(\boldsymbol{r},t) &= \boldsymbol{b}(z)e^{-i\omega t}e^{i\boldsymbol{p}_\perp\cdot\boldsymbol{r}_\perp},\end{aligned} \tag{9.45}$$

where ω and $\boldsymbol{p}_\perp$ are the conjugate frequency and the transverse momentum. Substituting this into eq. (9.42), we find

$$\left(-\omega^2 - \partial_z^2 + \boldsymbol{p}_\perp^2 + m_\pi^2\cos\phi\right)\Pi - CHe_z = 0, \tag{9.46}$$

where $\phi = \langle\pi^0\rangle / f_\pi$. Next, we use the Bianchi identity $\boldsymbol{\nabla}\times\boldsymbol{E} = -\dot{\boldsymbol{B}}$ to solve for the magnetic field amplitude. Using index notation gives step by step

$$\begin{aligned}-\dot{B}_i &= (\boldsymbol{\nabla}\times\boldsymbol{E})_i,\\ i\omega b_i e^{i\boldsymbol{p}_\perp\cdot\boldsymbol{r}_\perp} &= \varepsilon_{ijk}\partial_j\left(e_k e^{i\boldsymbol{p}_\perp\cdot\boldsymbol{r}_\perp}\right),\\ i\omega b_i &= \varepsilon_{ijk}\left[\partial_j e_k + ie_k\partial_j\left(p_1x_1 + p_2x_2\right)\right],\\ b_i &= \frac{1}{iw}\left[\varepsilon_{i3k}\partial_3 e_k + i\varepsilon_{ijk}e_k\partial_j\left(p_1x_1 + p_2x_2\right)\right].\end{aligned} \tag{9.47}$$

The magnetic field amplitude can be used to show that (9.43) is redundant. This is stated in [47]. Finally, we recast eq. (9.44) by writing it on component form

$$\varepsilon_{ijk}\partial_j\delta B_k = \delta\dot{E}_i + CB_{\mathrm{ex,i}}\delta\dot{\pi}^0 - Cf_\pi\varepsilon_{ijk}\delta E_j\partial_k\phi. \tag{9.48}$$

Setting $i = 1$ yields step by step

$$\begin{aligned} \varepsilon_{1jk}\partial_j\left(b_k e^{i\boldsymbol{p}_\perp\cdot\boldsymbol{r}_\perp}\right) &= -i\omega e_1 e^{i\boldsymbol{p}_\perp\cdot\boldsymbol{r}_\perp} - Cf_\pi\varepsilon_{1jk}e_j\left(\partial_k\phi\right)e^{i\boldsymbol{p}_\perp\cdot\boldsymbol{r}_\perp} \\ -\partial_3 b_2 + ib_3 p_2 &= -i\omega e_1 - Cf_\pi e_2\partial_3\phi \\ i\left(\omega^2+\partial_z^2-p_y^2\right)e_x + \left(ip_x p_y + \omega C f_\pi\partial_z\phi\right)e_y + p_x\partial_z e_z &= 0, \end{aligned} \tag{9.49}$$

where we have inserted the result from eq. (9.47) going to the last line. Two more equations can be derived in a similar way by setting $i = 2$ and $i = 3$ in eq. (9.48). Thus, recalling eq. (9.46) leaves us with four equations that determine the dispersion relations of the quasiparticle excitations. These are

$$\begin{aligned} \left(-\omega^2-\partial_z^2+\boldsymbol{p}_\perp^2+m_\pi^2\cos\phi\right)\Pi - CHe_z &= 0, \\ i\omega^2 CH\Pi + \boldsymbol{p}_\perp\cdot\partial_z\boldsymbol{e}_\perp + i\left(\omega^2-\boldsymbol{p}_\perp^2\right)e_z &= 0, \\ i\left(\omega^2+\partial_z^2-p_y^2\right)e_x + \left(ip_x p_y+\omega C f_\pi\partial_z\phi\right)e_y + p_x\partial_z e_z &= 0, \\ \left(ip_x p_y - \omega C f_\pi\partial_z\phi\right)e_x + i\left(\omega^2+\partial_z^2-p_x^2\right)e_y + p_y\partial_z e_z &= 0. \end{aligned} \tag{9.50}$$

Before actually solving these, we can point out some general characteristics of the solutions. When the modes are propagating along the external magnetic field, $\boldsymbol{p}_\perp = 0$, the second equation reduces to $e_z = -CH\Pi$. Consequently, the first equation reads

$$\left(-\partial_z^2-\omega^2+C^2H^2+m_\pi^2\cos\phi\right)\Pi = 0, \tag{9.51}$$

which describes a pion that propagates on the CSL background. We know that the anomaly results in an electric charge of the neutral pion. Neutral pion fluctuations will therefore imply a fluctuation of local electric charge. Hence, it is no surprise that this generates a fluctuating electric field with a nonzero z-component. Next, we compare eq. (9.51) to eq. (9.6) where the electromagnetic field is fixed to the background value and the dispersion relation is always gapless. In the case of dynamical electromagnetic fields, there is an additional term C^2H^2 which gives rise to a gap of the pion being equal to

$$\omega = CH = \frac{H}{4\pi^2 f_\pi}. \tag{9.52}$$

This gap will exist both in the chiral limit and away from it. Furthermore, the two last equations in eq. (9.50) reduce to

$$\left(-\partial_z^2-\omega^2\pm\omega C f_\pi\partial_z\phi\right)e_\pm = 0, \tag{9.53}$$

where the helicity eigenstates of the electric field are denoted by $e_\pm \equiv e_x \pm ie_y$. These states are pure electromagnetic waves propagating in the z-direction. Furthermore, we note that one of the states will always be gapless.

9.4 Chiral limit

As a benchmark, we will first consider the dispersion relations in the chiral limit. The Hamiltonian of the neutral pion field with a fixed external magnetic field $\boldsymbol{H} = (0, 0, H)$ follows from eq. (9.26). In the chiral limit it is minimized when

$$\partial_z\phi = \frac{\mu_I CH}{2f_\pi}. \tag{9.54}$$

In figures 8.2 and 8.3 we observed that the CSL approaches a linear profile relatively fast as the magnetic field is increased above the critical magnetic field for the formation of the CSL. This was the case for a baryon chemical potential. However, we expect identical behavior for an isospin chemical potential since the equation of motion is the same in the two cases. The chiral limit is therefore representative for a large region of the QCD phase diagram in the μ_I-H plane. A constant gradient implies that we can perform a Fourier transform in the z-coordinate as well. The equations of motion (9.50) then reads

$$\begin{aligned}
\left(-\omega^2+\boldsymbol{p}^2\right)\pi - CHe_z &= 0,\\
\omega^2 CH\Pi + p_z \boldsymbol{p}_\perp\cdot\boldsymbol{e}_\perp + \left(\omega^2-\boldsymbol{p}_\perp^2\right)e_z &= 0,\\
\left(\omega^2-p_y^2-p_z^2\right)e_x + \left(p_xp_y - \frac{1}{2}i\mu_I\omega C^2H\right)e_y + p_xp_ye_z &= 0,\\
\left(p_xp_y + \frac{1}{2}i\mu_I\omega C^2H\right)e_x + \left(\omega^2-p_x^2-p_z^2\right)e_y + p_yp_ze_z &= 0.
\end{aligned} \tag{9.55}$$

This set of equations are solved by setting the determinant of the coefficients of Π, e_x, e_y and e_z to zero. Denoting the coefficient matrix by A, we have

$$\begin{aligned}
\mathrm{Det}(A) = \frac{1}{4}\omega^2\Big\{ &4\left[\boldsymbol{p}^2-\omega^2\right]^3 - \mu_I^2C^6H^4\omega^2\\
&+C^2H^2\left[\boldsymbol{p}^2-\omega^2\right]\left[4\boldsymbol{p}^2+\boldsymbol{p}_\perp^2\left(\mu_I^2C^2-4\right)-\omega^2\left(\mu_I^2C^2+4\right)\right]\Big\} = 0.
\end{aligned} \tag{9.56}$$

This has a cumbersome analytic solution. Instead, the low-momentum expansion of the dispersion relations is

$$\begin{aligned}
\omega_1 &= \frac{|\boldsymbol{p}|}{CH}\sqrt{\boldsymbol{p}_\perp^2+\frac{4p_z^2}{\mu_I^2C^2}} + \mathcal{O}(\boldsymbol{p}^4),\\
\omega_2 &= \frac{\mu_IC^2H}{2} + \mathcal{O}(\boldsymbol{p}^4),\\
\omega_3 &= CH + \mathcal{O}(\boldsymbol{p}^4).
\end{aligned} \tag{9.57}$$

Thus, we have two gapped modes, as well as one gapless mode which is anisotropic and quadratic at low momentum. Exact dispersion relations can be found if we consider for instance only propagation in the z-direction giving

$$\begin{aligned}
\omega_{1,2} &= \frac{1}{4}\left[\mp\mu_IC^2H + \sqrt{16p_z^2+\left(\mu_IC^2H\right)^2}\right],\\
\omega_3 &= \sqrt{p_z^2+C^2H^2}.
\end{aligned} \tag{9.58}$$

Inserting the dispersion relations into eqs. (9.51) and (9.53) we find that $\omega_{1,2}$ satisfies the equations of motion for the two circularly polarized photons, and ω_3 satisfies the equation of motion for the neutral pion field. Propagation solely in the transverse plane yields

$$\begin{aligned}
\omega_{1,3} &= \frac{1}{2}\left(\mp CH + \sqrt{4\boldsymbol{p}_\perp^2+C^2H^2}\right),\\
\omega_2 &= \frac{1}{2}\sqrt{4\boldsymbol{p}_\perp^2+\left(\mu_IC^2H\right)^2}.
\end{aligned} \tag{9.59}$$

The behavior of theses modes is found by substituting them into the equations of motion (9.55) setting $p_z = 0$. The two modes ω_1 and ω_3 are a mixture of a pion and an electromagnetic wave polarized linearly in the z-direction. The ω_2 mode is a purely electromagnetic wave polarized elliptically in the xy-plane. Taking the low-momentum limit reveals that the gapless ω_1 mode becomes primarily pion-like. As a result, both photon polarizations are gapped in this limit.

9.5 Single domain wall

Before considering the general CSL case, we want to discuss the case with a single domain wall where $k \to 1$. In section 8.5, we saw that $k \to 1$ at the critical external field $H = H_{\text{CSL}}$. In section 11.4, it is shown that this holds almost exactly even when dynamical electromagnetic fields are introduced. We will only consider propagation in the z-direction since the case of a single domain wall is only of limited interest. An isolated domain wall has the form [22]

$$\phi(z) = 4 \arctan \mathrm{e}^{m_\pi z}. \tag{9.60}$$

Thus, we have

$$\cos\phi = 1 - \frac{2}{\cosh^2 \tilde{z}}, \tag{9.61}$$

where $\tilde{z} \equiv m_\pi z$ is a dimensionless coordinate. Substituting this into the equation of motion (9.51) yields

$$\left(-\partial_{\tilde{z}}^2 - \frac{2}{\cosh^2 \tilde{z}}\right) \Pi = \frac{1}{m_\pi^2} \left(\omega^2 - m_\pi^2 - C^2 H^2\right) \Pi. \tag{9.62}$$

This represents an eigenvalue problem, $\mathcal{H}\Pi = \lambda\Pi$, where the Hamiltonian $\mathcal{H}$ can be recognized as the Pöschl-Teller Hamiltonian with one bound state [52]. The bound state corresponds to $\lambda = -1$ and has the dispersion relation

$$\omega = CH, \tag{9.63}$$

written in physical units. It describes a pion fluctuation that is localized on the domain wall. Such a fluctuation is expected since the domain wall completely breaks translational invariance in the z-direction leading to a Goldstone boson. This mode will propagate in the direction of the unbroken translations [53, 54]. However, the would-be Goldstone boson does in this case acquire a gap due to the interaction with the electromagnetic field. The gapless mode will instead appear in the electromagnetic sector, recalling that the helicity eigenstates of the electric field will always have one gapless mode.

9.6 General chiral soliton lattice

We will now turn our attention towards the dispersion relations for a general CSL background. Solving the equations of motion (9.50) for a general CSL background with a general direction of propagation needs to be done numerically. However, if we restrict our attention to modes propagating in the z-direction, we have shown in

eqs. (9.51) and (9.53) that the pion and photon degrees of freedom decouple. Eq. (9.51) is identical to the equation of motion (9.7) for CSL phonons except for the term C^2H^2. Hence, the dispersion relation of the neutral pion can simply be read off eq. (9.21) yielding

$$\omega_3^2 = C^2H^2 + (1-k^2)\left[\frac{K(k)}{E(k)}\right]^2 p_z^2 + \mathcal{O}(p_z^4), \tag{9.64}$$

where we have introduced the corresponding shift of the phonon dispersion relation. We confirm that the gap is the same as in eq. (9.52). The gap is also the same as in the chiral limit in eq. (9.57) and for a single pion domain wall in eq. (9.63). This must be the case because the gap in eq. (9.52) was independent of the background. The remaining task is therefore to determine the dispersion relation of the photon degrees of freedom. This will be done for very strong magnetic fields where $k \to 0$ and for close-to-critical magnetic fields where $k \to 1$. Ultimately, we conjecture a closed expression for the photon dispersion relation valid at all magnetic fields for the CSL. We start out by considering photons in very strong magnetic fields. Inserting the CSL background given by eq. (9.4) into the equation of motion (9.53) for the photons gives

$$\left[-\partial_{\bar{z}}^2 - \bar{\omega}^2 \mp \frac{\bar{\omega}}{2\pi^2}\mathrm{dn}(\bar{z},k)\right] e_\pm = 0, \tag{9.65}$$

where we have introduced the dimensionless frequency $\bar{\omega} = \omega k/m_\pi$ and $\bar{z} = zm_\pi/k$ as previously. Additionally, we used that $\partial_{\bar{z}}\phi(\bar{z}) = -2\mathrm{dn}(\bar{z},k)$. The Jacobi dn function can for small k be approximated to

$$\mathrm{dn}(\bar{z},k) \approx 1 - \frac{k^2}{2}\sin^2\bar{z}. \tag{9.66}$$

The value of k is found from the relation

$$\frac{E(k)}{k} = \frac{\mu_I H}{32\pi m_\pi f_\pi^2}, \tag{9.67}$$

which is the same relation as in eq. (8.30) when $\mu_I \to 2\mu_B$. The factor two arises because the anomaly for an isospin chemical potential is different by a factor two compared to the anomaly for a baryon chemical potential as argued in section 6.4. The relation is found without including dynamical electromagnetic fields. However, we will show in section 11.4 that it also holds almost exactly when they are included. Using the condition for k and rescaling the period of the sine function, it can easily be checked that the approximation to $\mathrm{dn}(\bar{z},k)$ is accurate within 5% for $H/H_{\mathrm{CSL}} > 2$ and within 1% for $H/H_{\mathrm{CSL}} > 3$ for all $\bar{z}$. Next, we define

$$a \equiv \bar{\omega}^2 \pm \frac{\bar{\omega}}{2\pi^2}\left(1 - \frac{k^2}{4}\right), \tag{9.68}$$

$$q \equiv \mp\frac{\bar{\omega}k^2}{16\pi^2}, \tag{9.69}$$

such that eq. (9.65) can be written as the Mathieu equation having the form

$$\left[\partial_{\bar{z}}^2 + (a - 2q\cos 2\bar{z})\right] e_\pm = 0. \tag{9.70}$$

This resembles the Schrödinger equation in a periodic potential. It is therefore expected that the solution can be written in the Bloch form $e_\pm(\bar{z}) = e^{i\bar{p}_z} P(\bar{z})$, where $P(\bar{z})$ is periodic in $\bar{z}$ and $\bar{p}_z \equiv p_z k/m_\pi$ is the dimensionless crystal momentum. Eq. (20.3.15) in [43] tells us that a in the Mathieu equation reads

$$a = \bar{p}_z^2 + \frac{q^2}{2(\bar{p}_z^2 - 1)} + \mathcal{O}(q^4). \tag{9.71}$$

The low-momentum behavior of the gapless mode is then determined by equating eqs. (9.68) and (9.71) arriving at

$$\omega = \frac{p_z^2}{m_\pi} \frac{2\pi^2 k}{1 - \frac{k^2}{4}} + \mathcal{O}(p_z^4), \tag{9.72}$$

which is written in terms of the physical units. The gapless dispersion relation is an exact solution to the Mathieu equation, and we can therefore expect it to be precise for medium-to-small k. Or, in other words, for very strong magnetic fields. We can check that the dispersion relation is consistent with the result in the chiral limit by noting that eq. (9.67) will for strong magnetic fields behave asymptotically as

$$\frac{k}{m_\pi} \approx \frac{16\pi^2 f_\pi^2}{\mu_I H}. \tag{9.73}$$

Substituting this into eq. (9.72) yields the gapless dispersion relation in the chiral limit in eq. (9.57) when $\boldsymbol{p}_\perp = 0$.

Next, we consider close-to-critical magnetic fields where the value of the elliptic modulus becomes $k \to 1$. This amounts to a lattice with well-separated thin domain walls. We can therefore make use of the thin-wall approximation wherein the domain walls are set to be infinitely thin. Considering a single domain wall discussed in section 9.5, we find that eq. (9.53) takes the form

$$\left(-\partial_{\tilde{z}}^2 - \tilde{\omega}^2 \mp \frac{\tilde{\omega}}{2\pi^2} \frac{1}{\cosh \tilde{z}} \right) e_\pm = 0. \tag{9.74}$$

If the wavelength of the photons is much longer than the thickness of the domain wall, the "potential" can be approximated by $1/\cosh \tilde{z} \to \pi\delta(\tilde{z})$. The factor π ensures correct normalization of the approximation. The full CSL is constructed by adding other domain walls with spacing $\ell = 2kK(k)/m_\pi$ given by eq. (8.15). Consequently, we are left with the Dirac comb, which we know from elementary quantum mechanics leads to the Hamiltonian

$$\mathcal{H} = -\frac{1}{2m} \frac{\mathrm{d}^2}{\mathrm{d}\tilde{z}^2} + \frac{\Omega}{m} \sum_{n \in \mathbb{Z}} \delta(\tilde{z} - na), \tag{9.75}$$

where $a \equiv m_\pi \ell$ and $\Omega \equiv \mp\tilde{\omega}/(4\pi)$ [52]. The known spectrum of the Hamiltonian gives the relation

$$\cos p_z \ell = \cos \omega\ell \mp \frac{1}{4\pi} \sin \omega\ell, \tag{9.76}$$

which implies that the only dependence on the external magnetic field H enters through the lattice spacing ℓ. The low-momentum behavior of the dispersion relations then reads

$$\begin{aligned}\omega_1 =& 4\pi k K(k)\frac{p_z^2}{m_\pi} + \mathcal{O}(p_z^4),\\ \omega_2 =& \frac{m_\pi}{kK(k)}\arctan\frac{1}{4\pi} + \mathcal{O}(p_z^2).\end{aligned} \tag{9.77}$$

Hence, one of the helicities is gapped. In eq. (9.72), we obtained an expression for the dispersion relation of the gapless mode in the opposite regime where $k \to 0$. Interestingly, the power expansion in k of this mode agrees with the power expansion of the gapless mode in eq. (9.77) up to a correction of order k^5. We will therefore investigate if there exists an approximate expression that is valid for the entire range $0 \leq k \leq 1$. We start off by considering the exact equation of motion (9.65) for the two photon helicities. A long enough wavelength of the photon makes it possible to replace the Jacobi dn function by its average value [43],

$$\mathrm{dn}(\bar{z}, k) \to \frac{\pi}{2K(k)}. \tag{9.78}$$

Hence, a Fourier transform of eq. (9.65) results in

$$\bar{p}_z^2 - \bar{\omega}^2 \mp \frac{\bar{\omega}}{4\pi K(k)} = 0, \tag{9.79}$$

which actually replicates the gapless dispersion relation in eq. (9.77) that was derived using a different technique. The argument used above is not rigorous. Nevertheless, we may conjecture that the dispersion relation of the gapless photon is given exactly or accurately by eq. (9.77) for all magnetic fields.[3] Furthermore, the gap of the second mode in eq. (9.79) is $\omega = m_\pi/\left[4\pi k K(k)\right]$. This has the same k-dependence as the gap in eq. (9.77). However, their prefactor differs by about 0.2%.

9.7 Background plasma oscillations and charged pion dynamics

Even though the EFT setup is constructed exclusively from symmetry arguments and consequently is model-independent, we made an assumption when we neglected the oscillation of the charged background and the dynamics of the charged pions. We will therefore provide a justification for why this is adequate. For simplicity, we will operate in the chiral limit. In eq. (9.40) we assumed that a charged background canceled the electric charge of the CSL. Moreover, we assumed that the dynamics of this background does not affect the low-energy dispersion relations. Such a background may for example consist of electrons, nucleons or charged pions [22]. We must therefore estimate the dispersion relation of the plasma oscillations. We assume a background that is made up of a gas of massless spin-1/2 particles

[3] See section 4.4 in [47] for a discussion of how the Goldstone boson arises in this theory.

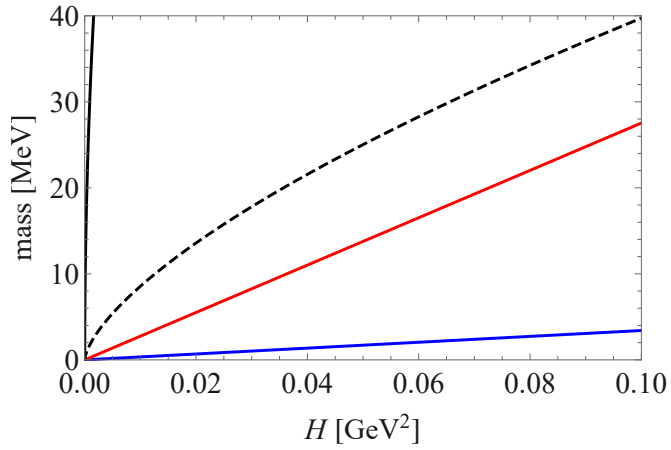

Figure 9.1: Gap of dispersion relations of charged pions $\omega_{\pi^\pm}$ (black) and the two neutral-pion-photon mixtures ω_2 and ω_3 (blue and red), as well as the frequency of plasma oscillations ω_{pl} (dashed). Plotted as a function of external magnetic field H at $\mu_I = 900$ MeV and $f_\pi = 92$ MeV.

with unit electric charge. Furthermore, we couple these particles minimally to the electromagnetic field. Such a gas will undergo plasma oscillations. The dispersion relation of these oscillations will in the long-wavelength limit take the form

$$\omega_{\text{pl}} = \sqrt{\frac{\rho_{\text{back}}}{\mu_{\text{back}}}} = \left(\frac{\rho_{\text{back}}}{\pi\sqrt{3}}\right)^{1/3}, \tag{9.80}$$

where ρ_{back} is the charge density of the gas, while μ_{back} is its chemical potential. The second equality is obtained using that a gas of massless spin-1/2 Dirac fermions has the relation $\rho_{\text{back}} = \mu_{\text{back}}^3/(3\pi^2)$ [55]. Since the charged background must neutralize the CSL, we have from eq. (9.40) that

$$\rho_{\text{back}} = \frac{\mu_I\,(CH)^2}{2}, \tag{9.81}$$

such that

$$\omega_{\text{pl}} = \left(\frac{\mu_I\,(CH)^2}{2\pi\sqrt{3}}\right)^{1/3}. \tag{9.82}$$

Hence, we can neglect the dynamics of the charged background for energies well below this plasma frequency. Finally, we note that the gap of the charged pions is given by the standard Landau level quantization discussed in section 2.3. In the chiral limit, we will therefore have four dispersion relations with a gap. These are

$$\omega_2 = \frac{\mu_I C^2 H}{2}, \qquad \omega_3 = CH, \qquad \omega_{\pi^\pm} = \sqrt{H}, \qquad \omega_{\text{pl}} = \left(\frac{\mu_I\,(CH)^2}{2\pi\sqrt{3}}\right)^{1/3}, \tag{9.83}$$

where the two first gaps are found in eq. (9.57). The validity of our theory is governed by the plasma oscillations, as seen in figure 9.1. The two neutral-pion-photon mixtures are significantly lighter than the plasma oscillations, implying that our assumptions are valid.

Chapter 10

Excitation spectrum in a Bose-Einstein condensate

The excitation spectrum in a BEC in presence of an isospin chemical potential was derived in section 5.3. The result was that two modes had a gap while one mode was gapless. We will in this chapter introduce an external magnetic field in addition to dynamical electromagnetic fields. This leads to a mass gap of the Goldstone boson of section 5.3. The dispersion relations under these conditions are derived by expanding the Lagrangian to second order and obtaining the zero modes of the inverse propagator. The Wess-Zumino-Witten term is not included in the Lagrangian as it does not affect the dispersion relations. This is shown in the final section.

The full Lagrangian in presence of dynamical electromagnetic fields at finite isospin chemical potential reads

$$\begin{aligned}\mathscr{L} &= \mathscr{L}_{\text{ChPT}} + \mathscr{L}_{\text{QED}} = \frac{f_\pi^2}{4}\left[\text{Tr}(D_\mu\Sigma^\dagger D^\mu\Sigma) + 2m_\pi^2\text{ReTr}\Sigma\right] - \frac{1}{4}F_{\mu\nu}F^{\mu\nu} - j^\mu_{\text{back}}A_\mu \\ &= \frac{f_\pi^2}{4}\left\{\text{Tr}\left[\partial_\mu\Sigma^\dagger\partial^\mu\Sigma\right] - \left[\frac{\mu_I^2}{2} + \frac{1}{2}e^2A_\mu A^\mu - \mu_I eA^0\right]\text{Tr}\left[\Sigma^\dagger\tau_3\Sigma\tau_3 - \mathbb{1}\right]\right. \\ &\qquad \left. + \frac{i}{2}\left(\mu_I\delta_{\mu 0} - eA_\mu\right)\text{Tr}\left[\left(\Sigma\tau_3 - \tau_3\Sigma\right)\partial^\mu\Sigma^\dagger + \left(\Sigma^\dagger\tau_3 - \tau_3\Sigma^\dagger\right)\partial^\mu\Sigma\right]\right\} \\ &\quad + \frac{f_\pi^2 m_\pi^2}{2}\text{ReTr}\Sigma - \frac{1}{4}F_{\mu\nu}F^{\mu\nu} - j^\mu_{\text{back}}A_\mu,\end{aligned} \tag{10.1}$$

where the ordinary derivatives in the ChPT Lagrangian in eq. (4.16) have been promoted to covariant derivatives of the form

$$D_\mu\Sigma \equiv \partial_\mu\Sigma - i[\delta_{\mu 0}\mu_I I_3 - eQ_\mu, \Sigma] = \partial_\mu\Sigma - \frac{1}{2}i\left(\delta_{\mu 0}\mu_I - eA_\mu\right)[\tau_3, \Sigma], \tag{10.2}$$

where $Q_\mu \equiv A_\mu\tau_3/2$. We have explicitly written out the electromagnetic coupling $e = 1$ such that the coupling to the electromagnetic fields can be turned off by setting $e = 0$. Moreover, the background current in the QED Lagrangian represents a classical charged background and will again ensure electrical neutrality of the ground state. We will assume that this background does not affect the dynamics of the excitation spectrum. The dispersion relations can be obtained by introducing fluctuations around the ground state and solving the equations of motion. However,

the procedure we choose is to work out the zero modes of the inverse propagator from the bilinear Lagrangian. Starting out with the parameterization $\Sigma = \exp\left(\frac{1}{f_\pi}\boldsymbol{\tau}\cdot\boldsymbol{\pi}\right)$, we calculate each term in the Lagrangian to second order. The first trace is found from eq. (5.13) to be

$$\mathrm{Tr}\left(\partial_\mu\Sigma^\dagger\partial^\mu\Sigma\right) = \frac{2}{f_\pi^2}\partial_\mu\pi_a\partial^\mu\pi_a + \mathcal{O}(\boldsymbol{\pi}^3). \tag{10.3}$$

The second trace in eq. (10.1) is the zeroth component of the third trace. The third trace can be written as

$$\begin{aligned}\mathrm{Tr}\left[(\Sigma\tau_3 - \tau_3\Sigma)\,\partial_\mu\Sigma^\dagger + \left(\Sigma^\dagger\tau_3 - \tau_3\Sigma^\dagger\right)\partial_\mu\Sigma\right] \\ = \mathrm{Tr}\left[\tau_3\left(\partial_\mu\Sigma\Sigma^\dagger - \Sigma\partial_\mu\Sigma^\dagger\right) + \tau_3\left(\partial_\mu\Sigma^\dagger\Sigma - \Sigma^\dagger\partial_\mu\Sigma\right)\right] \\ = \frac{8}{if_\pi}\left[\sin\alpha\,\partial_\mu\pi_1 - \frac{1}{f_\pi}\cos\alpha\,(\boldsymbol{\pi}\times\partial_\mu\boldsymbol{\pi})_3\right] + \mathcal{O}(\boldsymbol{\pi}^3),\end{aligned} \tag{10.4}$$

where the zeroth component of this was calculated in eqs. (5.18) and (5.19). Furthermore, we reuse the result of eq. (5.20) to cast the fourth trace in the Lagrangian into the form

$$\begin{aligned}\mathrm{Tr}\left(\Sigma^\dagger\tau_3\Sigma\tau_3 - \mathbb{1}\right) = -2\Bigg(2\sin^2\alpha + \frac{4}{if_\pi}\sin 2\alpha\,\pi_2 + \frac{2}{f_\pi^2}\cos^2\alpha\,\pi_1^2 \\ + \frac{2}{f_\pi^2}\cos 2\alpha\,\pi_2^2 - \frac{2}{f_\pi^2}\sin^2\alpha\,\pi_3^2\Bigg) + \mathcal{O}(\boldsymbol{\pi}^3).\end{aligned} \tag{10.5}$$

The last trace in the Lagrangian in eq. (10.1) is

$$\mathrm{ReTr}\Sigma = 2\left(\cos\alpha - \frac{1}{f_\pi}\sin\alpha\,\pi_2 - \frac{1}{2f_\pi^2}\cos\alpha\,\boldsymbol{\pi}^2\right) + \mathcal{O}(\boldsymbol{\pi}^3), \tag{10.6}$$

where we have used the result of eq. (5.21). The bilinear part of the Lagrangian is found by collecting the terms in eqs. (10.3)-(10.6) yielding

$$\begin{aligned}\mathscr{L}^{(2)} =& \frac{1}{2}\partial_\mu\pi_a\partial^\mu\pi_a - \frac{1}{2}m_{12}(\pi_1\partial_0\pi_2 - \pi_2\partial_0\pi_1) - \frac{1}{2}(m_1^2\pi_1^2 + m_2^2\pi_2^2 + m_3^2\pi_3^2) \\ & - f_\pi e\sin\alpha A^\mu\partial_\mu\pi_1 - f_\pi\mu_I e\sin 2\alpha A^0\pi_2 + \frac{f_\pi^2e^2}{2}\sin^2\alpha A_\mu A^\mu - \frac{1}{4}F_{\mu\nu}F^{\mu\nu},\end{aligned} \tag{10.7}$$

where we again defined the masses m_{12}, m_1, m_2 and m_3 in accordance with eq. (5.23). Hence, the introduction of dynamical electromagnetic fields has given rise to a mixing between the pion fields and the electromagnetic fields. Because of the $U(1)$ electromagnetic gauge freedom in the Lagrangian, we must add a gauge-fixing that ensures a well-defined generating functional. This guarantees that we obtain the correct physical results. The gauge-fixing can be added through the Faddeev-Popov procedure where the effective Lagrangian becomes

$$\mathscr{L}_{\mathrm{eff}} = \mathscr{L} + \mathscr{L}_{\mathrm{gf}} + \mathscr{L}_{\mathrm{FP}} = \mathscr{L} - \frac{1}{2\xi}G^2 + \bar{c}\frac{\partial G}{\partial\vartheta}c, \tag{10.8}$$

where $\mathscr{L}_{\mathrm{gf}}$ is the gauge-fixing and $\mathscr{L}_{\mathrm{FP}}$ is the Faddeev-Popov ghost term. Furthermore, $G(A^\mu,\boldsymbol{\pi}) = 0$ is an appropriate gauge-condition, ξ is an arbitrary parameter,

ϑ is the generator of the gauge symmetry and $c, \bar{c}$ are Grassmannian ghost fields. However, we can drop the last term in the effective Lagrangian since the ghosts do not affect results at tree level [28]. Choosing

$$G = \partial_\mu A^\mu + \xi f_\pi e \sin\alpha\ \pi_1, \tag{10.9}$$

we will be able to remove the mixing of A^μ and π_1. This is known as the R_ξ gauge. Picking another gauge or G does not affect physical results but may affect the length of the calculations. The resulting gauge-fixing is

$$\begin{aligned}\mathscr{L}_{\text{gf}} &= -\frac{1}{2\xi}G^2 = -\frac{1}{2\xi}(\partial_\mu A^\mu)^2 - f_\pi e\sin\alpha\ \pi_1\partial_\mu A^\mu - \frac{1}{2}\xi f_\pi^2 e^2\sin^2\alpha\ \pi_1^2 \\ &= -\frac{1}{2\xi}(\partial_\mu A^\mu)^2 + f_\pi e\sin\alpha\ A^\mu\partial_\mu\pi_1 - \frac{1}{2}\xi f_\pi^2 e^2\sin^2\alpha\ \pi_1^2,\end{aligned} \tag{10.10}$$

where we have performed a partial integration of the second term in the first line. Hence, the effective bilinear Lagrangian in eq. (10.8) becomes

$$\begin{aligned}\mathscr{L}_{\text{eff}}^{(2)} &= \frac{1}{2}\partial_\mu\pi_a\partial^\mu\pi_a - \frac{1}{2}m_{12}(\pi_1\partial_0\pi_2 - \pi_2\partial_0\pi_1) \\ &\quad - \frac{1}{2}\left[\left(m_1^2 + \xi f_\pi^2 e^2\sin^2\alpha\right)\pi_1^2 + m_2^2\pi_2^2 + m_3^2\pi_3^2\right] \\ &\quad - f_\pi\mu_I e\sin 2\alpha A^0\pi_2 + \frac{f_\pi^2 e^2}{2}\sin^2\alpha A_\mu A^\mu - \frac{1}{2\xi}\left(\partial_\mu A^\mu\right)^2 - \frac{1}{4}F_{\mu\nu}F^{\mu\nu}.\end{aligned} \tag{10.11}$$

We will from now on drop the subscript of the effective Lagrangian. The last term can be cast into the form

$$\begin{aligned}-\frac{1}{4}F_{\mu\nu}F^{\mu\nu} &= -\frac{1}{2}\left(\partial_\mu A_\nu\partial^\mu A^\nu - \partial_\mu A_\nu\partial^\nu A^\mu\right) \\ &= \frac{1}{2}\left(A_\mu\partial_\nu\partial^\nu A^\mu - A_\mu\partial^\mu\partial^\nu A_\nu\right) \\ &= \frac{1}{2}A_\mu\left(\eta^{\mu\nu}\Box - \partial^\mu\partial^\nu\right)A_\nu,\end{aligned} \tag{10.12}$$

where we performed a partial integration of both terms going to the penultimate line. Substituting this into the bilinear Lagrangian in eq. (10.11) gives

$$\begin{aligned}\mathscr{L}^{(2)} &= -\frac{1}{2}\pi_a\partial_\mu\partial^\mu\pi_a - \frac{1}{2}m_{12}(\pi_1\partial_0\pi_2 - \pi_2\partial_0\pi_1) \\ &\quad - \frac{1}{2}\left[\left(m_1^2 + \xi f_\pi^2 e^2\sin^2\alpha\right)\pi_1^2 + m_2^2\pi_2^2 + m_3^2\pi_3^2\right] \\ &\quad - f_\pi\mu_I e\sin 2\alpha A^0 + \frac{1}{2}A_\mu\left[\eta^{\mu\nu}\left(\Box + f_\pi^2 e^2\sin^2\alpha\right) - \left(1 - \frac{1}{\xi}\right)\partial^\mu\partial^\nu\right]A_\nu,\end{aligned} \tag{10.13}$$

where the first term is a result of partial integration. The bilinear Lagrangian can be written on matrix form as

$$\mathscr{L}^{(2)} = \frac{1}{2}\begin{pmatrix}\pi_1 & \pi_2 & \pi_3 & A_0 & A_1 & A_2 & A_3\end{pmatrix} \quad D^{-1} \quad \begin{pmatrix}\pi_1 \\ \pi_2 \\ \pi_3 \\ A_0 \\ A_1 \\ A_2 \\ A_3\end{pmatrix}, \tag{10.14}$$

where D^{-1} is the inverse propagator. The nonzero entries in the Fourier transformed inverse propagator are

$$\begin{aligned}
D_{11}^{-1} &= E^2 - \boldsymbol{p}^2 - m_1^2 - \xi f_\pi^2 e^2 \sin^2\alpha, & D_{21}^{-1} &= -D_{12}^{-1} = iEm_{12},\\
D_{33}^{-1} &= E^2 - \boldsymbol{p}^2 - m_3^2, & D_{42}^{-1} &= D_{24}^{-1} = -f_\pi \mu_I e \sin 2\alpha,\\
D_{44}^{-1} &= \boldsymbol{p}^2 - E^2 + f_\pi^2 e^2 \sin^2\alpha + \left(1 - \frac{1}{\xi}\right) E^2, & D_{54}^{-1} &= D_{45}^{-1} = \left(1 - \frac{1}{\xi}\right) E p_x,\\
D_{55}^{-1} &= E^2 - \boldsymbol{p}^2 - f_\pi^2 e^2 \sin^2\alpha + \left(1 - \frac{1}{\xi}\right) p_x^2, & D_{64}^{-1} &= D_{46}^{-1} = \left(1 - \frac{1}{\xi}\right) E p_y,\\
D_{66}^{-1} &= E^2 - \boldsymbol{p}^2 - f_\pi^2 e^2 \sin^2\alpha + \left(1 - \frac{1}{\xi}\right) p_y^2, & D_{65}^{-1} &= D_{56}^{-1} = \left(1 - \frac{1}{\xi}\right) p_x p_y,\\
D_{77}^{-1} &= E^2 - \boldsymbol{p}^2 - f_\pi^2 e^2 \sin^2\alpha + \left(1 - \frac{1}{\xi}\right) p_z^2, & D_{74}^{-1} &= D_{47}^{-1} = \left(1 - \frac{1}{\xi}\right) E p_z,\\
D_{75}^{-1} &= D_{57}^{-1} = \left(1 - \frac{1}{\xi}\right) p_x p_z, & D_{76}^{-1} &= D_{67}^{-1} = \left(1 - \frac{1}{\xi}\right) p_y p_z.
\end{aligned} \tag{10.15}$$

The determinant of the inverse propagator then becomes

$$\begin{aligned}
\mathrm{Det}\left(D^{-1}\right) = \frac{1}{\mu_I^2 \xi} &\left\{E^2 - \mathbf{p}^2 - \xi f_\pi^2 e^2 \left(1 - \frac{m_\pi^4}{\mu_I^4}\right)\right\}^2 \left\{E^2 - \mathbf{p}^2 - f_\pi^2 e^2 \left(1 - \frac{m_\pi^4}{\mu_I^4}\right)\right\}^2\\
&\left\{\mu_I^2 (\mathbf{p} - E)(\mathbf{p} + E)\left(\mu_I^2 + \mathbf{p}^2 - E^2\right) - m^4\left(3E^2 + \mathbf{p}^2\right) + f_\pi^2 e^2 \left[1 - \frac{m_\pi^4}{\mu_I^4}\right]\right.\\
&\left.\times \left[3m^4 + \mu_I^2\left(\mu_I^2 + \mathbf{p}^2 - E^2\right)\right]\right\}\left\{\mu_I^2 + \mathbf{p}^2 - E^2\right\},
\end{aligned} \tag{10.16}$$

where we have used that $\cos\alpha = m_\pi^2/\mu_I^2$, which was the case for a BEC with an isospin chemical potential. This was an on shell tree level result. In section 11.2, we will show that this also holds when dynamical electromagnetic fields are present. The zero modes of the inverse propagator are found by setting the determinant to zero and solving for E. We then find

$$\begin{aligned}
E_\pm(\mathbf{p}) &= \left[\mathbf{p}^2 + \frac{1}{2}(m_1^2 + m_2^2 + m_{12}^2)\right.\\
&\qquad \left.\pm \frac{1}{2}\sqrt{4\mathbf{p}^2 m_{12}^2 + (m_1^2 + m_2^2 + m_{12}^2)^2 + m_1^2 m_{12}^2 - 4m_1^2\left(m_2^2 + m_{12}^2\right)}\right]^{1/2},\\
E_{\mathrm{n}}(\mathbf{p}) &= \sqrt{\mathbf{p}^2 + \mu_I^2} = \sqrt{\mathbf{p}^2 + m_3^2},\\
E_{1,2}(\mathbf{p}) &= \sqrt{\mathbf{p}^2 + e^2 f_\pi^2\left(1 - \frac{m_\pi^4}{\mu_I^4}\right)} = \sqrt{\mathbf{p}^2 + m_1^2},\\
E_{3,4}(\mathbf{p}) &= \sqrt{\mathbf{p}^2 + \xi e^2 f_\pi^2\left(1 - \frac{m_\pi^4}{\mu_I^4}\right)} = \sqrt{\mathbf{p}^2 + \xi m_1^2},
\end{aligned} \tag{10.17}$$

where E_{n} corresponds to the neutral pion mode while the other modes are pion-

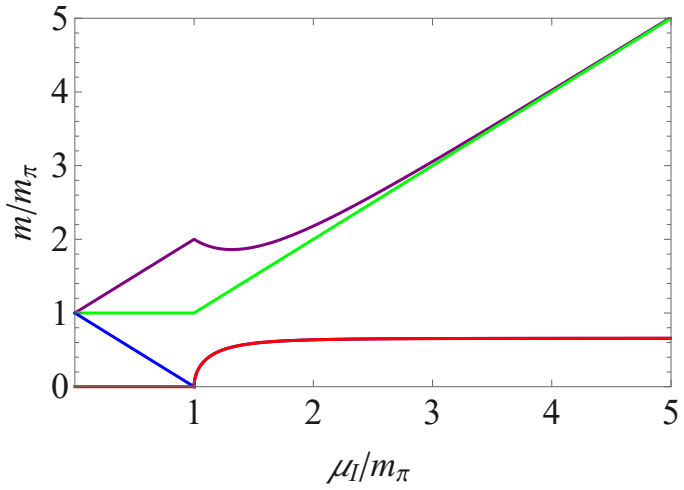

Figure 10.1: Mass spectrum in the normal phase for $\mu_I \leq m_\pi$ and in the Bose-Einstein condensate for $\mu_I \geq m_\pi$. In the normal phase, the curves correspond to the photons (red), the negatively charged pion (blue), the neutral pion (green) and the positively charged pion (purple). The red and blue curves overlap in the Bose-Einstein condensate.

photon mixtures. In this we have redefined the mass m_1 leaving us with

$$\begin{aligned} m_1^2 &\equiv m_\pi^2 \cos\alpha - \mu_I^2 \cos^2\alpha + f_\pi^2 e^2 \sin^2\alpha = f_\pi^2 e^2 \left(1 - \frac{m_\pi^4}{\mu_I^4}\right), \\ m_2^2 &= m_\pi^2 \cos\alpha - \mu_I^2 \cos 2\alpha = \mu_I^2 \left(1 - \frac{m_\pi^4}{\mu_I^4}\right), \\ m_3^2 &= m_\pi^2 \cos\alpha + \mu_I^2 \sin^2\alpha = \mu_I^2, \\ m_{12}^2 &= 4\mu_I^2 \cos^2\alpha = \frac{4m_\pi^4}{\mu_I^2}. \end{aligned} \tag{10.18}$$

Two of the seven modes are unphysical since they depend on the gauge-parameter ξ. As a consistency check, we can turn off the interaction between the electromagnetic fields and the pions by setting $e = 0$. We will then reproduce the dispersion relations in section 5.3 for a BEC with an isospin chemical potential. Moreover, the two physical photon modes become massless as they ought to be. If we instead set $\mu_I = m_\pi$, we recover the dispersion relations in the normal phase where there is no interaction between the pions and the electromagnetic fields. Letting $\boldsymbol{p} \to 0$ in eq. (10.17) yields the mass spectrum

$$\begin{aligned} m_+ &= \mu_I \sqrt{1 + 3\cos^2\alpha} = \mu_I \sqrt{1 + 3\frac{m_\pi^4}{\mu_I^4}}, \\ m_{\mathrm{n}} &= \mu_I, \\ m_{1,2,-} &= f_\pi e \sin\alpha = f_\pi e \sqrt{1 - \frac{m_\pi^4}{\mu_I^4}}, \end{aligned} \tag{10.19}$$

which are plotted in figure 10.1. First, we note that m_+ and m_{n} are the same as before we introduced an external magnetic field along with dynamical photons. In

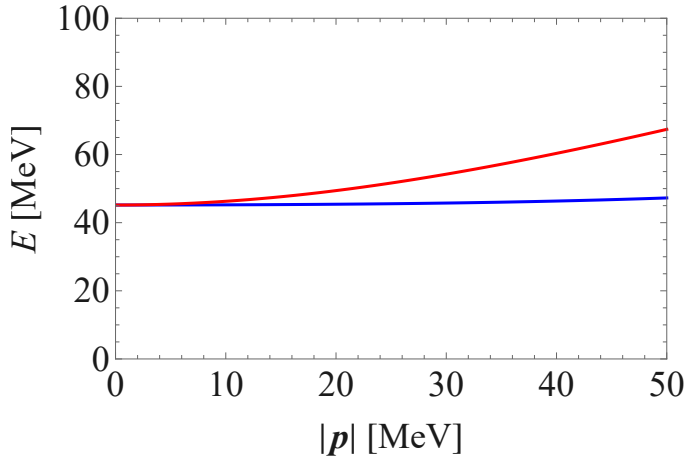

Figure 10.2: Dispersion relations of the three originally gapless modes E_- (blue) and $E_{1,3}$ (red) at $\mu_I = 150$ MeV and $m_\pi = 140$ MeV. Plotted as a function of the magnitude of the momentum $|\boldsymbol{p}|$ with $f_\pi = 92$ MeV.

contrast, the originally gapless photon modes and negatively charged pion mode have now acquired a gap. We can say that the electromagnetic gauge field has "eaten" the Goldstone boson. This is known as the Anderson-Higgs mechanism [56, 57]. Moreover, we see from the dispersion relations in figure 10.2 that E_- is a slower longitudinal mode in contrast to $E_{1,3}$ which are faster transverse modes. At zero momentum, there is no distinction between the longitudinal and transverse modes. It is therefore expected that these three modes have the same gap [55].

10.1 Excitation spectrum in presence of anomalies

We will in the following determine if the Wess-Zumino-Witten term affects the dispersion relations of a BEC with isospin chemical potential and dynamical electromagnetic fields. In other words, we must see if the Wess-Zumino-Witten term contributes to the bilinear Lagrangian. The term is found in eq. (7.20) and with no baryon chemical potential it takes the form

$$\mathscr{L}_{\text{WZW}} = \frac{\lambda}{2} A_\mu^{\text{Q}} \varepsilon^{\mu\nu\alpha\beta} \text{Tr}\left[(\Sigma D_\nu \Sigma^\dagger)(\Sigma D_\alpha \Sigma^\dagger)(\Sigma D_\beta \Sigma^\dagger) - \frac{3i}{4}\tau_3 (D_\nu \Sigma\Sigma^\dagger - D_\nu \Sigma^\dagger \Sigma)(F^I_{\alpha\beta} + F^Q_{\alpha\beta})\right], \tag{10.20}$$

where λ is the constant obtained in eq. (7.27). We will proceed by expanding $\Sigma = \exp\left(\frac{1}{f_\pi}\boldsymbol{\tau}\cdot\boldsymbol{\pi}\right)$ in powers of the fields. First, we note that $D_i\Sigma = \mathcal{O}(\boldsymbol{\pi}^1)$. Hence, the first term will only be of second order in the fields if one of the greek indices in the first trace is zero. Consequently, the first term becomes

$$\frac{\lambda}{2}\varepsilon^{i0jk} A_i^{\text{Q}} \text{Tr}\left[(\Sigma D_0 \Sigma^\dagger)(\Sigma D_j \Sigma^\dagger)(\Sigma D_k \Sigma^\dagger)\right] = \mathcal{O}(\text{fields}^3). \tag{10.21}$$

The second term in eq. (10.20) can be expanded as

$$
\begin{aligned}
&-\frac{3i\lambda}{8}\varepsilon^{\mu\nu\alpha\beta}A_\mu^{\mathrm{Q}}\mathrm{Tr}\left[\tau_3\left(D_\nu\Sigma\Sigma^\dagger - D_\nu\Sigma^\dagger\Sigma\right)\left(F^I_{\alpha\beta}+F^Q_{\alpha\beta}\right)\right]\\
&\qquad= -\frac{3i\lambda}{8}\varepsilon^{\mu\nu\alpha\beta}A_\mu^{\mathrm{Q}}\mathrm{Tr}\left\{\tau_3\left[\left(\frac{i}{f_\pi}\boldsymbol{\tau}\cdot\partial_\nu\boldsymbol{\pi}\Sigma - \frac{i}{2}\left(A_\nu^{\mathrm{I}}+A_\nu^{\mathrm{Q}}\right)\left[\tau_3,\Sigma\right]\right)\Sigma^\dagger\right.\right.\\
&\qquad\qquad\left.\left.-\left(-\frac{i}{f_\pi}\boldsymbol{\tau}\cdot\partial_\nu\boldsymbol{\pi}\Sigma^\dagger - \frac{i}{2}\left(A_\nu^{\mathrm{I}}+A_\nu^{\mathrm{Q}}\right)\left[\tau_3,\Sigma^\dagger\right]\right)\Sigma\right]\left[F^{\mathrm{I}}_{\alpha\beta}+F^{\mathrm{Q}}_{\alpha\beta}\right]\right\}\\
&\qquad= -\frac{3i\lambda}{8}\varepsilon^{\mu\nu\alpha\beta}A_\mu^{\mathrm{Q}}\mathrm{Tr}\left\{\tau_3\left[\frac{i}{f_\pi}\boldsymbol{\tau}\cdot\partial_\nu\boldsymbol{\pi} - \frac{i}{2}\left(A_\nu^{\mathrm{I}}+A_\nu^{\mathrm{Q}}\right)\left(\tau_3-\Sigma\tau_3\Sigma^\dagger\right)\right.\right.\\
&\qquad\qquad\left.\left.+\frac{i}{f_\pi}\boldsymbol{\tau}\cdot\partial_\nu\boldsymbol{\pi} + \frac{i}{2}\left(A_\nu^{\mathrm{I}}+A_\nu^{\mathrm{Q}}\right)\left(\tau_3-\Sigma^\dagger\tau_3\Sigma\right)\right]\left[F^{\mathrm{I}}_{\alpha\beta}+F^{\mathrm{Q}}_{\alpha\beta}\right]\right\}\\
&\qquad= \frac{3\lambda}{4f_\pi}\varepsilon^{\mu\nu\alpha\beta}A_\mu^{\mathrm{Q}}\left(F^{\mathrm{I}}_{\alpha\beta}+F^{\mathrm{Q}}_{\alpha\beta}\right)\mathrm{Tr}\left(\tau_3\boldsymbol{\tau}\cdot\partial_\nu\boldsymbol{\pi}\right)\\
&\qquad= \frac{3\lambda}{2f_\pi}\varepsilon^{\mu\nu\alpha\beta}A_\mu^{\mathrm{Q}}\left(F^{\mathrm{I}}_{\alpha\beta}+F^{\mathrm{Q}}_{\alpha\beta}\right)\partial_\nu\pi_3 \qquad (10.22)\\
&\qquad= \frac{3\lambda}{2f_\pi}\varepsilon^{\mu\nu\alpha\beta}A_\mu^{\mathrm{Q}}F^{\mathrm{I}}_{\alpha\beta}\partial_\nu\pi_3 + \mathcal{O}(\mathrm{fields}^3)\\
&\qquad= \frac{3\lambda\mu_I}{2f_\pi}\pi_3\left(\varepsilon^{ijk0}\partial_k\partial_i + \varepsilon^{kji0}\partial_k\partial_i\right)A_j^{\mathrm{Q}} + \mathcal{O}(\mathrm{fields}^3)\\
&\qquad= \mathcal{O}(\mathrm{fields}^3),
\end{aligned}
$$

where the different steps are achieved by exploiting the cyclic property of the trace, the Bianchi identity and the complete antisymmetry of the Levi-Civita symbol, as well as partial integration. We conclude from eqs. (10.21) and (10.22) that the Wess-Zumnio-Witten term in eq. (10.20) is of order three in the fields. Consequently, the bilinear Lagrangian stays the same, and the Wess-Zumino-Witten term does not affect the dispersion relations in the BEC.

Chapter 11

QCD phase diagram

In section 8.6, we established that the CSL is energetically favored over the QCD vacuum above a certain strength of the external magnetic field. However, it has not been established when the CSL is energetically more favorable than the BEC. For that reason, we will in this chapter determine the low-energy QCD phase diagram as a function of isospin chemical potential and external magnetic field. The electromagnetic fields are dynamical, and we will allow for three phases to exist. These are the QCD vacuum, the BEC and the CSL. A fourth phase involving a magnetic vortex lattice is discussed in chapter 12. Since simulations in lattice QCD allow for a variation of the pion mass, we will start out by obtaining the phase diagram in the chiral limit [58].

The phase diagram at a *fixed* external magnetic field is determined by comparing the total Gibbs free energy of the different phases. At a given external field and isospin density, the phase with the lowest total Gibbs free energy will be present in the phase diagram. The Gibbs free energy (density) is given by

$$\mathscr{G} = \mathscr{F} - \boldsymbol{B}\cdot\boldsymbol{H} = \mathscr{H} - \boldsymbol{B}\cdot\boldsymbol{H}, \tag{11.1}$$

where $\mathscr{F}$ is the Helmholtz free energy (density) and the magnetic field $\boldsymbol{B} = \boldsymbol{M} + \boldsymbol{H}$ is the sum of the magnetization $\boldsymbol{M}$ and the external magnetic field $\boldsymbol{H}$ [59]. The isospin chemical potential and the dynamical electromagnetic fields are included in the ChPT Lagrangian in eq. (4.16) by promoting the ordinary derivatives to covariant derivatives reading

$$D_\mu\Sigma = \partial_\mu\Sigma - i[\delta_{\mu 0}\mu_I I_3 - eQ_\mu, \Sigma], \tag{11.2}$$

where $Q_\mu \equiv A_\mu\tau_3/2$. Furthermore, we use units in which the electromagnetic coupling is $e = \sqrt{4\pi/137}$. This ensures correct dimensions when we include the magnetic field in the Gibbs free energy. The dynamics of the electromagnetic fields is governed by the Lagrangian of quantum electrodynamics (QED),

$$\mathscr{L}_{\text{QED}} = -\frac{1}{4}F_{\mu\nu}F^{\mu\nu} = -\frac{1}{2}\boldsymbol{B}^2, \tag{11.3}$$

in which we have assumed time-independence of A_i and sat $A^0 = 0$. The latter is justified by the fact that no electric fields $\boldsymbol{E} = -\boldsymbol{\nabla}A^0 - \partial_0\boldsymbol{A}$ implies that A^0 is a constant that can be treated as a chemical potential. As a result, the full

Lagrangian, including the Wess-Zumino-Witten term in eq. (7.20), becomes

$$\begin{aligned}\mathscr{L} &= \mathscr{L}_{\text{ChPT}} + \mathscr{L}_{\text{QED}} + \mathscr{L}_{\text{WZW}} \\ &= \frac{f_\pi^2}{4}\left[\text{Tr}(D_\mu \Sigma^\dagger D^\mu \Sigma) + 2m_\pi^2 \text{ReTr}\Sigma\right] - f_\pi^2 m_\pi^2 - \frac{1}{2}\boldsymbol{B}^2 + \mathscr{L}_{\text{WZW}},\end{aligned} \tag{11.4}$$

where we have subtracted a term $f_\pi^2 m_\pi^2$ making the ChPT Lagrangian vanish in the QCD vacuum. Finally, we choose the external magnetic field to be oriented in the z-direction, $\boldsymbol{H} = (0, 0, H)$.

11.1 Gibbs free energy of the QCD vacuum

First of all, we determine the Gibbs free energy of the QCD vacuum. The vacuum has $\Sigma = \mathbb{1}$, which yields the Hamiltonian

$$\mathscr{H}_{\text{V}} = -\mathscr{L}_{\text{V}} = \frac{1}{2}\boldsymbol{B}^2. \tag{11.5}$$

A system with only a magnetic field will have no magnetization. Hence, $\boldsymbol{B} = (0, 0, H)$ and the total Gibbs free energy per unit volume is

$$\frac{G_{\text{V}}}{V} = \frac{1}{V}\int \mathrm{d}^3x\, \mathscr{G}_{\text{V}} = -\frac{1}{2}H^2. \tag{11.6}$$

This energy will in the following be subtracted from the Gibbs free energy of the BEC and the CSL. These phases will therefore be preferred over the vacuum when their total Gibbs free energy drops below zero.

11.2 Gibbs free energy of a Bose-Einstein condensate

The BEC is a uniform phase, meaning that there will be no gradient energy. Thus, the spatial part of the covariant derivative $D_i\Sigma$ is zero, and we have from eq. (11.2) that

$$\partial_i \Sigma = -\frac{1}{2} ieA_i[\tau_3, \Sigma]. \tag{11.7}$$

Taking the curl of both sides of the equation will, for a charged condensate, give $\boldsymbol{B} = \boldsymbol{\nabla} \times \boldsymbol{A} = 0$. A uniform condensate of charged pions will therefore expel the external magnetic field completely. Time-independence together with $D_i\Sigma = 0$ will also make the Wess-Zumino-Witten term vanish. The electromagnetic field will effectively drop out of the ChPT Lagrangian when $A^0 = 0$. We can therefore perform the same calculation as in section 5.1, and we are left with the Hamiltonian

$$\mathscr{H}_{\text{BEC}} = -\mathscr{L}_{\text{BEC}} = -\frac{f_\pi^2 m_\pi^2}{2}\sin\alpha - f_\pi^2 m_\pi^2 (\cos\alpha - 1), \tag{11.8}$$

where $\cos\alpha = m_\pi^2/\mu_I^2$ and $\mu_I \geq m_\pi$. The Gibbs free energy is

$$\mathscr{G}_{\text{BEC}} = \mathscr{H}_{\text{BEC}} - \boldsymbol{B}\cdot\boldsymbol{H} = -\frac{f_\pi^2 m_\pi^2}{2}\sin\alpha - f_\pi^2 m_\pi^2 (\cos\alpha - 1) + \frac{1}{2}H^2, \tag{11.9}$$

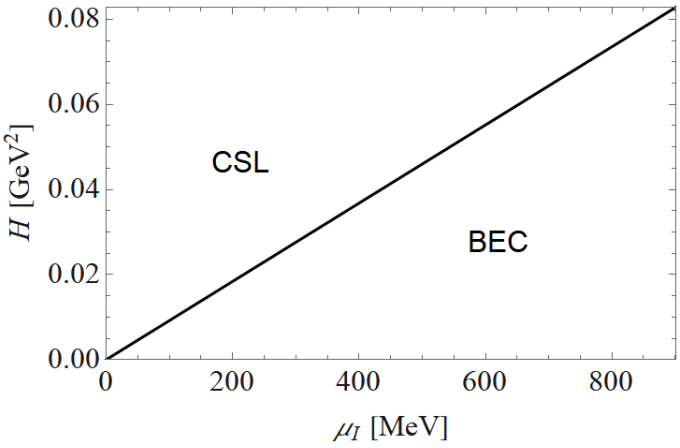

Figure 11.1: The QCD phase diagram in presence of an external magnetic field H and an isospin chemical potential μ_I in the chiral limit. The CSL exists above the curve, while the BEC exists below the curve. Numerical values are obtained with $f_\pi = 92$ MeV.

where we have subtracted the Gibbs free energy of the QCD vacuum. The total Gibbs free energy per unit volume reads

$$\frac{G_{\text{BEC}}}{V} = -\frac{f_\pi^2}{2\mu_I^2}\left(\mu_I^2 - m_\pi^2\right)^2 + \frac{1}{2}H^2. \tag{11.10}$$

Consequently, the transition from the QCD vacuum to the BEC happens when the external field satisfies

$$H < \frac{f_\pi\left(\mu_I^2 - m_\pi^2\right)}{\mu_I} \equiv H_{\text{V/BEC}}. \tag{11.11}$$

This agrees with the result obtained in [17], and $H_{\text{V/BEC}}$ is plotted in figure 11.2.

11.3 Phase diagram in the chiral limit

We will start out by determining how the phase diagram looks in the chiral limit. We must therefore obtain the Gibbs free energy of the CSL in the chiral limit. The CSL consists solely of neutral pions, implying that we can set $\Sigma = e^{i\tau_3\phi}$, where $\phi = \pi^0/f_\pi$. Hence, the covariant derivatives in eq. (11.2) will reduce to ordinary derivatives resulting in the Lagrangian

$$\mathscr{L}_{\text{CSL}} = \frac{f_\pi^2}{2}\dot{\phi}\dot{\phi} - \frac{f_\pi^2}{2}\left(\boldsymbol{\nabla}\phi\right)^2 - m_\pi^2 f_\pi^2(1-\cos\phi) + \frac{\mu_I e}{8\pi^2}\boldsymbol{B}\cdot\boldsymbol{\nabla}\phi - \frac{1}{2}\boldsymbol{B}^2, \tag{11.12}$$

where $e = \sqrt{4\pi/137}$ is also included in the anomaly to ensure correct dimensions. We can gain more information about the magnetic field by calculating the Euler-Lagrange equations for the electromagnetic field $\boldsymbol{A}$ reading

$$\frac{\partial\mathscr{L}_{\text{CSL}}}{\partial A_i} - \partial_j\left(\frac{\partial\mathscr{L}_{\text{CSL}}}{\partial\left(\partial_j A_i\right)}\right) = 0. \tag{11.13}$$

The fourth term in the CSL Lagrangian is a surface term and so does not contribute to the equations of motion. We have

$$\frac{\partial \mathscr{L}_{\text{CSL}}}{\partial A_i} = 0. \tag{11.14}$$

Thus, using $\boldsymbol{B}_i = (\boldsymbol{\nabla} \times \boldsymbol{A})_i = \varepsilon_{ijk}\partial_j A_k$ we find

$$\begin{aligned}\partial_j \left(\frac{\partial \mathscr{L}_{\text{CSL}}}{\partial (\partial_j A_i)} \right) &= -\frac{1}{2}\partial_j \left(\frac{\partial}{\partial (\partial_j A_i)} \varepsilon_{lmn}\partial_m A_n \varepsilon^{lpq}\partial^p A^q \right) = -\partial_j \left[\left(\delta_j^q \delta_i^q - \delta_j^q \delta_i^p \right) \partial^p A^q \right] \\ &= -\partial_j F^{ji} = -(\boldsymbol{\nabla} \times \boldsymbol{B})^j = 0. \end{aligned} \tag{11.15}$$

Since the external magnetic field $\boldsymbol{H}$ points in the z-direction, it is reasonable to assume that the magnetic field $\boldsymbol{B}$ will also point in the z-direction. Consequently, eq. (11.15) together with Gauss's law for magnetism $\boldsymbol{\nabla} \cdot \boldsymbol{B} = 0$ tells us that $\boldsymbol{B} = (0, 0, B)$ is actually a constant. The CSL Lagrangian in eq. (11.12) then takes the form

$$\mathscr{L}_{\text{CSL}} = \frac{f_\pi^2}{2}\dot{\phi}\dot{\phi} - \frac{f_\pi^2}{2}(\boldsymbol{\nabla}\phi)^2 - m_\pi^2 f_\pi^2 (1 - \cos\phi) + \frac{\mu_I e B}{8\pi^2}\partial_z \phi - \frac{1}{2}B^2. \tag{11.16}$$

A Legendre transformation of the Lagrangian, as in eq. (8.4), results in the Hamiltonian

$$\begin{aligned}\mathscr{H}_{\text{CSL}} &= \sum_a \pi_a \dot{\phi}_a - \mathscr{L}_{\text{CSL}} = f_\pi^2 \dot{\phi}^2 - \mathscr{L}_{\text{CSL}} \\ &= \frac{f_\pi^2}{2}\left[\dot{\phi}^2 + (\partial_x \phi)^2 + (\partial_y \phi)^2 + (\partial_z \phi)^2 \right] + m_\pi^2 f_\pi^2 (1 - \cos\phi) - \frac{\mu_I e B}{8\pi^2}\partial_z \phi + \frac{1}{2}B^2. \end{aligned} \tag{11.17}$$

Thereby, we arrive at the CSL Gibbs free energy

$$\mathscr{G}_{\text{CSL}} = \mathscr{H}_{\text{CSL}} - \boldsymbol{B} \cdot \boldsymbol{H} = \frac{f_\pi^2}{2}(\partial_z \phi)^2 + m_\pi^2 f_\pi^2 (1 - \cos\phi) - \frac{\mu_I e B}{8\pi^2}\partial_z \phi + \frac{1}{2}B^2 - BH + \frac{1}{2}H^2, \tag{11.18}$$

where we used that a pion field configuration independent of t, x and y minimizes the energy. Furthermore, we subtracted the Gibbs free energy of the QCD vacuum. The total Gibbs free energy is minimal in the chiral limit when

$$\phi = \frac{\mu_I e B z}{8\pi^2 f_\pi^2}. \tag{11.19}$$

Inserting this into eq. (11.18) gives the total Gibbs free energy per unit volume

$$\frac{G_{\text{CSL}}}{V} = \frac{1}{2}B^2 \left[1 - \left(\frac{e\mu_I}{8\pi^2 f_\pi} \right)^2 \right] - BH + \frac{1}{2}H^2. \tag{11.20}$$

Minimizing with respect to B yields

$$B = \frac{H}{1 - \left(\frac{e\mu_I}{8\pi^2 f_\pi} \right)^2}, \tag{11.21}$$

which results in

$$\frac{G_{\text{CSL}}}{V} = \frac{1}{2}H^2 \frac{1}{1 - \left(\frac{8\pi^2 f_\pi}{e\mu_I}\right)^2} < 0. \tag{11.22}$$

The energy is less than zero because $e\mu_I < 8\pi^2 f_\pi$ within the validity of ChPT. The CSL is therefore preferred over the QCD vacuum for all values of H and μ_I in the chiral limit. Taking the chiral limit of eq. (11.10) gives a negative Gibbs free energy of the BEC when

$$H < f_\pi \mu_I. \tag{11.23}$$

The BEC is energetically favored over the QCD vacuum when this condition is satisfied. The next step is to compare the Gibbs free energies of the CSL and the BEC. Using eqs. (11.10) and (11.22), we see that the BEC is preferred over the CSL when

$$H < f_\pi \mu_I \sqrt{1 - \left(\frac{e\mu_I}{8\pi^2 f_\pi}\right)^2} \equiv H_{\text{chiral}}, \tag{11.24}$$

which is slightly less than $f_\pi \mu_I$ in eq. (11.23). The phase diagram in the chiral limit will therefore consist solely of the CSL and the BEC. H_{chiral} is plotted in figure 11.1, and determines the external magnetic field at which the transition between the two phases takes place.

11.4 Phase diagram away from the chiral limit

In order to determine the phase diagram away from the chiral limit, we must obtain the Gibbs free energy of the CSL for nonzero pion mass. The CSL Lagrangian in eq. (11.16) has the same ϕ-dependence as the Lagrangian in eq. (8.3) except for a different surface term. The equation of motion for ϕ will therefore be the same. Thus, eq. (8.9) gives us the relation

$$\partial_z^2 \phi = m_\pi^2 \sin\phi. \tag{11.25}$$

The same derivation as in section 8.2 gives a lattice structure with the same period as in eq. (8.15). We can also use the result of eq. (8.24) when we integrate the Gibbs free energy of the CSL in eq. (11.18). The total Gibbs free energy per unit volume then becomes

$$\frac{G_{\text{CSL}}}{V} = \frac{m_\pi}{2kK(k)} \left[F(k) - \frac{\mu_I e B}{4\pi}\right] + \frac{1}{2}(B - H)^2, \tag{11.26}$$

where we have exploited that B is a constant in space and $F(k)$ is

$$F(k) \equiv 4m_\pi f_\pi^2 \left[\frac{2E(k)}{k} + \left(k - \frac{1}{k}\right) K(k)\right]. \tag{11.27}$$

The energy is minimized when

$$B = H + \frac{m_\pi}{2kK(k)} \frac{\mu_I e}{4\pi}. \tag{11.28}$$

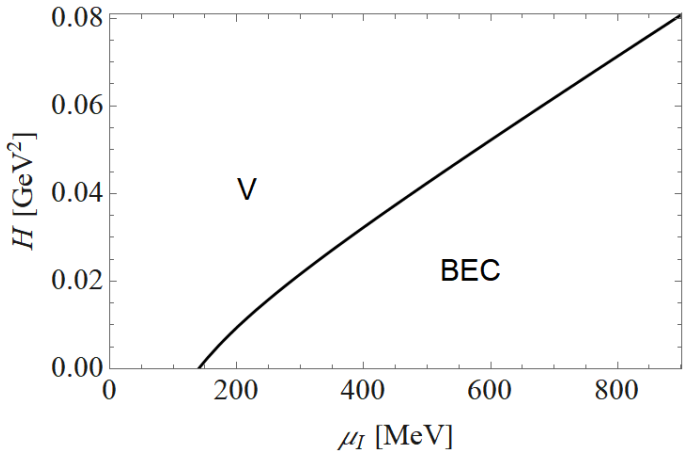

Figure 11.2: The external magnetic field H at which the transition between the BEC and the QCD vacuum (V) occurs. Plotted as a function of isospin chemical potential μ_I with pion mass $m_\pi = 140$ MeV and $f_\pi = 92$ MeV. The BEC exists below the graph.

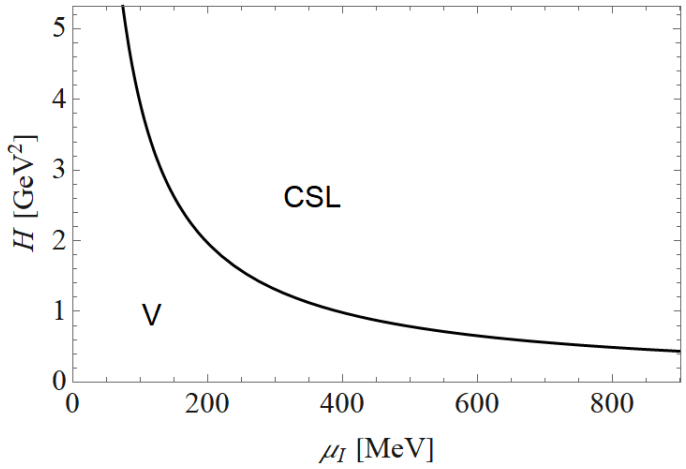

Figure 11.3: The external magnetic field H at which the transition between the QCD vacuum (V) and the CSL occurs. Plotted as a function of isospin chemical potential μ_I with pion mass $m_\pi = 140$ MeV and $f_\pi = 92$ MeV. The CSL exists above the graph.

The second term can, in analogy with eq. (3.4) of [23], be verified as the magnetization per unit volume of the CSL. Substituting the value of the magnetic field B into eq. (11.26) results in

$$\frac{G_{\text{CSL}}}{V} = \frac{m_\pi}{2kK(k)}\left[F(k) - \frac{1}{2}\frac{m_\pi}{2kK(k)}\left(\frac{\mu_I e}{4\pi}\right)^2 - \frac{\mu_I e}{4\pi}H\right]. \tag{11.29}$$

Minimizing this with respect to k gives the condition

$$H = \frac{m_\pi}{e\mu_I k}\left(32\pi f_\pi^2 E(k) - \frac{e^2\mu_I^2}{8\pi K(k)}\right) \equiv H_{\text{CSL}}, \tag{11.30}$$

where H_{CSL} is, for the optimal value of k, the lowest external magnetic field at which the CSL can exist. We observe that the optimal value of k is unaffected by the value of the pion mass.

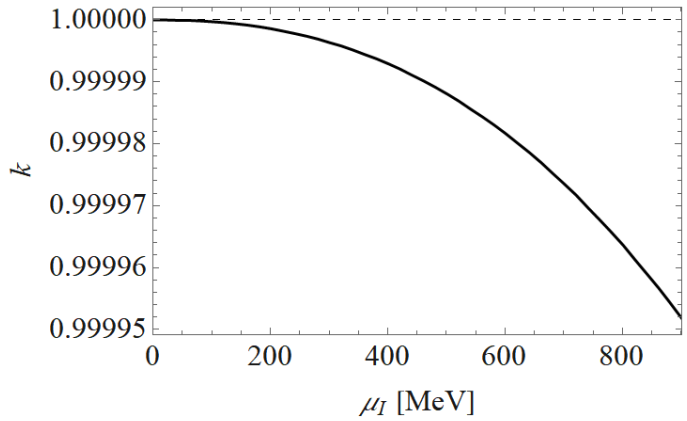

Figure 11.4: The value of the elliptic modulus k at the transition between the QCD vacuum and the CSL as a function of isospin chemical potential μ_I. The pion mass is set to $m_\pi = 140$ MeV and $f_\pi = 92$ MeV.

The transition from the QCD vacuum to the CSL happens when the total Gibbs free energy of the CSL drops below zero. The external magnetic field, $H_{\mathrm{V/CSL}}$, at which this happens is found by numerical minimization of the total Gibbs free energy with respect to k and then solving $G_{\mathrm{CSL}}/V = 0$ for H. The result is plotted in figure 11.3. The necessary external field for a transition to the CSL decreases with increasing isospin chemical potential. This is expected from the case of a baryon chemical potential. It can be verified numerically that $H_{\mathrm{V/CSL}} \geq H_{\mathrm{CSL}}$, implying that the transition does actually take place where the CSL can exist. The value of k at the transition between the QCD vacuum and the CSL is displayed in figure 11.4. We observe that k deviates slightly from one, indicating a weakly first order transition. The deviation is however so small that any higher order corrections may erase it.

The transition between the BEC and the CSL takes place when $G_{\mathrm{BEC}} = G_{\mathrm{CSL}}$. Eqs. (11.10) and (11.29) give this equality when

$$\frac{m_\pi}{2kK(k)}\left[F(k) - \frac{1}{2}\frac{m_\pi}{2kK(k)}\left(\frac{\mu_I e}{4\pi}\right)^2 - \frac{\mu_I e}{4\pi}H\right] - \frac{1}{2}H^2 + \frac{f_\pi^2}{2\mu_I^2}\left(\mu_I^2 - m_\pi^2\right)^2 = 0, \quad (11.31)$$

where k is found by numerical minimization of G_{CSL}. A scenario where $k \to 1$ gives $H_{\mathrm{BEC/CSL}} = H_{\mathrm{V/BEC}}$, where $H_{\mathrm{BEC/CSL}}$ is the external magnetic field at which the transition between the BEC and the CSL occurs. When m_π is comparable to the physical value of the pion mass, $m_\pi = 140$ MeV, there will be no transition directly from the BEC to the CSL. Instead, the CSL and the BEC are well separated in the phase diagram. This is seen by comparing figures 11.2 and 11.3, where we have plotted $H_{\mathrm{V/CSL}}$ and $H_{\mathrm{V/BEC}}$, respectively.

The region where the QCD vacuum separates the BEC and the CSL in the phase diagram shrinks as the pion mass is reduced. Figure 11.5 displays the phase diagram at $m_\pi = 50$ MeV. Reducing the pion mass further leads to the possibility of a direct transition between the BEC and the CSL phase. This can happen when $\mu_I \gtrsim 175$ MeV for $m_\pi = 1$ MeV as seen in figure 11.6. The QCD vacuum is eventually squeezed out of the phase diagram when $m_\pi \to 0$, and we are left with the phase diagram obtained in figure 11.1.

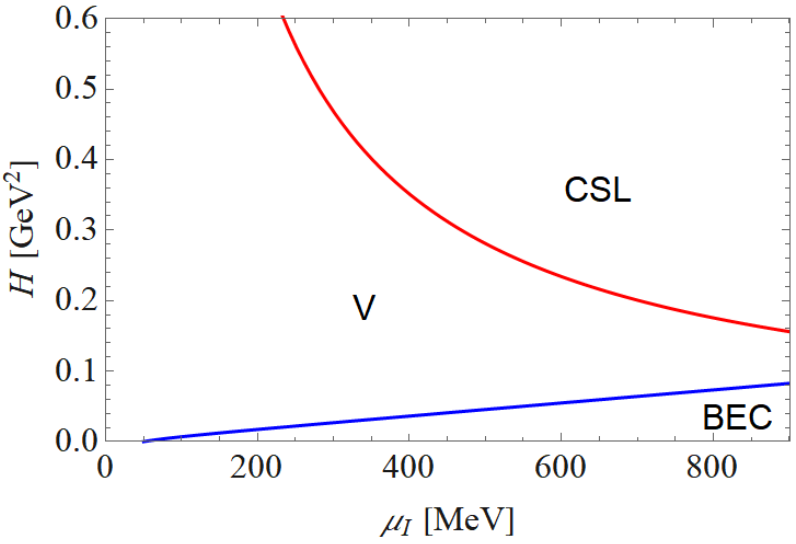

Figure 11.5: The QCD phase diagram as a function of isospin chemical potential μ_I with pion mass $m_\pi = 50$ MeV and $f_\pi = 92$ MeV. The QCD vacuum (V) separates the BEC and the CSL.

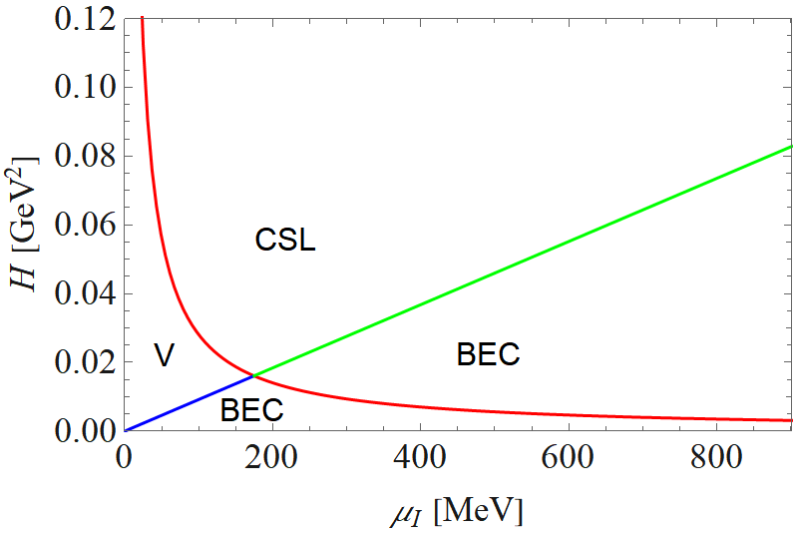

Figure 11.6: The QCD phase diagram as a function of isospin chemical potential μ_I with pion mass $m_\pi = 1$ MeV and $f_\pi = 92$ MeV. The QCD vacuum (V) is nearly squeezed out of the phase diagram by the BEC and the CSL.

Chapter 12

Magnetic vortex lattice

In this chapter, we consider the possibility of a magnetic vortex lattice in the QCD phase diagram. Such a phase can be expected since we already know that an external field causes the BEC to set up currents that expel the external magnetic field. The question is therefore whether the nature of this superconductivity is type-I or type-II. In [17], it is established that the type-II superconductivity is by far the dominant type in the phase diagram. We will therefore expect a phase where the external magnetic field starts to penetrate the BEC as vortices. The transition from a uniform BEC to a vortex phase occurs at the lower critical field H_{c1}. As the external field is increased, the density of magnetic vortices will increase. The vortices will arrange themselves into a lattice, forming a magnetic vortex lattice. At the upper critical field H_{c2}, these vortices will be so closely packed that the superconducting phase makes a transition to the QCD vacuum, where the external field completely penetrates the system. The QCD magnetic vortex lattice has been studied at the lower critical field in [17] and at the upper critical field in [26]. However, it has not been found any method to determine the structure and the energy of the lattice for arbitrary external field and isospin chemical potential. This problem has been addressed in the Ginzburg-Landau theory for conventional superconductors by Brandt [60]. In [61], he solves the equations of motion iteratively in order to obtain both the structure and the energy of the magnetic vortex lattice.

As it turns out, this procedure may also be adapted to the vortex lattice in QCD. We start out by writing the Helmholtz free energy of the system on a gauge-invariant form. The degrees of freedom are then expanded into Fourier series consisting of a solution to the equations of motion at the upper critical field. After deriving this solution, we propose an iteration procedure that solves the equations of motion numerically for a given average magnetic field of the system. Next, we derive a virial theorem for QCD which makes it possible to compute the external magnetic field for a given average magnetic field. Having both the Helmholtz free energy and the external magnetic field at hand, we can obtain the Gibbs free energy of the vortex lattice. This can in turn be used to establish the presence of the lattice in the phase diagram.

12.1 Helmholtz free energy

The Lagrangian in presence of an isospin chemical potential and dynamical electromagnetic fields is given by eq. (11.4). It may be written as

$$\begin{aligned}\mathscr{L} &= \mathscr{L}_{\text{ChPT}} + \mathscr{L}_{\text{QED}} \\ &= -\frac{f_\pi^2}{4}\text{Tr}\left\{\partial_i\Sigma^\dagger\partial_i\Sigma + \frac{1}{2}ieA_i\left(\partial_i\Sigma^\dagger[\tau_3,\Sigma] + \left[\tau_3,\Sigma^\dagger\right]\partial_i\Sigma\right)\right. \\ &\quad \left. +\frac{1}{4}\left(\mu_I^2 - e^2A_iA_i\right)\left[\tau_3,\Sigma^\dagger\right][\tau_3,\Sigma]\right\} + \frac{f_\pi^2 m_\pi^2}{2}\text{ReTr}\Sigma - f_\pi^2 m_\pi^2 - \frac{1}{4}F_{ij}F^{ij},\end{aligned} \tag{12.1}$$

where we have assumed time-independence, as well as no electric fields implying that we can set $A^0 = 0$. We choose the parameterization $\Sigma = \frac{1}{f_\pi}(\sigma + i\boldsymbol{\tau}\cdot\boldsymbol{\pi})$, subject to the constraint $\sigma^2 + \boldsymbol{\pi}^2 = f_\pi^2$. This makes it possible to draw parallels to the Ginzburg-Landau theory. We will proceed by assuming no neutral pion condensation, $\pi_3 = 0$. The possibility of neutral pion condensation has been discussed in the literature, but the existence of such condensation has not been established [26]. The first term in the Lagrangian becomes

$$-\frac{f_\pi^2}{4}\text{Tr}\left(\partial_i\Sigma^\dagger\partial_i\Sigma\right) = -\frac{1}{2}\left[(\boldsymbol{\nabla}\sigma)^2 + (\boldsymbol{\nabla}\pi_1)^2 + (\boldsymbol{\nabla}\pi_2)^2\right]. \tag{12.2}$$

The second term in the Lagrangian becomes

$$-\frac{if_\pi^2 e}{8}A_i\text{Tr}\left(\partial_i\Sigma^\dagger[\tau_3,\Sigma]\right) = \frac{1}{2}e\boldsymbol{A}\left(\pi_1\boldsymbol{\nabla}\pi_2 - \pi_2\boldsymbol{\nabla}\pi_1\right). \tag{12.3}$$

Next, the third term in the Lagrangian becomes

$$-\frac{if_\pi^2 e}{8}A_i\text{Tr}\left(\left[\tau_3,\Sigma^\dagger\right]\partial_i\Sigma\right) = \left[-\frac{if_\pi^2 e}{8}A_i\text{Tr}\left(\partial_i\Sigma^\dagger[\tau_3,\Sigma]\right)\right]^\dagger = \frac{1}{2}e\boldsymbol{A}\left(\pi_1\boldsymbol{\nabla}\pi_2 - \pi_2\boldsymbol{\nabla}\pi_1\right). \tag{12.4}$$

The fourth term in the Lagrangian can be written as

$$-\frac{f_\pi^2}{16}\left(\mu_I^2 - e^2A_iA_i\right)\text{Tr}\left(\left[\tau_3,\Sigma^\dagger\right][\tau_3,\Sigma]\right) = \frac{1}{2}\left(\mu_I^2 - e^2\boldsymbol{A}^2\right)\left(\pi_1^2 + \pi_2^2\right). \tag{12.5}$$

Adding the terms in eqs. (12.2)-(12.5), the Lagrangian in eq. (12.1) can be cast into the form

$$\begin{aligned}\mathscr{L} =& -\frac{1}{2}(\boldsymbol{\nabla}\sigma)^2 - \frac{1}{2}(\boldsymbol{\nabla}\pi_1)^2 - \frac{1}{2}(\boldsymbol{\nabla}\pi_2)^2 + e\boldsymbol{A}\left(\pi_1\boldsymbol{\nabla}\pi_2 - \pi_2\boldsymbol{\nabla}\pi_1\right) \\ &+ \frac{1}{2}\left(\mu_I^2 - e^2\boldsymbol{A}^2\right)\left(\pi_1^2 + \pi_2^2\right) - f_\pi m_\pi^2\left(f_\pi - \sigma\right) - \frac{1}{2}\boldsymbol{B}^2.\end{aligned} \tag{12.6}$$

The canonical conjugate momenta in a Legendre transform of the Lagrangian vanish since there is no time-dependence. The Hamiltonian is therefore given by

$$\mathscr{H} = -\mathscr{L} = \frac{1}{2}(\boldsymbol{\nabla}\sigma)^2 + \frac{1}{2}e^2\left|\left(\frac{\boldsymbol{\nabla}}{ie} - \boldsymbol{A}\right)\pi\right|^2 - \frac{1}{2}\mu_I\pi^*\pi - f_\pi m_\pi^2(\sigma - f_\pi) + \frac{1}{2}\boldsymbol{B}^2, \tag{12.7}$$

where we have defined the complex field $\pi \equiv \pi_1 + i\pi_2$, in which we drop the conventional factor $1/\sqrt{2}$. In addition, we used that

$$\frac{1}{2}e^2\left|\left(\frac{\boldsymbol{\nabla}}{ie} - \boldsymbol{A}\right)\pi\right|^2 = \frac{1}{2}\left(\boldsymbol{\nabla}\pi_1\right)^2 + \frac{1}{2}\left(\boldsymbol{\nabla}\pi_2\right)^2 - e\boldsymbol{A}\left(\pi_1\boldsymbol{\nabla}\pi_2 - \pi_2\boldsymbol{\nabla}\pi_1\right) + \frac{1}{2}e^2\boldsymbol{A}^2\left(\pi_1^2 + \pi_2^2\right). \tag{12.8}$$

Writing $\pi \equiv \omega^{1/2}e^{i\phi}$, where $\omega = |\pi|^2$, the condition $\sigma^2 + \pi_1^2 + \pi_2^2 = f_\pi^2$ becomes $\sigma^2 + \omega = f_\pi^2$. This allows us to eliminate the dependence on σ by inserting $\sigma = \sqrt{f_\pi^2 - \omega}$ into the Hamiltonian. This yields the Helmholtz free energy

$$\begin{aligned}\mathscr{F} &= \frac{\left(\boldsymbol{\nabla}\omega\right)^2}{8\left(f_\pi^2 - \omega\right)} + \frac{1}{2}e^2\left|\left(\frac{\boldsymbol{\nabla}}{ie} - \boldsymbol{A}\right)\omega^{1/2}e^{i\phi}\right|^2 - \frac{1}{2}\mu_I^2\omega \\ &\quad - f_\pi m_\pi^2\left(\sqrt{f_\pi^2 - \omega} - f_\pi\right) + \frac{1}{2}\boldsymbol{B}^2 \\ &= \frac{\left(\boldsymbol{\nabla}\omega\right)^2}{8}\left(\frac{1}{f_\pi^2 - \omega} + \frac{1}{\omega}\right) - \frac{1}{2}\left(\mu_I^2 - e^2\boldsymbol{Q}^2\right)\omega - f_\pi m_\pi^2\left(\sqrt{f_\pi^2 - \omega} - f_\pi\right) + \frac{1}{2}\boldsymbol{B}^2,\end{aligned} \tag{12.9}$$

where we have defined the gauge-invariant supervelocity $\boldsymbol{Q} = \boldsymbol{A} - \frac{\boldsymbol{\nabla}\phi}{e}$ and applied the product rule in order to find $\boldsymbol{\nabla}\omega = 2\omega^{1/2}\boldsymbol{\nabla}\omega^{1/2}$, such that $\left(\boldsymbol{\nabla}\omega^{1/2}\right)^2 = \frac{(\boldsymbol{\nabla}\omega)^2}{4\omega}$. Thus, we are left with a gauge-invariant free energy without any unfixed degrees of freedom. This means that we can minimize the energy and compare it to other phases such as the CSL. The next step is to exploit the resemblance to the Ginzburg-Landau theory. In [61], Brandt solves the Ginzburg-Landau equations iteratively by writing ω, $\boldsymbol{B}$ and $\boldsymbol{Q}$ as Fourier series with the same periodicity as the lattice. Since the external magnetic field is uniform and points in the z-direction, we will assume that $\boldsymbol{B} = (0, 0, B(x, y))$. In addition, we write $\omega = \omega(x, y)$. Consequently, we have a two-dimensional problem and we let $\boldsymbol{r} = (x, y)$. The inversion symmetry of the lattice makes it possible to write

$$\omega(\boldsymbol{r}) = \sum_{\boldsymbol{K}} a_{\boldsymbol{K}}\left(1 - \cos\boldsymbol{K}\cdot\boldsymbol{r}\right), \tag{12.10}$$

$$B(\boldsymbol{r}) = \bar{B} + \sum_{\boldsymbol{K}} b_{\boldsymbol{K}}\cos\boldsymbol{K}\cdot\boldsymbol{r}, \tag{12.11}$$

where $\bar{B} = \langle B(\boldsymbol{r})\rangle = (1/V)\int_V \mathrm{d}^3 r B(r)$ is the spatially averaged magnetic field over a unit cell of volume V. The sums are over all reciprocal lattice vectors $\boldsymbol{K} \neq 0$, and the Fourier series in B represents the variation of B away from the average magnetic field. Next, we turn our attention to the supervelocity $\boldsymbol{Q}$. Close to a vortex core, we have that $\phi = p\theta$, where θ is the polar angle and p is an integer denoting the amount of flux going through a vortex. This ensures the single-valuedness of ω. Furthermore, it implies that $\boldsymbol{\nabla}\phi = \frac{p}{r}\hat{\theta}$, which diverges when $r \to 0$ at the vortex cores. Applying Stoke's theorem to the divergent part of $\boldsymbol{Q}$ yields the relation

$$\boldsymbol{\nabla}\times\left(-\frac{p}{er}\hat{\theta}\right) = -\frac{2\pi p}{e}\delta_2\left(\boldsymbol{r}\right)\hat{z}. \tag{12.12}$$

However, excluding the singularities at the vortex cores gives $\boldsymbol{\nabla}\times\boldsymbol{Q} = \boldsymbol{\nabla}\times\boldsymbol{A} = B(\boldsymbol{r})\hat{z}$. The full expression for the curl of the supervelocity is therefore

$$\boldsymbol{\nabla}\times\boldsymbol{Q} = \left[B(\boldsymbol{r}) - \Phi_0\sum_{\boldsymbol{R}}\delta_2\left(\boldsymbol{r} - \boldsymbol{R}\right)\right]\hat{z}, \tag{12.13}$$

where $\boldsymbol{R}$ are lattice vectors pointing to the vortex positions and we assumed that each vortex carries the lowest amount of flux $\Phi_0 = 2\pi/e$. Furthermore, we can split the supervelocity $\boldsymbol{Q}$ into the two terms

$$\boldsymbol{Q} = \boldsymbol{Q}_{\mathrm{A}} + \boldsymbol{Q}_{\mathrm{B}}, \tag{12.14}$$

where $\boldsymbol{Q}_{\mathrm{A}}$ is the supervelocity of the Abrikosov solution. This is the solution at the upper critical field H_{c2}. It represents the singular contributions at the vortex cores,

$$\boldsymbol{\nabla} \times \boldsymbol{Q}_{\mathrm{A}} = \left[\bar{B} - \Phi_0 \sum_{\boldsymbol{R}} \delta_2 \left(\boldsymbol{r} - \boldsymbol{R} \right) \right] \hat{z}, \tag{12.15}$$

where the average magnetic field $\bar{B} = \Phi_0/S$, in which S is the area of a unit cell. An exact expression for $\boldsymbol{Q}_{\mathrm{A}}$ in terms of Fourier coefficients will be derived in section 12.2. Consequently, $\boldsymbol{\nabla} \times \boldsymbol{Q}_{\mathrm{B}} = B(\boldsymbol{r})\hat{z} - \bar{B}\hat{z}$ describes the spatial variation of the magnetic field away from the Abrikosov H_{c2} solution. We note that the average vorticities over a unit cell of these velocity fields vanish,

$$\langle \boldsymbol{\nabla} \times \boldsymbol{Q} \rangle = \langle \boldsymbol{\nabla} \times \boldsymbol{Q}_{\mathrm{A}} \rangle = \langle \boldsymbol{\nabla} \times \boldsymbol{Q}_{\mathrm{B}} \rangle = \bar{B} - \Phi_0/S = 0. \tag{12.16}$$

Moreover, eq. (12.11) allows us to write

$$\boldsymbol{Q} = \boldsymbol{Q}_{\mathrm{A}} + \sum_{\boldsymbol{K}} b_{\boldsymbol{K}} \frac{\hat{z} \times \boldsymbol{K}}{K^2} \sin \boldsymbol{K} \cdot \boldsymbol{r}, \tag{12.17}$$

where the sum is still running over all reciprocal lattice vectors $\boldsymbol{K} \neq 0$ [62]. We position the vortices at $\boldsymbol{R} = \boldsymbol{R}_{mn} = (mx_1 + nx_2, ny_2)$, yielding the reciprocal lattice vectors

$$\boldsymbol{K} = \boldsymbol{K}_{mn} = \frac{2\pi}{S} \left(my_2, -mx_2 + nx_1 \right), \tag{12.18}$$

where m, n are integers and $S = x_1 y_2$. For a triangular lattice, we have $x_2 = x_1/2$ and $y_2 = \sqrt{3}x_1/2$. Requiring that $S\bar{B} = \Phi_0$ results in the vortex spacing

$$x_1 = \sqrt{\frac{4\pi}{\sqrt{3}e\bar{B}}}. \tag{12.19}$$

12.2 The Abrikosov solution

At the upper critical field, the order parameter $\omega = \pi^*\pi$ will be small compared to f_π^2. We will in the following use this to solve the linearized equation of motion for π^* in order to find an expression for $\boldsymbol{Q}_{\mathrm{A}}$. This expression should be computed with high accuracy as it typically is the dominating term in $\boldsymbol{Q}$. The equation of motion is found by using the Euler-Lagrange equations for the Lagrangian in eq. (12.7). We start out by writing

$$\sigma = \sqrt{f_\pi^2 - \pi^*\pi} = f_\pi \left(1 - \frac{\pi^*\pi}{2f_\pi^2} + \mathcal{O}\left(\pi^4\right) \right), \tag{12.20}$$

implying that $(\boldsymbol{\nabla}\sigma)^2$ is of order four in the pion fields and so does not contribute to the linearized equation of motion. To first order in the pion fields we have

$$\frac{\partial \mathscr{L}}{\partial \pi^*} = \frac{1}{2}e^2 \boldsymbol{A}\left(\frac{\boldsymbol{\nabla}}{ie} - \boldsymbol{A}\right)\pi + \frac{1}{2}\left(\mu_I^2 - m_\pi^2\right)\pi, \tag{12.21}$$

and

$$\boldsymbol{\nabla}\cdot\frac{\partial \mathscr{L}}{\partial\left(\boldsymbol{\nabla}\boldsymbol{\pi}^*\right)} = \frac{1}{2}ie\boldsymbol{A}\cdot\boldsymbol{\nabla}\pi + \frac{1}{2}ie\pi\boldsymbol{\nabla}\cdot\boldsymbol{A} - \frac{1}{2}\boldsymbol{\nabla}^2\pi. \tag{12.22}$$

Hence, the linearized equation of motion is

$$\left(-\frac{i}{e}\boldsymbol{\nabla} - \boldsymbol{A}\right)^2 \pi_{\mathrm{A}} = \frac{\mu_I^2 - m_\pi^2}{e^2}\pi_{\mathrm{A}} \equiv \frac{H_{\mathrm{c2}}}{e}\pi_{\mathrm{A}}, \tag{12.23}$$

where the subscript A denotes that π is the solution near the upper critical field, also known as the Abrikosov solution in the Ginzburg-Landau theory. The strength of the upper critical field H_{c2} is found in [26] by looking at where the dispersion relation of a charged pion becomes tachyonic. The magnetic field B will be nearly uniform close to H_{c2}, and we can therefore make the approximation $\boldsymbol{B} = (0, 0, H_{\mathrm{c2}})$. Thus, in the symmetric gauge we have $\boldsymbol{A} = \frac{H_{\mathrm{c2}}}{2}(-y, x, 0)$. This can be used to rewrite the linearized equation of motion in terms of creation and annihilation operators. We start out by defining

$$\begin{aligned}
\Pi_x &\equiv -\frac{i}{e}\partial_x + \frac{H_{\mathrm{c2}}}{2}y, \\
\Pi_y &\equiv -\frac{i}{e}\partial_y - \frac{H_{\mathrm{c2}}}{2}x, \\
\Pi_z &\equiv 0,
\end{aligned} \tag{12.24}$$

as well as

$$\begin{aligned}
a &\equiv \Pi_x + i\Pi_y, \\
a^\dagger &\equiv \Pi_x - i\Pi_y.
\end{aligned} \tag{12.25}$$

The commutator of the annihilation operator a and the creation operator $a^\dagger$ reads

$$\left[a, a^\dagger\right] = 2i[\Pi_y, \Pi_x] = \frac{2H_{\mathrm{c2}}}{e}. \tag{12.26}$$

Next, we calculate

$$a^\dagger a = \Pi_x^2 + \Pi_y^2 + i[\Pi_x, \Pi_y] = -\frac{1}{e^2}\left(\partial_x^2 + \partial_y^2\right) + \frac{iH_{\mathrm{c2}}}{e}\left(x\partial_y - y\partial_x\right) + \frac{H_{\mathrm{c2}}^2}{4}\left(x^2 + y^2\right) - \frac{H_{\mathrm{c2}}}{e}, \tag{12.27}$$

where the commutator of Π_x and Π_y is found in eq. (12.26). This can in turn be used to rewrite the linearized equation of motion (12.23) as

$$\begin{aligned}
\frac{e}{H_{\mathrm{c2}}}\left(-\frac{i}{e}\boldsymbol{\nabla} - \boldsymbol{A}\right)^2 \pi_{\mathrm{A}} &= \frac{e}{H_{\mathrm{c2}}}\left[-\frac{1}{e^2}\left(\partial_x^2 + \partial_y^2\right) + \frac{iH_{\mathrm{c2}}}{e}\left(x\partial_y - y\partial_x\right) + \frac{H_{\mathrm{c2}}^2}{4}\right]\pi_{\mathrm{A}} \\
&= \frac{e}{H_{\mathrm{c2}}}\left(a^\dagger a + \frac{H_{\mathrm{c2}}}{e}\right)\pi_{\mathrm{A}} = \pi_{\mathrm{A}}.
\end{aligned} \tag{12.28}$$

Since π_A can be interpreted as the lowest Landau level, the annihilation operator a must satisfy $a\pi_\mathrm{A} = 0$. Inserting a from eq. (12.25) and writing $\pi_\mathrm{A} = |\pi_\mathrm{A}|e^{i\phi_\mathrm{A}}$ gives

$$\left(-\frac{i}{e}\partial_x + \frac{H_{c2}}{2}y + \frac{1}{e}\partial_y - \frac{iH_{c2}}{2}x\right)|\pi_\mathrm{A}|e^{i\phi_\mathrm{A}} = 0. \tag{12.29}$$

This equation agrees with the linearized equation of motion obtained in [26] using a different approach. Demanding that the real and imaginary terms must separately be zero provides us with the two equations

$$\begin{aligned}\partial_x|\pi_\mathrm{A}| &= e|\pi_\mathrm{A}|\left(-A_y + \frac{1}{e}\partial_y\phi_\mathrm{A}\right),\\ \partial_y|\pi_\mathrm{A}| &= e|\pi_\mathrm{A}|\left(A_x - \frac{1}{e}\partial_x\phi_\mathrm{A}\right).\end{aligned} \tag{12.30}$$

The derivatives of the modulus squared are $\partial_x|\pi_\mathrm{A}|^2 = 2|\pi_\mathrm{A}|\partial_x|\pi_\mathrm{A}|$ and $\partial_y|\pi_\mathrm{A}|^2 = 2|\pi_\mathrm{A}|\partial_y|\pi_\mathrm{A}|$. Substituting this into the linearized equations of motion yields

$$\begin{aligned}\partial_x\omega_\mathrm{A} &= -2e\omega_\mathrm{A}\left(A_y - \frac{1}{e}\partial_y\phi_\mathrm{A}\right),\\ \partial_y\omega_\mathrm{A} &= 2e\omega_\mathrm{A}\left(A_x - \frac{1}{e}\partial_x\phi_\mathrm{A}\right),\end{aligned} \tag{12.31}$$

where we used that $|\pi_\mathrm{A}|^2 = \omega_\mathrm{A}$. Thus, the nonzero components of Q_A becomes

$$\begin{aligned}Q_{\mathrm{A}x} &= A_x - \frac{1}{e}\partial_{x\mathrm{A}} = \frac{1}{2e}\frac{\partial_y\omega_\mathrm{A}}{\omega_\mathrm{A}},\\ Q_{\mathrm{A}y} &= A_y - \frac{1}{e}\partial_{y\mathrm{A}} = -\frac{1}{2e}\frac{\partial_x\omega_\mathrm{A}}{\omega_\mathrm{A}}.\end{aligned} \tag{12.32}$$

A more compact form reads

$$\boldsymbol{Q}_\mathrm{A} = \frac{1}{2e}\frac{\boldsymbol{\nabla}\omega_\mathrm{A}\times\hat{z}}{\omega_\mathrm{A}}. \tag{12.33}$$

The supervelocity at the upper critical field is therefore perpendicular to the order parameter gradient [63]. The solution to the linearized equations of motion in eq. (12.31) is given by the rapidly converging series in eq. (12.10) with coefficients [61]

$$a^\mathrm{A}_{\boldsymbol{K}} = -(-1)^{m+mn+n}\exp\left(-\frac{\boldsymbol{K}^2_{mn}S}{8\pi}\right). \tag{12.34}$$

For any lattice symmetry, ω_A is normalized to $\langle\omega_\mathrm{A}(\boldsymbol{r})\rangle = 1$. Figure 12.1 shows that the solution forms a fishnet pattern where ω_A goes to zero at the vortex cores. This is expected at magnetic fields close to the upper critical field H_{c2}.

12.3 Ginzburg-Landau equations of QCD

One way to find the minimum Gibbs free energy of the magnetic vortex lattice is to use a finite number of Fourier coefficients $a_{\boldsymbol{K}}$ and $b_{\boldsymbol{K}}$, and minimize the energy with

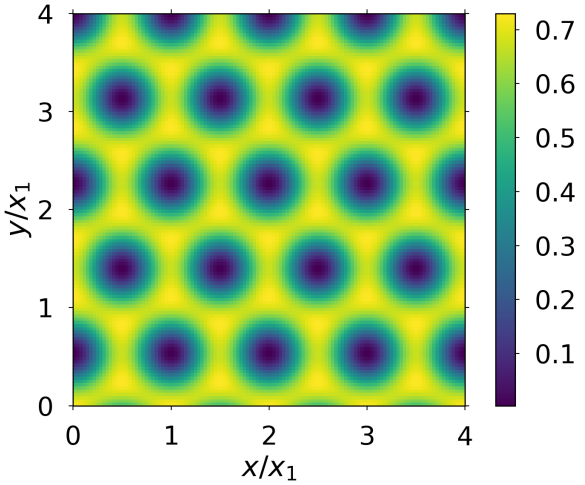

Figure 12.1: The solution ω_{A} to the linearized equation of motion near the upper critical field H_{c2}. The order parameter goes to zero at the vortex cores which are separated by a distance x_1.

respect to these coefficients. This has been done for the Ginzburg-Landau theory in [64]. However, a faster way is to iterate the equations of motion for ω and $\boldsymbol{A}$. In that way, we can obtain the correct solutions to the equations of motion for a given average magnetic field $\bar{B}$. The average magnetic field is our input parameter. This means that we do not know the external magnetic field at which we solve the equations of motion. Hence, the Gibbs free energy is unknown. Only the Helmholtz free energy, in which the external field is not present, is known. We must therefore find a way to get the external field for a given average magnetic field. One way to obtain the external field is to calculate the average Helmholtz free energy $\bar{F} = \langle \mathscr{F} \rangle = F/V$ and then use the relation $H = \partial \bar{F}/\partial \bar{B}$. This relation is found by minimizing the average Gibbs free energy with respect to $\bar{B}$. The external field is then found by taking the numerical derivative of $\bar{F}$. However, a numerically faster and more accurate method is to use a version of the so-called virial theorem, which we will derive in section 12.4.

The equation of motion for ω is found by setting the variation $\delta\mathscr{F}/\delta\omega$ of the free energy in eq. (12.9) to zero. First, we have

$$\frac{\partial \mathscr{F}}{\partial \omega} = \frac{1}{8}\left[(\boldsymbol{\nabla}\omega)^2\left(\frac{1}{(f_\pi^2-\omega)^2} - \frac{1}{\omega^2}\right) + \frac{4 f_\pi m_\pi^2}{\sqrt{f_\pi^2-\omega}} - 4\left(\mu_I^2 - e^2\boldsymbol{Q}^2\right)\right]. \tag{12.35}$$

Next, we have

$$\boldsymbol{\nabla}\cdot\left(\frac{\partial \mathscr{F}}{\partial\left(\boldsymbol{\nabla}\omega\right)}\right) = \frac{\boldsymbol{\nabla}^2\omega}{4}\left(\frac{1}{f_\pi^2-\omega} + \frac{1}{\omega}\right) + \frac{\boldsymbol{\nabla}\omega}{4}\left(\frac{\boldsymbol{\nabla}\omega}{(f_\pi^2-\omega)^2} - \frac{\boldsymbol{\nabla}\omega}{\omega^2}\right), \tag{12.36}$$

which together gives the equation of motion for ω in the form

$$\left(-\boldsymbol{\nabla}^2 + 2e^2 f_\pi^2\right)\omega = \frac{1}{2}\left\{\omega - \frac{\omega^2}{f_\pi^2}\right\}\left\{4\left(\mu_I^2 - e^2\boldsymbol{Q}^2\right) + (\boldsymbol{\nabla}\omega)^2\left[\frac{1}{\left(f_\pi^2-\omega\right)^2} - \frac{1}{\omega^2}\right] - \frac{4f_\pi m_\pi^2}{\sqrt{f_\pi^2-\omega}}\right\} + 2e^2 f_\pi^2\omega, \tag{12.37}$$

where we have added a term $2e^2 f_\pi^2\omega$ to both sides of the equation for stable and more rapid convergence. Expanding the left-hand side into the Fourier series of eq. (12.10) yields

$$\sum_{\boldsymbol{K}} a_{\boldsymbol{K}}\left[-\boldsymbol{K}^2\cos\boldsymbol{K}\cdot\boldsymbol{r} + 2e^2 f_\pi^2\left(1-\cos\boldsymbol{K}\cdot\boldsymbol{r}\right)\right] = \frac{1}{2}\left\{\omega - \frac{\omega^2}{f_\pi^2}\right\}\left\{4\left(\mu_I^2 - e^2\boldsymbol{Q}^2\right) + (\boldsymbol{\nabla}\omega)^2\left[\frac{1}{\left(f_\pi^2-\omega\right)^2} - \frac{1}{\omega^2}\right] - \frac{4f_\pi m_\pi^2}{\sqrt{f_\pi^2-\omega}}\right\} + 2e^2 f_\pi^2\omega. \tag{12.38}$$

Next, we multiply both sides by $\cos\boldsymbol{K}'\cdot\boldsymbol{r}$, take the spatial average $\langle ...\rangle$ and use the property $\langle\cos\boldsymbol{K}\cdot\boldsymbol{r}\cos\boldsymbol{K}'\cdot\boldsymbol{r}\rangle = \frac{1}{2}\delta_{\boldsymbol{K},\boldsymbol{K}'}$ to obtain the iteration equation for the Fourier coefficients

$$a_{\boldsymbol{K}} = \frac{-2}{\boldsymbol{K}^2 + 2e^2 f_\pi^2}\left\langle\left\{2\left[\omega - \frac{\omega^2}{f_\pi^2}\right]\left[\mu_I^2 - e^2\boldsymbol{Q}^2\right] + \frac{1}{2f_\pi^2}\left[\frac{\omega\left(\boldsymbol{\nabla}\omega\right)^2}{f_\pi^2-\omega} - \frac{\left(f_\pi^2-\omega\right)\left(\boldsymbol{\nabla}\omega\right)^2}{\omega}\right] - \frac{2m_\pi^2}{f_\pi}\omega\sqrt{f_\pi^2-\omega} + 2e^2 f_\pi^2\omega\right\}\cos\boldsymbol{K}\cdot\boldsymbol{r}\right\rangle, \tag{12.39}$$

where we have dropped the prime in $\boldsymbol{K}'$. Updated Fourier coefficients for ω are found by inserting the old values of ω and $\boldsymbol{Q}$ on the right-hand side. Points where $\omega \to f_\pi^2$ or $\omega \to 0$ are not problematic since $\boldsymbol{\nabla}\omega$ goes faster to zero at these points. A second iteration equation can be found from the equations of motion for the vector potential $\boldsymbol{A}$. The equations of motion are obtained by requiring that the variation $\delta\mathscr{F}/\delta\boldsymbol{A}$ of the Helmholtz free energy in eq. (12.9) vanishes. Hence, we are left with

$$\boldsymbol{\nabla}\times\boldsymbol{B} = -e^2\omega\boldsymbol{Q}. \tag{12.40}$$

Taking the curl of both sides yields

$$\begin{aligned}\boldsymbol{\nabla}^2\boldsymbol{B} &= e^2\boldsymbol{\nabla}\times(\omega\boldsymbol{Q})\\ &= e^2\left(\boldsymbol{\nabla}\omega\times\boldsymbol{Q} + \omega\boldsymbol{\nabla}\times\boldsymbol{Q}\right)\\ &= e^2\left(\boldsymbol{\nabla}\omega\times\boldsymbol{Q} + \omega\boldsymbol{\nabla}\times\boldsymbol{A} - \frac{1}{e}\omega\boldsymbol{\nabla}\times\boldsymbol{\nabla}\phi\right),\end{aligned} \tag{12.41}$$

where we used Gauss's law $\boldsymbol{\nabla}\cdot\boldsymbol{B} = 0$. Since $\boldsymbol{\nabla}\phi$ is singular at the vortex core, ϕ is not twice continuously differentiable and the identity $\boldsymbol{\nabla}\times\boldsymbol{\nabla}f = 0$ for a function f

does not hold. We must therefore consider the term $\omega\boldsymbol{\nabla}\times\boldsymbol{\nabla}\phi$ more closely. At the vortex cores, the complex order parameter π will go to zero. Thus, for small r we can assume that $\pi = cr^n e^{ip\theta}$ for a p-quanta vortex, where $n > 0$, θ is the polar angle and c is a constant. Because all fields are radially symmetric in this region we have $\boldsymbol{A} = A(r)\hat{\theta}$ and $\boldsymbol{B} = B(\boldsymbol{r})\hat{z} = \frac{1}{r}\frac{\partial}{\partial r}(rA)$. The magnitude of the vector potential is therefore given by

$$A(r) = \frac{1}{r}\int_0^r \mathrm{d}r' r' B(r') \approx \frac{1}{2} rB(0), \tag{12.42}$$

where the last equality follows from the fact that we are near a vortex core. Close to a vortex core we will also have $\phi = p\theta$ so that $\boldsymbol{\nabla}\phi = \frac{p}{r}\hat{\theta}$. Hence, the supervelocity becomes $\boldsymbol{Q} = \left(\frac{1}{2}rB(0) - \frac{p}{er}\right)\hat{\theta}$. The r-dependence in π is determined by inserting $\omega = \pi^*\pi = c^2 r^{2n}$ into the equation of motion (12.37) resulting in

$$\begin{aligned} -4n^2c^2r^{2n-2} = \frac{1}{2}\left\{c^2r^{2n} - \frac{c^4r^{4n}}{f_\pi^2}\right\}\Bigg\{4\mu_I^2 - 4e^2\left(\frac{1}{2}rB(0) - \frac{p}{er}\right)^2 \\ +4n^2c^4r^{4n-2}\left[\frac{1}{\left(f_\pi^2 - c^2r^{2n}\right)^2} - \frac{1}{c^4r^{4n}}\right] - \frac{4f_\pi m_\pi^2}{\sqrt{f_\pi^2 - c^2r^{2n}}}\Bigg\}. \end{aligned} \tag{12.43}$$

When $r \to 0$, this is dominated by three terms giving

$$-4n^2c^2r^{2n-2} = \frac{1}{2}c^2r^{2n}\left(-4e^2\frac{p^2}{e^2r^2} - 4n^2c^4r^{4n-2}\frac{1}{c^4r^{4n}}\right). \tag{12.44}$$

This equality holds when $p = n$ and we conclude that $\pi = cr^p e^{ip\theta}$ near a p-quanta vortex. Since $\boldsymbol{\nabla}\phi = \frac{p}{r}\hat{\theta} \to \infty$ when $r \to 0$, we know that $\boldsymbol{\nabla}\times\boldsymbol{\nabla}\phi$ will give a delta function near a vortex core. However, with our result for π near a vortex core, we can easily show that $\omega\boldsymbol{\nabla}\times\boldsymbol{\nabla}\phi$ is well behaved at all locations. Using $\omega = c^2r^{2p}$ and exploiting the product rule we find

$$\begin{aligned} \omega\boldsymbol{\nabla}\times\boldsymbol{\nabla}\phi =& \boldsymbol{\nabla}\times(\omega\boldsymbol{\nabla}\phi) - \boldsymbol{\nabla}\omega\times\boldsymbol{\nabla}\phi \\ =& c^2\left[\boldsymbol{\nabla}\times\left(r^{2p}\frac{p}{r}\hat{\theta}\right) - 2pr^{2p-1}\hat{r}\times\frac{p}{r}\hat{\theta}\right] \\ =& c^2\left[\frac{1}{r}\left(\frac{\partial\left(pr^{2p}\right)}{\partial r}\right) - 2p^2r^{2p-2}\right]\hat{z} \\ =& c^2\left[2p^2r^{2p-2} - 2p^2r^{2p-2}\right]\hat{z} \\ =& 0. \end{aligned} \tag{12.45}$$

This is valid close to a vortex core. Away from a vortex core, $\boldsymbol{\nabla}\phi$ will not be singular and $\boldsymbol{\nabla}\times\boldsymbol{\nabla}\phi$ is zero. The equation of motion (12.41) is thus

$$\boldsymbol{\nabla}^2\boldsymbol{B} = e^2\left(\boldsymbol{\nabla}\omega\times\boldsymbol{Q} + \omega\boldsymbol{B}\right). \tag{12.46}$$

Having $\boldsymbol{B} = (0, 0, B)$, $\boldsymbol{Q} = (Q_x, Q_y, 0)$ and adding a stabilizing term $-e^2\bar{\omega}B$ gives

$$\left(\boldsymbol{\nabla}^2 - e^2\bar{\omega}\right)B = e^2\left[Q_y\partial_x\omega - Q_x\partial_y\omega + (\omega - \bar{\omega})B\right], \tag{12.47}$$

where $\bar{\omega} = \langle\omega\rangle$ is the spatial average of ω. Inserting the Fourier series of B in eq. (12.11) on the left-hand side yields

$$\left(\boldsymbol{\nabla}^2 - e^2\bar{\omega}\right)\left(\bar{B} + \sum_{\boldsymbol{K}} b_{\boldsymbol{K}}\cos\boldsymbol{K}\cdot\boldsymbol{r}\right) = e^2\left[Q_y\partial_x\omega - Q_x\partial_y\omega + (\omega - \bar{\omega})B\right]. \tag{12.48}$$

Multiplying both sides by $\cos \boldsymbol{K}' \cdot \boldsymbol{r}$, averaging over space $\langle ... \rangle$ and exploiting that $\langle \cos \boldsymbol{K} \cdot \boldsymbol{r} \cos \boldsymbol{K}' \cdot \boldsymbol{r} \rangle = \frac{1}{2} \delta_{\boldsymbol{K},\boldsymbol{K}'}$, we arrive at

$$b_{\boldsymbol{K}} = -\frac{2e^2}{\boldsymbol{K}^2 + e^2 \bar{\omega}} \left\langle \left[Q_y \partial_x \omega - Q_x \partial_y \omega + (\omega - \bar{\omega})\, B \right] \cos \boldsymbol{K} \cdot \boldsymbol{r} \right\rangle , \tag{12.49}$$

where the prime in $\boldsymbol{K}'$ is dropped. Thus, we have an iteration equation for the Fourier coefficients $b_{\boldsymbol{K}}$ where we insert the old values of ω and $\boldsymbol{Q}$ on the right-hand side. The convergence of the iteration may be accelerated if we optimize the amplitude of ω after each use of eq. (12.39). This is done by assuming a change of ω that modifies its amplitude but maintains its shape,

$$\omega = (1 + c)\omega. \tag{12.50}$$

The right-hand side, with the old value of ω, updates the left-hand side with the new value of ω. The constant c is found by minimizing the average Helmholtz free energy $\bar{F}$ at each iteration step. First, we substitute eq. (12.50) into eq. (12.9). Then, taking the spatial average and setting the variation of $\bar{F}$ with respect to c to zero, we find

$$\begin{aligned} \frac{\delta \bar{F}}{\delta c} = \Bigg\langle \frac{1}{8} \Bigg[& \frac{2 f_\pi^2 \left(\boldsymbol{\nabla} \omega\right)^2}{\omega \left(f_\pi^2 - (1+c)\omega\right)} + \frac{4 f_\pi m_\pi^2 \omega}{\sqrt{f_\pi^2 - (1+c)\omega}} \\ & + \frac{\left(\boldsymbol{\nabla} \omega\right)^2}{\omega} \frac{f_\pi^2 \left(2(1+c)\omega - f_\pi^2\right)}{\left(f_\pi^2 - (1+c)\omega\right)^2} - 4\omega \left(\mu_I^2 - e^2 \boldsymbol{Q}^2\right) \Bigg] \Bigg\rangle \\ = 0. & \end{aligned} \tag{12.51}$$

After iterating the two eqs. (12.39) and (12.49) a few times, we expect the correction c to be small, $|c| \ll 1$. The linear approximation of eq. (12.51) is therefore sufficient. Expanding to first order in c gives

$$c = -\frac{\left\langle \frac{(\boldsymbol{\nabla}\omega)^2}{\omega} \left(\frac{f_\pi^2}{f_\pi^2 - \omega}\right)^2 + \frac{4 f_\pi m_\pi^2 \omega}{\sqrt{f_\pi^2 - \omega}} - 4\omega \left(\mu_I^2 - e^2 \boldsymbol{Q}^2\right) \right\rangle}{2 \left\langle \frac{f_\pi^4 (\boldsymbol{\nabla}\omega)^2}{(f_\pi^2 - \omega)^3} + \frac{f_\pi m_\pi^2 \omega^2}{(f_\pi^2 - \omega)^{3/2}} \right\rangle}. \tag{12.52}$$

Expanding both sides of eq. (12.50) into the Fourier series of eq. (12.10) yields

$$\sum_{\boldsymbol{K}} a_{\boldsymbol{K}} \left(1 - \cos \boldsymbol{K} \cdot \boldsymbol{r}\right) = \sum_{\boldsymbol{K}} (1 + c)\, a_{\boldsymbol{K}} \left(1 - \cos \boldsymbol{K} \cdot \boldsymbol{r}\right). \tag{12.53}$$

Inserting c from eq. (12.52), multiplying both sides by $\cos \boldsymbol{K}' \cdot \boldsymbol{r}$, averaging over space $\langle ... \rangle$ and exploiting that $\langle \cos \boldsymbol{K} \cdot \boldsymbol{r} \cos \boldsymbol{K}' \cdot \boldsymbol{r} \rangle = \frac{1}{2} \delta_{\boldsymbol{K},\boldsymbol{K}'}$ results in

$$a_{\boldsymbol{K}} = a_{\boldsymbol{K}} \left[1 - \frac{\left\langle \frac{(\boldsymbol{\nabla}\omega)^2}{\omega} \left(\frac{f_\pi^2}{f_\pi^2 - \omega}\right)^2 + \frac{4 f_\pi m_\pi^2 \omega}{\sqrt{f_\pi^2 - \omega}} - 4\omega \left(\mu_I^2 - e^2 \boldsymbol{Q}^2\right) \right\rangle}{2 \left\langle \frac{f_\pi^4 (\boldsymbol{\nabla}\omega)^2}{(f_\pi^2 - \omega)^3} + \frac{f_\pi m_\pi^2 \omega^2}{(f_\pi^2 - \omega)^{3/2}} \right\rangle} \right], \tag{12.54}$$

where we have dropped the prime in $\boldsymbol{K}'$. Updated Fourier coefficients $a_{\boldsymbol{K}}$ are obtained by inserting the old values of ω, $\boldsymbol{Q}$ and $a_{\boldsymbol{K}}$ on the right-hand side. However,

this iteration equation is numerically problematic. If $\omega \to f_\pi^2$ at some points in space, the second term in the nominator and denominator will diverge. Thus, the two spatial averages will diverge. This can lead to an overflow in the numerical procedure since the averages need to be stored before they are divided by each other. This should not be a problem at high external fields where ω does not reach f_π^2. For convenience, we state all three iteration equations (12.39), (12.49) and (12.54),

$$a_{\boldsymbol{K}} = \frac{-2}{\boldsymbol{K}^2 + 2e^2 f_\pi^2} \left\langle \left\{ 2\left[\omega - \frac{\omega^2}{f_\pi^2}\right]\left[\mu_I^2 - e^2\boldsymbol{Q}^2\right] + \frac{1}{2f_\pi^2}\left[\frac{\omega\left(\boldsymbol{\nabla}\omega\right)^2}{f_\pi^2 - \omega} - \frac{\left(f_\pi^2 - \omega\right)\left(\boldsymbol{\nabla}\omega\right)^2}{\omega}\right] - \frac{2m_\pi^2}{f_\pi}\omega\sqrt{f_\pi^2 - \omega} + 2e^2 f_\pi^2 \omega \right\} \cos \boldsymbol{K}\cdot\boldsymbol{r} \right\rangle, \tag{12.55}$$

$$a_{\boldsymbol{K}} = a_{\boldsymbol{K}}\left[1 - \frac{\left\langle \frac{(\boldsymbol{\nabla}\omega)^2}{\omega}\left(\frac{f_\pi^2}{f_\pi^2-\omega}\right)^2 + \frac{4f_\pi m_\pi^2 \omega}{\sqrt{f_\pi^2-\omega}} - 4\omega\left(\mu_I^2 - e^2\boldsymbol{Q}^2\right)\right\rangle}{2\left\langle \frac{f_\pi^4(\boldsymbol{\nabla}\omega)^2}{(f_\pi^2-\omega)^3} + \frac{f_\pi m_\pi^2 \omega^2}{(f_\pi^2-\omega)^{3/2}}\right\rangle}\right], \tag{12.56}$$

$$b_{\boldsymbol{K}} = -\frac{2e^2}{\boldsymbol{K}^2 + e^2\bar{\omega}}\left\langle \left[Q_y\partial_x\omega - Q_x\partial_y\omega + (\omega - \bar{\omega})\,B\right]\cos \boldsymbol{K}\cdot\boldsymbol{r}\right\rangle. \tag{12.57}$$

The iteration procedure starts out by iterating eqs. (12.55) and (12.56) a few times, setting $b_{\boldsymbol{K}} = 0$. Next, we iterate eqs. (12.55)-(12.57) until we reach the desired precision. After each iteration step, we update ω, $B(\boldsymbol{r})$ and $\boldsymbol{Q}$ using the Fourier series in eqs. (12.10), (12.11) and (12.17). Eq. (12.56) is skipped for low magnetic fields so that overflow is avoided.

12.4 Virial theorem for QCD and Gibbs free energy

The input parameter of the numerical method is the average magnetic field $\bar{B}$. We must therefore find the external magnetic field in order to obtain the Gibbs free energy. A fast and accurate way to do this is to use a version of the virial theorem. The virial theorem gives a relation between the external magnetic field and the solutions to the equations of motion. The external field is therefore calculated after the iteration procedure. The viral theorem for Ginzburg-Landau theories is proved in [65]. The fundamental idea of the proof is the fact that the average magnetic field $\bar{B}$ adjusts itself to minimize the free energy. For a given external field, there is an optimal vortex density $\bar{B}/\Phi_0$, which gives the minimal free energy of the system. Consequently, the external field acts as a pressure. We can formally change this pressure by scaling the coordinate system. Such a scaling will for an optimal vortex density result in an increased free energy [62]. We start off by introducing a parameter λ, which scales the x- and y-coordinates as

$$\boldsymbol{r}' = \boldsymbol{r}/\lambda. \tag{12.58}$$

The transformed order parameter then becomes

$$\pi'(\boldsymbol{r}) = \pi(\lambda \boldsymbol{r}). \tag{12.59}$$

In addition we have that

$$\omega'(\boldsymbol{r}) = \omega(\lambda \boldsymbol{r}). \tag{12.60}$$

To see how the coordinate scaling affects the average magnetic field, we must investigate how the magnetic field is quantized in the vortex lattice. The average magnetic field is determined by implementing what can be described as "periodic boundary conditions". Since the physical quantities $\boldsymbol{B}$ and $|\pi|$ has the same periodicity as the lattice, we must require that

$$\begin{aligned} \boldsymbol{A}\left(\boldsymbol{r}+\boldsymbol{R}_\nu\right) &= \boldsymbol{A}\left(\boldsymbol{r}\right) + \boldsymbol{\nabla}\chi_\nu(\boldsymbol{r}), \\ \pi\left(\boldsymbol{r}+\boldsymbol{R}_\nu\right) &= \pi(\boldsymbol{r})\mathrm{e}^{ie\chi_\nu(\boldsymbol{r})}, \end{aligned} \tag{12.61}$$

where $\boldsymbol{R}_\nu$ are lattice vectors and χ_ν are the gauge potentials associated with each lattice vector. Hence, a translation by a lattice vector amounts to a gauge transformation. Furthermore, $\boldsymbol{A}$ and π are single-valued. Circling along the edges of a unit cell will therefore require

$$\begin{aligned} \pi\left(\boldsymbol{r}+\boldsymbol{R}_1+\boldsymbol{R}_2\right) - \pi\left(\boldsymbol{r}+\boldsymbol{R}_2+\boldsymbol{R}_1\right) &= \pi\left(\boldsymbol{r}+\boldsymbol{R}_1\right)\mathrm{e}^{ie\chi_2(\boldsymbol{r}+\boldsymbol{R}_1)} - \pi\left(\boldsymbol{r}+\boldsymbol{R}_2\right)\mathrm{e}^{ie\chi_1(\boldsymbol{r}+\boldsymbol{R}_2)} \\ &= \pi\left(\boldsymbol{r}\right)\mathrm{e}^{ie[\chi_2(\boldsymbol{r}+\boldsymbol{R}_1)+\chi_1(\boldsymbol{r})]} - \pi\left(\boldsymbol{r}\right)\mathrm{e}^{ie[\chi_1(\boldsymbol{r}+\boldsymbol{R}_2)+\chi_2(\boldsymbol{r})]} \\ &= 0. \end{aligned} \tag{12.62}$$

This leads to the condition

$$\chi_1\left(\boldsymbol{r}\right) + \chi_2\left(\boldsymbol{r}+\boldsymbol{R}_1\right) - \chi_1\left(\boldsymbol{r}+\boldsymbol{R}_2\right) - \chi_2\left(\boldsymbol{r}\right) = \frac{2\pi p}{e}, \tag{12.63}$$

where p is an integer. The total magnetic flux Φ passing through a unit cell is found from eqs. (12.61) and (12.63) by integrating $\boldsymbol{B}$ over a unit cell

$$\Phi = \int \boldsymbol{B}\cdot \mathrm{d}\boldsymbol{A} = \int \boldsymbol{A}\cdot \mathrm{d}\boldsymbol{l} = p\Phi_0. \tag{12.64}$$

The magnetic flux is therefore quantized in units of $\Phi_0 = 2\pi/e$. Thus, the spatial average of $\boldsymbol{B}$ over a unit cell with area A becomes

$$\bar{\boldsymbol{B}} = \frac{p\Phi_0}{A}\hat{z}. \tag{12.65}$$

Consequently, the average magnetic field has been fixed by the boundary conditions. The scaling of the coordinates changes the boundary conditions to

$$\begin{aligned} \boldsymbol{A}'\left(\boldsymbol{r}+\boldsymbol{R}_\nu\right) &= \boldsymbol{A}'\left(\boldsymbol{r}\right) + \boldsymbol{\nabla}'\chi'_\nu\left(\boldsymbol{r}\right), \\ \pi'\left(\boldsymbol{r}+\boldsymbol{R}_\nu\right) &= \pi'\mathrm{e}^{ie\chi'_\nu(\boldsymbol{r})}. \end{aligned} \tag{12.66}$$

Furthermore, the number of flux quanta p is unchanged, but eq. (12.65) results in a changed average magnetic field

$$\bar{\boldsymbol{B}}' = \frac{\lambda^2 p\Phi_0}{A'} = \lambda^2\bar{\boldsymbol{B}}. \tag{12.67}$$

The average Helmholtz free energy $\bar{F}$ depends on the boundary conditions. Hence, the changed boundary conditions may be taken into account by including a dependence of $\bar{F}$ on the average magnetic field. From the scaling of $\boldsymbol{B} = \boldsymbol{\nabla} \times \boldsymbol{A}$, we see that the vector potential scales in the same manner as the gradient,

$$\boldsymbol{A}'(\boldsymbol{r}) = \frac{1}{\lambda}\boldsymbol{A}(\lambda \boldsymbol{r}). \tag{12.68}$$

Inserting the primed variables into the Helmholtz free energy in eq. (12.9) and taking the spatial average gives the free energy per unit volume

$$\begin{aligned}\bar{F}' = \Bigg\langle & \frac{1}{\lambda^2}\frac{(\boldsymbol{\nabla}'\omega')^2}{8}\left(\frac{1}{f_\pi^2-\omega'}+\frac{1}{\omega'}\right) - \frac{1}{2}\mu_I^2\omega' + \frac{1}{2\lambda^2}e^2\boldsymbol{Q}'^2\omega' \\ & - f_\pi m_\pi^2\left(\sqrt{f_\pi^2-\omega'}-f_\pi\right) + \frac{1}{2\lambda^4}\boldsymbol{B}'^2\Bigg\rangle.\end{aligned} \tag{12.69}$$

Next, demanding that $\partial\bar{F}'/\partial\lambda = 0$ when $\lambda = 1$ yields

$$0 = \left\langle -\frac{(\boldsymbol{\nabla}\omega)^2}{4}\left(\frac{1}{f_\pi^2-\omega}+\frac{1}{\omega}\right) - e^2\boldsymbol{Q}^2\omega - 2\boldsymbol{B}^2\right\rangle + 2\bar{\boldsymbol{B}}\cdot\frac{\partial\bar{F}}{\partial\bar{\boldsymbol{B}}}. \tag{12.70}$$

The last term arises from the dependence of $\bar{F}$ on the changed boundary conditions, which leads to a scaled average magnetic field in eq. (12.67). The λ dependence of π and $\boldsymbol{A}$ can be neglected since $\mathscr{F}$ is stationary under variations of π and $\boldsymbol{A}$. Exploiting the relation $\boldsymbol{H} = \partial\bar{F}/\partial\bar{\boldsymbol{B}}$ gives the virial theorem for QCD in the form

$$\boldsymbol{H}\cdot\bar{\boldsymbol{B}} = \left\langle \frac{(\boldsymbol{\nabla}\omega)^2}{8}\left(\frac{1}{f_\pi^2-\omega}+\frac{1}{\omega}\right) + \frac{1}{2}e^2\boldsymbol{Q}^2\omega + \boldsymbol{B}^2\right\rangle. \tag{12.71}$$

The total Gibbs free energy per unit volume of the magnetic vortex lattice is given by eqs. (12.9) and (12.71). By the use of the virial theorem, it takes the simple form

$$\begin{aligned}\frac{G}{V} &= \bar{F} - \boldsymbol{H}\cdot\bar{\boldsymbol{B}} + \frac{1}{2}H^2 \\ &= \left\langle -\frac{1}{2}\mu_I^2\omega - f_\pi m_\pi^2\left(\sqrt{f_\pi^2-\omega}-f_\pi\right) - \frac{1}{2}\boldsymbol{B}^2\right\rangle + \frac{1}{2}H^2,\end{aligned} \tag{12.72}$$

where ω and $\boldsymbol{B}$ are the solutions to the iteration equations (12.55)-(12.57). Furthermore, we have subtracted the Gibbs free energy of the QCD vacuum.

12.5 Numerical procedure and results

Because all terms in the iteration equations (12.55)-(12.57) are smooth periodic functions of $\boldsymbol{r}$, we can achieve high accuracy by simulating on an equidistant 2D grid. In order to avoid the divergences at the vortex cores, we choose $x_i = (i-1/2)x_1/N_x$ for $i = 1,...,N_x$ and $y_j = (j-1/2)y_2/N_y$ for $j = 1,...,N_y$, where $2N_y \approx N_x y_2/x_1$. This fills a rectangular basic area $0 \le x \le x_1$, $0 \le y \le y_2/2$ with $N = N_x N_y = 100-7000$ grid points. This is valid for any unit cell shaped like a parallelogram. Taking the

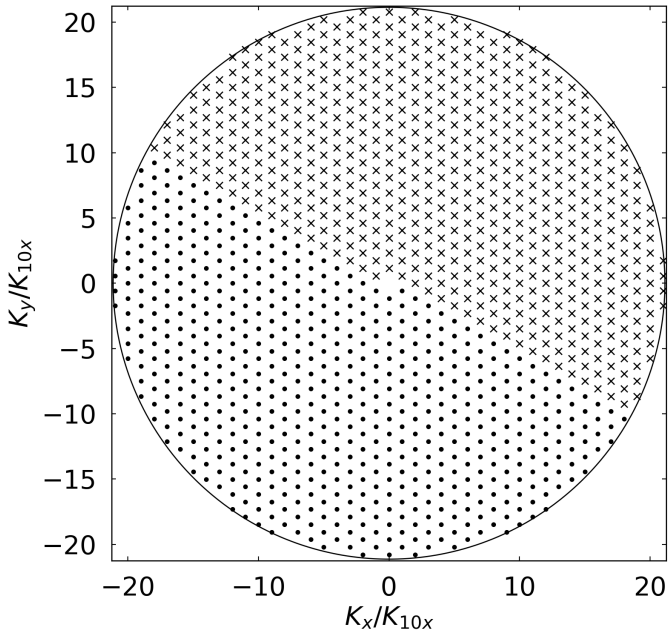

Figure 12.2: The reciprocal lattice vectors $\boldsymbol{K}$ used in the two-dimensional Fourier series are marked with a cross. Any half circle of reciprocal lattice vectors is sufficient due to symmetry. All vectors are divided by the x-component of $\boldsymbol{K}_{10}$ and the number of grid points is $N = N_x \cdot N_y = 42 \cdot 18$.

spatial average $\langle ... \rangle$ means summing N terms with a constant weight $1/N$. Since the Fourier series are written in terms of cosine and sine, we will only need to consider the reciprocal lattice vectors $\boldsymbol{K}_{mn}$ within a half-circle $|\boldsymbol{K}_{mn}| \leq K_{\max}$. We choose $K_{\max}^2 \approx 20N/S$ such that the number of reciprocal lattice vectors is slightly less than the number of grid points N. Figure 12.2 displays a plot of the reciprocal lattice vectors for $N = N_x \cdot N_y = 42 \cdot 18$. The numerical procedure is substantially accelerated by computing the matrices $\cos \boldsymbol{K} \cdot \boldsymbol{r}$ and $\sin \boldsymbol{K} \cdot \boldsymbol{r}$ ahead of the iteration. For a given average magnetic field $\bar{B}$, the iteration procedure runs in less than a minute depending on the necessary precision. The code is written in Python 3.7 and is found in appendix B. The second iteration equation (12.56) is left out since it makes the iteration procedure unstable. This should not affect the result, only the speed of convergence. We can easily adapt the code in order to solve the same problem as Brandt did in [61]. Unfortunately, it turns out that the code must have a bug as it does not reproduce the results of Brandt exactly. However, the general form of the order parameter and the magnetic field is correct. We will therefore skip a detailed analysis of the results and instead look at the qualitative behavior of the results. Figure 12.3 shows plots of the magnetic field B and the order parameter ω at an external magnetic field $H = 0.0139$ GeV^2 for two different isospin densities. It is important to note that the upper critical field H_{c2} is dependent on the isospin density. As expected, the order parameter goes to zero at the vortex cores, where the magnetic field is maximal. Furthermore, the magnetic field B satisfies $B < H$, which implies a vortex lattice that screens out a fraction of the external field H. This is expected since type-II superconductors exhibit a partial Meissner effect. In addition, we observe that a higher isospin density at a fixed external field allows

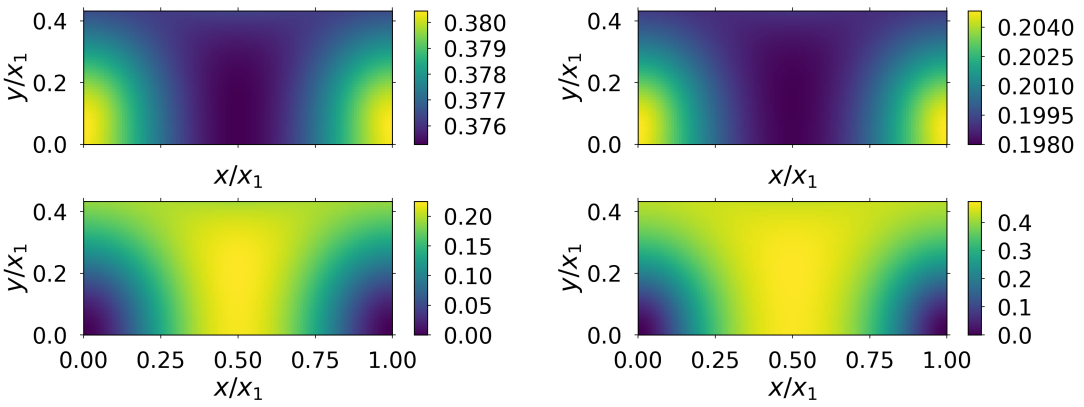

Figure 12.3: The upper plots shows the magnetic field B in units of the upper critical field H_{c2}. The lower plots shows the order parameter ω/f_π^2. The isospin chemical potential is set to $\mu_I = 175$ MeV in the left plots and $\mu_I = 200$ MeV in the right plots. Vortex cores are located at $(x, y) = (0, 0)$ and $(x, y) = (x_1, 0)$. All numerical values are obtained at an external magnetic field $H = 0.0139$ GeV^2 with $f_\pi = 92$ MeV and $m_\pi = 140$ MeV.

for a higher order parameter away from the vortex cores. This can be explained by the fact that higher density gives the system a possibility of producing stronger opposing magnetic fields. The order parameter can therefore take a higher value since the magnetic field is lower in the system. Finally, we see in figure 12.4 that we have fast convergence of the Gibbs free energy.

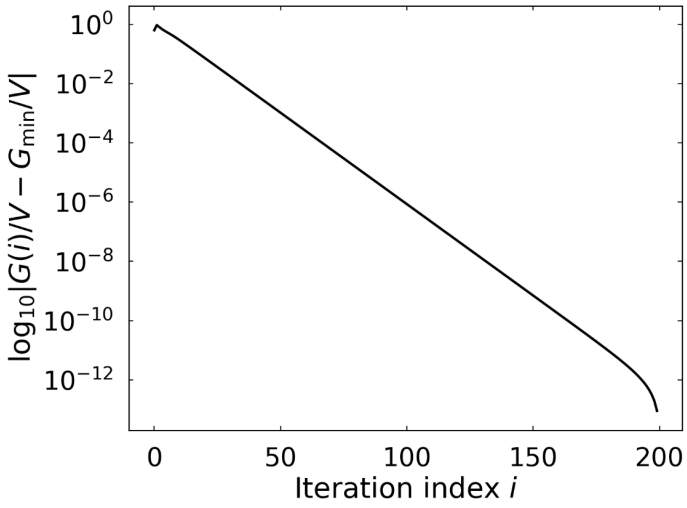

Figure 12.4: The convergence of the iteration procedure illustrated by the logarithmic difference $\log|G(i)/V - G_{\min}/V|$, where $G(i)$ is the total Gibbs free energy after iteration i and $G_{\min}$ is the total Gibbs free energy after 200 iterations. The numerical values were obtained having $H = 0.0139$ GeV^2, $\mu_I = 175$ MeV, $m_\pi = 140$ MeV, $f_\pi = 92$ MeV and $N = NxNy = 6235$.

Chapter 13

Conclusion and outlook

The main body of this thesis consists of three parts. We will in this chapter summarize the most important results from each of these parts. Moreover, we will address a few topics for future work.

13.1 Part I and II

In part I, we started out by examining how a complex scalar field undergoes SSB of a $U(1)$ symmetry by acquiring a nonzero vev. We saw how the dispersion relations of massive and massless modes were affected by a chemical potential and an external magnetic field. A key result was the Landau level quantization of charged particles with a chemical potential in a magnetic field. Moreover, we saw how the SSB in a linear $SO(3)$ sigma model led to two Goldstone bosons in accordance with Goldstone's theorem. A chemical potential in the nonlinear $SO(3)$ sigma model made one of these Goldstone bosons massive.

In part II, we investigated how the low-energy regime of QCD behaves. Using ChPT, we found that two-flavor QCD at low energies describes three degrees of freedom with equal mass m_π. The degrees of freedom are a result of SSB of the $SU(2)_L \times SU(2)_R$ symmetry of QCD to an $SU(2)_V$ symmetry. Introducing an isospin chemical potential μ_I resulted in a phase where the QCD vacuum was rotated when $\mu_I \geqslant m_\pi$. The rotation was accompanied by a BEC of charged pions with one gapless mode. When $\mu_I \leqslant m_\pi$, the chemical potential leads to a Zeeman-like splitting of the relativistic dispersion relations of the charged pions. Furthermore, the dispersion relation of the neutral pion remained relativistic but with mass μ_I.

In order to gain more insight into the behavior of low-energy QCD, we calculated the chiral isospin anomaly in presence of electromagnetic, baryon number and isospin background gauge fields. We included the anomaly into the ChPT Lagrangian by restricting our attention to neutral pions. A remarkable consequence was that nonuniform *neutral* pion fields carried electric charge, baryon number and isospin even though neutral pions have none of these. Next, we calculated the Wess-Zumino-Witten term which captures the anomalies of QCD and is the only anomalous term that can be added to the two-flavor Lagrangian. The starting point was the GW current. First, we saw how the divergence of the GW current vanished when the background gauge fields became purely vector-like. By restrict-

ing the Wess-Zumino-Witten term to neutral pions, we were able to determine the coefficient of the GW current.

13.2 Part III

Part III started out by realizing that the Wess-Zumino-Witten term would affect the ground state of QCD in the presence of an external magnetic field at finite baryon chemical potential, μ_B. By solving the equation of motion exactly under these circumstances, we established the possibility of a CSL when $\mu_B B \geqslant 16\pi m_\pi f_\pi^2$. CSL was found to be an array of parity-violating topological solitons carrying baryon charge. The CSL was proven to be energetically more favorable than the QCD vacuum when $\mu_B \leqslant m_N$, where m_N is the nucleon mass. Additionally, the CSL is energetically more favorable than nuclear matter when $\mu_B \approx m_N$. Hence, the presence of CSL in the QCD phase diagram was firmly established.

The rest of the thesis focused on an isospin chemical potential instead of a baryon chemical potential. However, the same CSL structure arose also with a finite isospin density since the anomaly was only present through a surface term of the Lagrangian. First, we noted that the CSL spontaneously breaks continuous translational and rotational symmetries leading to a gapless phonon of the soliton lattice. Next, we introduced dynamical electromagnetic fields. In the case of no coupling between the photons and the pion, we found three gapless modes, namely the phonon of the CSL and the two photon polarizations. However, turning on the coupling gave two gapped modes and only one gapless mode. This is fascinating since we had spontaneous breaking of spatial translations as well as the absence of the Higgs mechanism for photons. The gapless mode was generally a mixture of the neutral pion and the photon polarizations. Nevertheless, we could remove the mixing by considering for example modes propagating in the direction of the external magnetic field. This made it possible to define helicity due to unbroken rotational invariance. The pion and photons modes were therefore clearly distinguished.

In part II we derived the excitation spectrum of a BEC in the presence of an isospin chemical potential. A next step was therefore to introduce an external magnetic field along with dynamical electromagnetic fields. Doing so, we assumed that a classical charged background ensured electrical neutrality of the ground state. Furthermore, we assumed that the charged background did not affect the dynamics of the excitation spectrum. The introduction of a dynamical electromagnetic field gave rise to a coupling between the charged pions and the two photon polarizations. As a result, the photon polarizations and the originally gapless charged pion acquired the same gap through the Anderson-Higgs mechanism. The gap of the two other modes remained the same. We also showed that the Wess-Zumino-Witten term does not affect the dispersion relations.

Moreover, we established where the CSL and the BEC are manifested in the μ_I-H plane of the QCD phase diagram, allowing for dynamical electromagnetic fields. For physical pion masses, we found that the QCD vacuum well separates the BEC and the CSL in the phase diagram. However, reducing the pion mass towards the chiral limit squeezes the QCD vacuum out of the phase diagram. Finally, we considered the existence of a magnetic vortex lattice by ignoring the possibility of

neutral pion condensation. We exploited the resemblance to the Ginzburg-Landau theory and established an iteration scheme that may make it possible to determine where such a lattice is manifested in the QCD phase diagram. In doing so, we needed to derive a virial theorem for QCD. The theorem gave a relation of the external magnetic field to the average magnetic field and the order parameter of the superconducting state. Using the virial theorem, we achieved fast convergence of the Gibbs free energy of the magnetic vortex lattice. The lattice was seen to exhibit an expected partial Meissner effect. Moreover, higher isospin density at a fixed external field allowed for a larger magnitude of the order parameter away from the vortex cores.

13.3 Outlook

Lastly, we will address some topics for future work. This thesis has not taken into account the effect of thermal fluctuations. This could potentially destroy the long-range order of the CSL in presence of dynamical electromagnetic fields [66]. The effects of thermal fluctuations can be determined by looking at the two-point correlator of the pion field. In [47] it is established that thermal fluctuations do not cause instability of the CSL at finite baryon density. The thermal fluctuations do instead lead to an anomalous contribution to pressure. We will therefore expect the same result at a finite isospin density.

In addition, we would like to verify our assumption that a charged background does not affect the dynamics of the excitation spectrum in a BEC. Initial calculations have shown that this might not be the case when the background is a gas of massless spin-1/2 Dirac fermions. The results may therefore be valid only below the scale of the plasma oscillation frequency. However, our assumption may be valid if we consider a different background with a larger gap.

Finally, a number of interesting aspects can be explored if the iteration procedure correctly solves the equations of motion in a magnetic vortex lattice. First of all, it allows us to determine the QCD phase diagram more completely. In this thesis, we have only considered a triangular unit cell. However, the numerical procedure allows us to consider any unit cell with the shape of a parallelogram. A consistency check can be performed by comparing our results to the results near the lower and upper critical field in [17, 26]. Furthermore, the numerical procedure makes it possible to determine the magnetization of the system.

Bibliography

[1] M. S. Grønli, *Chiral soliton lattice in quantum chromodynamics with isospin chemical potential*, Specialization project (Norwegian University of Science and Technology, 2020).

[2] Y. Nambu, *Quasi-particles and gauge invariance in the theory of superconductivity*, Physical Review **117**, 648–663 (1960).

[3] J. Goldstone, *Field theories with « Superconductor » solutions*, Il Nuovo Cimento **19**, 154–164 (1961).

[4] J. Goldstone, A. Salam and S. Weinberg, *Broken symmetries*, Physical Review **127**, 965–970 (1962).

[5] Y. Nambu, *Axial vector current conservation in weak interactions*, Physical Review Letters **4**, 380–382 (1960).

[6] H. Fritzsch and M. Gell–Mann, *Current Algebra: Quarks and What Else?*, Physics, Proceedings of the XVI International Conference, 135–165 (1972).

[7] H. Fritzsch, M. Gell-Mann and H. Leutwyler, *Advantages of the color octet gluon picture*, Physics Letters B **47**, 365–368 (1973).

[8] H. D. Politzer, *Reliable perturbative results for strong interactions?*, Physical Review Letters **30**, 1346–1349 (1973).

[9] D. J. Gross and F. Wilczek, *Ultraviolet behavior of non-abelian gauge theories*, Physical Review Letters **30**, 1343–1346 (1973).

[10] S. Weinberg, *Phenomenological Lagrangians*, Physica A: Statistical Mechanics and its Applications **96**, 327–340 (1979).

[11] D. T. Son and M. A. Stephanov, *QCD at finite isospin density*, Physical Review Letters **86**, 592–595 (2001).

[12] K. Splittorff, D. T. Son and M. A. Stephanov, *QCD-like theories at finite baryon and isospin density*, Physical Review D **64** (2001).

[13] M. G. Alford, A. Schmitt, K. Rajagopal and T. Schäfer, *Color superconductivity in dense quark matter*, Reviews of Modern Physics **80**, 1455–1515 (2008).

[14] D. K. Sinclair, *Quenched lattice QCD at finite isospin density and related theories*, Physical Review D - Particles, Fields, Gravitation and Cosmology **66**, 1 (2002).

[15] B. B. Brandt, G. Endrodi and S. Schmalzbauer, *QCD phase diagram for nonzero isospin-asymmetry*, Physical Review D **97** (2018).

[16] T. D. Cohen, *Functional integrals for qcd at nonzero chemical potential and zero density*, Physical Review Letters **91** (2003).

[17] P. Adhikari, T. D. Cohen and J. Sakowitz, *Finite isospin chiral perturbation theory in a magnetic field*, Physical Review C **91** (2015).

[18] G. Endrődi, *Magnetic structure of isospin-asymmetric QCD matter in neutron stars*, Physical Review D **90**, 94501 (2014).

[19] K. Fukushima and T. Hatsuda, *The phase diagram of dense QCD*, Reports on Progress in Physics **74**, 14001 (2010).

[20] S. L. Adler, *Axial-vector vertex in spinor electrodynamics*, Physical Review **177**, 2426–2438 (1969).

[21] J. S. Bell and R. Jackiw, *A PCAC puzzle:* $\pi^0 \to \gamma\gamma$ *in the* σ*-model*, Nuovo Cimento A Serie **A60**, 47 (1969).

[22] D. T. Son and M. A. Stephanov, *Axial anomaly and magnetism of nuclear and quark matter*, Physical Review D - Particles, Fields, Gravitation and Cosmology **77** (2008).

[23] T. Brauner and N. Yamamoto, *Chiral soliton lattice and charged pion condensation in strong magnetic fields*, Journal of High Energy Physics **2017** (2017).

[24] P. Adhikari, J. O. Andersen and P. Kneschke, *Two-flavor chiral perturbation theory at nonzero isospin: pion condensation at zero temperature*, European Physical Journal C **79** (2019).

[25] A. A. Abrikosov, *On the Magnetic properties of superconductors of the second group*, Soviet Physics - Journal of Experimental and Theoretical Physics **5**, 1174–1182 (1957).

[26] P. Adhikari, *Magnetic vortex lattices in finite isospin chiral perturbation theory*, Physics Letters, Section B: Nuclear, Elementary Particle and High-Energy Physics **790**, 211–217 (2019).

[27] M. F. Jakobsen, *A Soft-Limit Theorem for the On-Shell Scattering Amplitudes Describing Processes Involving Massive Nambu-Goldstone Bosons,* Master's thesis at The Norwegian University of Science and Technology (2017), https://ntnuopen.ntnu.no/ntnu-xmlui/handle/11250/2451918.

[28] M. Kachelriess, *Quantum Fields: From the Hubble to the Planck Scale*, Oxford Graduate Texts (Oxford University Press, 2017).

[29] H. Watanabe, *Counting Rules of Nambu-Goldstone Modes*, Annual Review of Condensed Matter Physics **11**, 169 (2020).

[30] A. Nicolis and F. Piazza, *Implications of relativity on nonrelativistic goldstone theorems: Gapped excitations at finite charged density*, Physical Review Letters **110** (2013).

[31] S. Scherer and M. R. Schindler, *A Chiral Perturbation Theory Primer*, Lecture Notes in Physics **830** (2005).

[32] J. Bardeen, L. N. Cooper and J. R. Schrieffer, *Microscopic theory of superconductivity*, Physical Review **106**, 162–164 (1957).

[33] C. Vafa and E. Witten, *Restrictions on symmetry breaking in vector-like gauge theories*, Nuclear Physics, Section B **234**, 173–188 (1984).

[34] R. J. Crewther, P. Di Vecchia, G. Veneziano and E. Witten, *Chiral estimate of the electric dipole moment of the neutron in quantum chromodynamics*, Physics Letters B **88**, 123–127 (1979).

[35] R. Zwicky, *Symmetries of Quantum Mechanics,* Lecture notes in "Symmetries of Quantum Mechanichs" at The University of Edinburgh (2015), https://www2.ph.ed.ac.uk/~rzwicky2/SoQM/romanSoQM_2015.pdf.

[36] P. Adhikari, J. O. Andersen and M. A. Mojahed, *Condensates and pressure of two-flavor chiral perturbation theory at nonzero isospin and temperature*, The European Physical Journal C **81** (2021).

[37] A. I. Vainshtein, V. I. Zakharov, V. A. Novikov and M. A. Shifman, *ABC's of Instantons*, Soviet Physics Uspekhi **25**, 195 (1982).

[38] K. Fujikawa, *Path Integral for Gauge Theories with Fermions*, Physical Review D **21**, 2848 (1980).

[39] M. F. Atiyah and I. M. Singer, *The index of elliptic operators on compact manifolds*, Bulletin of the American Society **69**, 422–433 (1969).

[40] J. Wess and B. Zumino, *Consequences of anomalous Ward identities*, Physics Letters B **37**, 95–97 (1971).

[41] J. Goldstone and F. Wilczek, *Fractional Quantum Numbers on Solitons*, Physical Review Letters **47**, 986–989 (1981).

[42] Y. Togawa, T. Koyama, K. Takayanagi, S. Mori, Y. Kousaka, J. Akimitsu, S. Nishihara, K. Inoue, A. S. Ovchinnikov and J. Kishine, *Chiral magnetic soliton lattice on a chiral helimagnet*, Physical Review Letters **108** (2012).

[43] M. Abramowitz and I. A. Stegun, *Handbook of mathematical functions with formulas, graphs, and mathematical tables*, ninth ed. (Dover, 1964).

[44] N. Manton and P. Sutcliffe, *Topological solitons*, Cambridge Monographs on Mathematical Physics (Cambridge University Press, 2004).

[45] V. E. Korepin and L. D. Faddeev, *Quantization of solitons*, Theoretical and Mathematical Physics **25** (1975).

[46] D. Son and A. R. Zhitnitsky, *Quantum anomalies in dense matter*, Physical Review D **70**, 074018 (2004).

[47] T. Brauner and S. V. Kadam, *Anomalous electrodynamics of neutral pion matter in strong magnetic fields*, Journal of High Energy Physics **2017** (2017).

[48] H. Watanabe and H. Murayama, *Redundancies in Nambu-Goldstone Bosons*, Physical Review Letters **110** (2013).

[49] E. T. Whittaker and G. N. Watson, *A course of modern analysis*, 4th ed., Cambridge Mathematical Library (Cambridge University Press, 1996).

[50] H. Li, D. Kusnezov and F. Iachello, *Group theoretical properties and band structure of the Lamé Hamiltonian*, Journal of Physics A: Mathematical and General **33**, 6413–6429 (2000).

[51] F. Wilczek, *Two applications of axion electrodynamics*, Physical Review Letters **58**, 1799–1802 (1987).

[52] S. Flügge, *Practical Quantum Mechanics*, Classics in Mathematics (Springer Berlin Heidelberg, 2012).

[53] I. Low and A. V. Manohar, *Spontaneously Broken Spacetime Symmetries and Goldstone's Theorem*, Physical Review Letters **88** (2002).

[54] H. Watanabe and H. Murayama, *Nambu-Goldstone bosons with fractional-power dispersion relations*, Physical Review D **89** (2014).

[55] J. I. Kapusta and C. Gale, *Finite-temperature field theory: principles and applications*, 2nd ed., Cambridge Monographs on Mathematical Physics (Cambridge University Press, 2006).

[56] P. W. Higgs, *Broken Symmetries and the Masses of Gauge Bosons*, Physical Review Letters **13**, 508–509 (1964).

[57] P. W. Anderson, *Plasmons, Gauge Invariance, and Mass*, Physical Review **130**, 439–442 (1963).

[58] Q.-Q. Bai, C.-X. Wang, Y. Xiao and L.-S. Geng, *Pion-mass dependence of the nucleon-nucleon interaction*, Physics Letters B **809**, 135745 (2020).

[59] P. Coleman, *Introduction to Many-Body Physics* (Cambridge University Press, 2015).

[60] The author would like to thank Professor Asle Sudbø for recommending the works of Brandt.

[61] E. Brandt, *Ideal and distorted vortex lattice in bulk and film superconductors (review)*, Low Temperature Physics **36**, 2–12 (2010).

[62] P. Lipavsky, J. Kolácek, K. Morawetz, E. H. Brandt and T. J. Yang, *Bernoulli Potential in Superconductors: How the Electrostatic Field Helps to Understand Superconductivity*, Lecture Notes in Physics (Springer Berlin Heidelberg, 2007).

[63] M. Sweeney, *Vortex phases in type-I superconductors*, Doctor of Philosophy (Colorado State University, 2010).

[64] E. Brandt, *Ginsburg-Landau Theory of the Vortex Lattice in Type-II Superconductors for All Values of and B*, Physica Status Solidi B - Basic Solid State Physics **51**, 345–358 (1972).

[65] M. M. Doria, J. E. Gubernatis and D. Rainer, *Virial theorem for Ginzburg-Landau theories with potential applications to numerical studies of type-II superconductors*, Physical Review B **39**, 9573–9575 (1989).

[66] Y. Hidaka, K. Kamikado, T. Kanazawa and T. Noumi, *Phonons, pions, and quasi-long-range order in spatially modulated chiral condensates*, Physical Review D **92** (2015).

Appendices

Appendix A

Useful properties for the Goldstone-Wilzcek current

Some properties we used in section 7.1 to determine the divergence of the Goldstone-Wilzcek current are

$$D_\mu \Sigma = -\Sigma (D_\mu \Sigma^\dagger)\Sigma, \tag{A.1}$$

$$D_\mu \Sigma^\dagger = -\Sigma^\dagger (D_\mu \Sigma)\Sigma^\dagger, \tag{A.2}$$

$$\varepsilon^{\mu\nu\alpha\beta} D_\mu D_\nu \Sigma = \frac{1}{2}\varepsilon^{\mu\nu\alpha\beta} \left[D_\mu, D_\nu\right] \Sigma, \tag{A.3}$$

$$\varepsilon^{\mu\nu\alpha\beta} D_\mu D_\nu \Sigma^\dagger = \frac{1}{2}\varepsilon^{\mu\nu\alpha\beta} \left[D_\mu, D_\nu\right] \Sigma^\dagger, \tag{A.4}$$

$$\varepsilon^{\mu\nu\alpha\beta} [D_\mu, D_\nu]\Sigma = \varepsilon^{\mu\nu\alpha\beta} \left(i\Sigma \mathcal{F}^R_{\mu\nu} - i\mathcal{F}^L_{\mu\nu}\Sigma\right), \tag{A.5}$$

$$\varepsilon^{\mu\nu\alpha\beta} [D_\mu, D_\nu]\Sigma^\dagger = \varepsilon^{\mu\nu\alpha\beta} \left(i\Sigma^\dagger \mathcal{F}^L_{\mu\nu} - i\mathcal{F}^R_{\mu\nu}\Sigma^\dagger\right). \tag{A.6}$$

The properties in eqs. (A.1) and (A.2) are shown by using the unitarity of the matrix field, $\Sigma\Sigma^\dagger = \mathbf{1}$. For eq. (A.1), this is done by writing

$$\begin{aligned} D_\mu \Sigma =& D_\mu(\Sigma\Sigma^\dagger\Sigma) = (D_\mu\Sigma)\Sigma^\dagger\Sigma + \Sigma(D_\mu\Sigma^\dagger)\Sigma + \Sigma\Sigma^\dagger(D_\mu\Sigma) \\ \implies & D_\mu\Sigma = -\Sigma(D_\mu\Sigma^\dagger)\Sigma. \end{aligned} \tag{A.7}$$

Next, the properties in eqs. (A.3) and (A.4) are shown by exploiting the complete antisymmetry of the Levi-Civita symbol $\varepsilon^{\mu\nu\alpha\beta}$. Considering eq. (A.3), we have

$$\begin{aligned} \varepsilon^{\mu\nu\alpha\beta} D_\mu D_\nu \Sigma &= \frac{1}{2}(\varepsilon^{\mu\nu\alpha\beta} D_\mu D_\nu + \varepsilon^{\mu\nu\alpha\beta} D_\mu D_\nu \Sigma)\Sigma \\ &= \frac{1}{2}(\varepsilon^{\mu\nu\alpha\beta} D_\mu D_\nu - \varepsilon^{\mu\nu\alpha\beta} D_\nu D_\mu \Sigma)\Sigma = \frac{1}{2}\varepsilon^{\mu\nu\alpha\beta}[D_\mu, D_\nu]\Sigma. \end{aligned} \tag{A.8}$$

Lastly, eqs. (A.5) and (A.6) are also derived by utilizing the complete antisymmetry of $\varepsilon^{\mu\nu\alpha\beta}$. Eq. (A.5) takes the form

$$\begin{aligned} &\varepsilon^{\mu\nu\alpha\beta}[D_\mu, D_\nu]\Sigma = \varepsilon^{\mu\nu\alpha\beta}(\partial_\mu\Sigma - i\mathcal{A}^L_\mu\Sigma + i\Sigma\mathcal{A}^R_\mu)(\partial_\nu\Sigma - i\mathcal{A}^L_\nu\Sigma + i\Sigma\mathcal{A}^R_\nu) \\ &= \varepsilon^{\mu\nu\alpha\beta}\left\{(-i\partial_\mu\mathcal{A}^L_\nu - \partial_\nu\mathcal{A}^L_\mu)\Sigma + i\Sigma(\partial_\mu\mathcal{A}^R_\nu - \partial_\nu\mathcal{A}^R_\mu) - \left[\mathcal{A}^L_\mu, \mathcal{A}^L_\nu\right]\Sigma + \Sigma\left[\mathcal{A}^R_\mu, \mathcal{A}^R_\nu\right]\right\} \\ &= \varepsilon^{\mu\nu\alpha\beta}(i\Sigma\mathcal{F}^R_{\mu\nu} - i\mathcal{F}^L_{\mu\nu}\Sigma). \end{aligned} \tag{A.9}$$

Appendix B

Code for the magnetic vortex lattice

This appendix presents the Python code used in section 12.5 for the magnetic vortex lattice. The second iteration equation (12.56) as well as several plot functions are not included in the code. The code plots the magnetic field B and the order parameter ω at a given isospin density and average magnetic field. Furthermore, it computes the corresponding external magnetic field and plots the convergence of the Gibbs free energy.

```
#Import
import numpy as np
import matplotlib.pyplot as plt
import numba

#Constants
mu = 175
m = 140
e = np.sqrt(4*np.pi/137)
Hc2 = (mu**2-m**2)/e
BBar = (mu**2-m**2)/e*0.2
f = 92
d = np.sqrt(4*np.pi/(np.sqrt(3)*e*BBar))
Nx = 80
Ny = int(np.sqrt(3)*Nx/4)
iterations = 100

#Functions
@numba.jit(parallel=True)
def makeKFunc():
    mnArray = np.array(0,dtype=tuple)
    Kx = np.array(0,dtype=np.double)
    Ky = np.array(0,dtype=np.double)
    for i in range(-int(Nx/2),int(Nx/2)+1):
        for j in range(int(Nx/2)+1):
            if (j==0 and i>=0):
```

```
                continue
            elif (i**2-i*j+j**2) < 15/(8*np.pi**2)*(Nx)**2:
                Kx = np.append(Kx,2*np.pi*i/d)
                Ky = np.append(Ky,2*np.pi/(np.sqrt(3)*d)*(-i+2*j))
                mnArray = np.append(mnArray, (i,j))
    Kx = np.delete(Kx,0)
    Ky = np.delete(Ky,0)
    mnArray = np.delete(mnArray,0)
    return Kx, Ky, mnArray

@numba.jit(parallel=True)
def aStartCoeffsFunc():
    aA = np.zeros(len(Kx[:]),dtype=np.double)
    for i in range(len(Kx[:])):
        m = mnMatrix[2*i]
        n = mnMatrix[2*i+1]
        aA[i] =
        ↪  -f**2*(-1)**(m+m*n+n)*np.exp(-np.pi/np.sqrt(3)*(m**2-m*n+n**2))
    return aA

@numba.jit(parallel=True)
def dotKrFunc():
    dotKrMatrix = np.full((len(Kx[:]),Nx,Ny),0,dtype=np.double)
    cosKrMatrix = np.full((len(Kx),Nx,Ny),0,dtype=np.double)
    sinKrMatrix = np.full((len(Kx),Nx,Ny),0,dtype=np.double)
    for i in range(len(Kx[:])):
        for j in range(1,Nx+1):
            for k in range(1,Ny+1):
                dotKrMatrix[i][j-1][k-1] =
                ↪  (d/Nx)*(Kx[i]*(j-1/2)+Ky[i]*(k-1/2))
        cosKrMatrix[i,:,:] = np.cos(dotKrMatrix[i,:,:])
        sinKrMatrix[i,:,:] = np.sin(dotKrMatrix[i,:,:])
    return dotKrMatrix[:,:,:], cosKrMatrix[:,:,:], sinKrMatrix[:,:,:]

def QAFunc():
    nominatorX = np.zeros((Nx,Ny),dtype=np.double)
    denominatorX = np.zeros((Nx,Ny),dtype=np.double)
    nominatorY = np.zeros((Nx,Ny),dtype=np.double)
    denominatorY = np.zeros((Nx,Ny),dtype=np.double)
    for i in range(len(Kx[:])):
        nominatorX[:,:] += aStart[i]*Ky[i]*sinKr[i,:,:]
        denominatorX[:,:] += aStart[i]*(1-cosKr[i,:,:])
        nominatorY[:,:] = aStart[i]*Kx[i]*sinKr[i,:,:]
        denominatorY[:,:] += aStart[i]*(1-cosKr[i,:,:])
    return nominatorX[:,:]/(2*e*denominatorX[:,:]),
    ↪  -nominatorY[:,:]/(2*e*denominatorY[:,:])
```

```
def wFourierFunc(a):
    w = np.full((Nx,Ny),0,dtype=np.double)
    for i in range(len(Kx[:])):
        w += a[i]*(1-cosKr[i,:,:])
    return w[:,:]

def bFourierFunc(b):
    B = np.full((Nx,Ny),BBar,dtype=np.double)
    for i in range(len(Kx[:])):
        B[:,:] += b[i]*cosKr[i,:,:]
    return B[:,:]

def gradientSquaredFunc(a):
    gradX2 = np.zeros((Nx,Ny),dtype=np.double)
    gradY2 = np.zeros((Nx,Ny),dtype=np.double)
    for i in range(len(Kx[:])):
        gradX2[:,:] += a[i]*Kx[i]*sinKr[i,:,:]
        gradY2[:,:] += a[i]*Ky[i]*sinKr[i,:,:]
    return gradX2[:,:]**2+gradY2[:,:]**2

def aCoeffs1Func(a,Qx,Qy):
    w = wFourierFunc(a[:])
    gradientWSquared = gradientSquaredFunc(a[:])
    newA = np.full(len(Kx[:]),0,dtype=np.double)
    firstTerm =
    ↪  2*(w[:,:]-w[:,:]**2/f**2)*(mu**2-e**2*(Qx[:,:]**2+Qy[:,:]**2))
    secondTerm =
    ↪  1/(2*f**2)*w[:,:]*gradientWSquared[:,:]/(f**2-w[:,:])
    thirdTerm =
    ↪  -1/(2*f**2)*(f**2-w[:,:])*gradientWSquared[:,:]/w[:,:]
    fourthTerm = -2*m**2/f*w[:,:]*(f**2-w[:,:])**(1/2)
    fifthTerm = 2*e**2*f**2*w[:,:]
    for i in range(len(Kx[:])):
        KSquared = Kx[i]**2+Ky[i]**2
        newA[i] = 1/(Nx*Ny)*np.sum((firstTerm[:,:] + secondTerm[:,:]
        ↪  + thirdTerm[:,:] + fourthTerm[:,:] +
        ↪  fifthTerm[:,:])*cosKr[i,:,:])
        newA[i] *= -2/(KSquared+2*e**2*f**2)
    return newA[:]

def bCoeffsFunc(a,b,Qx,Qy):
    w = wFourierFunc(a[:])
    B = bFourierFunc(b[:])
    wBar = 1/(Nx*Ny)*np.sum(w[:,:])
    gradX = np.zeros((Nx,Ny),dtype=np.double)
    gradY = np.zeros((Nx,Ny),dtype=np.double)
    for i in range(len(Kx[:])):
        gradX[:,:] += a[i]*Kx[i]*sinKr[i,:,:]
```

```
        gradY[:,:] += a[i]*Ky[i]*sinKr[i,:,:]
    p = Qy[:,:]*gradX[:,:]-Qx[:,:]*gradY[:,:]
    wB = w[:,:]*B[:,:]
    wBarB = wBar*B[:,:]
    bNew = np.full(len(Kx[:]),0,dtype=np.double)
    for i in range(len(Kx[:])):
        KSquared = Kx[i]**2+Ky[i]**2
        bNew[i] =
        ↪  1/(Nx*Ny)*np.sum((wB[:,:]-wBarB[:,:]+p[:,:])*cosKr[i,:,:])
        bNew[i] *= -2*e**2/(KSquared+e**2*wBar)
    return bNew[:]

@numba.jit(parallel=True)
def iterateFunc():
    a = np.copy(aStart[:])
    b = np.copy(bStart[:])
    Qx = np.copy(QAx[:,:])
    Qy = np.copy(QAy[:,:])
    freeEnergies = np.array(0,dtype=np.double)
    for i in range(iterations):
        print(i)
        aTemp = np.copy(a[:])
        bTemp = np.copy(b[:])
        a = aCoeffs1Func(a[:],Qx[:,:],Qy[:,:])
        b = bCoeffsFunc(a[:],b[:],Qx[:,:],Qy[:,:])
        Qx = np.copy(QAx[:,:])
        Qy = np.copy(QAy[:,:])
        for j in range(len(Kx[:])):
            Qx[:,:] += -b[j]*Ky[j]/(Kx[j]**2+Ky[j]**2)*sinKr[j,:,:]
            Qy[:,:] += b[j]*Kx[j]/(Kx[j]**2+Ky[j]**2)*sinKr[j,:,:]
        free = GibbsFreeEnergyFunc(a[:],b[:],Qx[:,:],Qy[:,:])
        freeEnergies = np.append(freeEnergies,free)
    freeEnergies = np.delete(freeEnergies[:],0)
    fig = plt.figure()
    ax = fig.add_subplot(111)
    x = np.linspace(0,len(freeEnergies[:]),len(freeEnergies[:]))
    plt.plot(x,freeEnergies[:]*10**(-9),color='black')
    plt.title('Gibbs free energy')
    plt.xlabel('Number of iterations')
    plt.ylabel(r'$G/V \times 10^9 \mathrm{\,\,[MeV}^4\mathrm{]}$')
    ax.xaxis.set_ticks_position('both')
    ax.yaxis.set_ticks_position('both')
    ax.xaxis.set_tick_params(direction='in')
    ax.yaxis.set_tick_params(direction='in')
    plt.tight_layout()
    plt.show()
```

```
    print('External magnetic field H
    ↪  =',round(externalFieldFunc(a[:],b[:],Qx[:,:],Qy[:,:])*10**(-6),4),
    ↪  'GeV^2')
    return a[:], b[:], Qx[:,:], Qy[:,:]

def GibbsFreeEnergyFunc(a,b,Qx,Qy):
    w = wFourierFunc(a[:])
    fMinW = f**2-w[:,:]
    B = bFourierFunc(b[:])
    H = externalFieldFunc(a,b,Qx,Qy)
    return
    ↪  1/(Nx*Ny)*np.sum(-1/2*mu**2*w[:,:]-f*m**2*(fMinW-f)-1/2*B[:,:]**2)

def externalFieldFunc(a,b,Qx,Qy):
    w = wFourierFunc(a[:])
    B = bFourierFunc(b[:])
    BBar = 1/(Nx*Ny)*np.sum(B[:,:])
    gradientWSquared = gradientSquaredFunc(a[:])
    fMinW = f**2-w[:,:]
    QSquared = Qx[:,:]**2+Qy[:,:]**2
    firstTerm = 1/8*gradientWSquared[:,:]*(1/fMinW[:,:]+1/w[:,:])
    secondTerm = 1/2*e**2*QSquared[:,:]*w[:,:]
    denominator =
    ↪  1/(Nx*Ny)*np.sum(firstTerm[:,:]+secondTerm[:,:]+B[:,:]**2)
    return denominator/BBar

def plotWBFunc(a,b):
    fig, ax = plt.subplots(2,1)
    B = bFourierFunc(b[:])/Hc2
    im1 = ax[0].imshow(np.real(B[:,:]).transpose(1,0),origin='lower',
    ↪  extent=[0,1,0,1*np.sqrt(3)/4])
    plt.colorbar(im1,ax=ax[0],aspect=10)
    ax[0].title.set_text('Magnetic field'r' $B/H_\mathrm{c2}$')
    ax[0].xaxis.set_ticks_position('both')
    ax[0].yaxis.set_ticks_position('both')
    ax[0].xaxis.set_tick_params(direction='out')
    ax[0].yaxis.set_tick_params(direction='out')
    empty_string_labels = ['']*len(B[0,:])
    ax[0].set_xticklabels(empty_string_labels)
    ax[0].set_xlabel(r'$x/x_1$')
    ax[0].set_ylabel(r'$y/x_1$')
    w = wFourierFunc(a[:])/f**2
    im2 = ax[1].imshow(np.real(w[:,:]).transpose(1,0),origin='lower',
    ↪  extent=[0,1,0,1*np.sqrt(3)/4],vmin=0)
    plt.colorbar(im2,ax=ax[1],aspect=10)
    ax[1].title.set_text('Order parameter'r' $\omega/f_\pi^2$')
    ax[1].xaxis.set_ticks_position('both')
    ax[1].yaxis.set_ticks_position('both')
```

```
    ax[1].xaxis.set_tick_params(direction='out')
    ax[1].yaxis.set_tick_params(direction='out')
    ax[1].set_xlabel(r'$x/x_1$')
    ax[1].set_ylabel(r'$y/x_1$')
    plt.tight_layout()
    plt.show()

#Run
Kx, Ky, mnMatrix = makeKFunc()
aStart = aStartCoeffsFunc()
bStart = np.zeros(len(Kx))
dotKr, cosKr, sinKr = dotKrFunc()
QAx, QAy = QAFunc()
a, b, Qx, Qy = iterateFunc()
plotWBFunc(a[:],b[:])
```